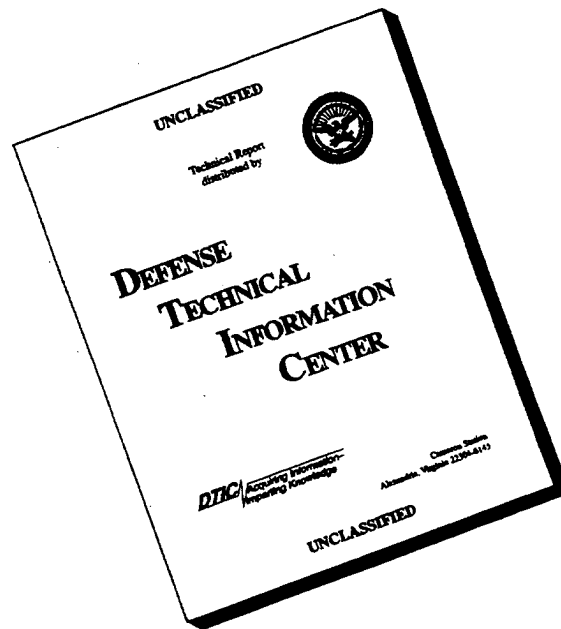


REPORT DOCUMENTATION PAGE			Form Approved OMB No. 0704-0188	
Public reporting burden for this collection of information is estimated to average 1 hour per response, including the time for reviewing instructions, searching existing data sources, gathering and maintaining the data needed, and completing and reviewing the collection of information. Send comments regarding this burden estimate or any other aspect of this collection of information, including suggestions for reducing this burden, to Washington Headquarters Services, Directorate for Information Operations and Reports, 1215 Jefferson Davis Highway, Suite 1204, Arlington, VA 22202-4302, and to the Office of Management and Budget, Paperwork Reduction Project (0704-0188), Washington, DC 20503.				
1. AGENCY USE ONLY (Leave blank)		2. REPORT DATE 2 Feb 96		3. REPORT TYPE AND DATES COVERED
4. TITLE AND SUBTITLE Adsorption and Catalysis on Carbonaceous Adsorbents-Electronic Factors			5. FUNDING NUMBERS	
6. AUTHOR(S) Edward George Marchand				
7. PERFORMING ORGANIZATION NAME(S) AND ADDRESS(ES) AFIT Student Attending: Michigan Technological University			8. PERFORMING ORGANIZATION REPORT NUMBER 96-001D	
9. SPONSORING / MONITORING AGENCY NAME(S) AND ADDRESS(ES) DEPARTMENT OF THE AIR FORCE AFIT/CI 2950 P STREET, BLDG 125 WRIGHT-PATTERSON AFB OH 45433-7765			10. SPONSORING / MONITORING AGENCY REPORT NUMBER	
11. SUPPLEMENTARY NOTES				
12a. DISTRIBUTION / AVAILABILITY STATEMENT Approved for Public Release IAW AFR 190-1 Distribution Unlimited BRIAN D. GAUTHIER, MSgt, USAF Chief Administration			12b. DISTRIBUTION CODE	
13. ABSTRACT (Maximum 200 words)				
14. SUBJECT TERMS			15. NUMBER OF PAGES 179	
			16. PRICE CODE	
17. SECURITY CLASSIFICATION OF REPORT		18. SECURITY CLASSIFICATION OF THIS PAGE		19. SECURITY CLASSIFICATION OF ABSTRACT
				20. LIMITATION OF ABSTRACT

19960531 079

DISCLAIMER NOTICE



THIS DOCUMENT IS BEST QUALITY AVAILABLE. THE COPY FURNISHED TO DTIC CONTAINED A SIGNIFICANT NUMBER OF PAGES WHICH DO NOT REPRODUCE LEGIBLY.

GENERAL INSTRUCTIONS FOR COMPLETING SF 298

The Report Documentation Page (RDP) is used in announcing and cataloging reports. It is important that this information be consistent with the rest of the report, particularly the cover and title page. Instructions for filling in each block of the form follow. It is important to **stay within the lines** to meet **optical scanning requirements**.

Block 1. Agency Use Only (Leave blank).

Block 2. Report Date. Full publication date including day, month, and year, if available (e.g. 1 Jan 88). Must cite at least the year.

Block 3. Type of Report and Dates Covered. State whether report is interim, final, etc. If applicable, enter inclusive report dates (e.g. 10 Jun 87 - 30 Jun 88).

Block 4. Title and Subtitle. A title is taken from the part of the report that provides the most meaningful and complete information. When a report is prepared in more than one volume, repeat the primary title, add volume number, and include subtitle for the specific volume. On classified documents enter the title classification in parentheses.

Block 5. Funding Numbers. To include contract and grant numbers; may include program element number(s), project number(s), task number(s), and work unit number(s). Use the following labels:

C - Contract	PR - Project
G - Grant	TA - Task
PE - Program Element	WU - Work Unit Accession No.

Block 6. Author(s). Name(s) of person(s) responsible for writing the report, performing the research, or credited with the content of the report. If editor or compiler, this should follow the name(s).

Block 7. Performing Organization Name(s) and Address(es). Self-explanatory.

Block 8. Performing Organization Report Number. Enter the unique alphanumeric report number(s) assigned by the organization performing the report.

Block 9. Sponsoring/Monitoring Agency Name(s) and Address(es). Self-explanatory.

Block 10. Sponsoring/Monitoring Agency Report Number. (If known)

Block 11. Supplementary Notes. Enter information not included elsewhere such as: Prepared in cooperation with...; Trans. of...; To be published in.... When a report is revised, include a statement whether the new report supersedes or supplements the older report.

Block 12a. Distribution/Availability Statement.

Denotes public availability or limitations. Cite any availability to the public. Enter additional limitations or special markings in all capitals (e.g. NOFORN, REL, ITAR).

DOD - See DoDD 5230.24, "Distribution Statements on Technical Documents."

DOE - See authorities.

NASA - See Handbook NHB 2200.2.

NTIS - Leave blank.

Block 12b. Distribution Code.

DOD - Leave blank.

DOE - Enter DOE distribution categories from the Standard Distribution for Unclassified Scientific and Technical Reports.

NASA - Leave blank.

NTIS - Leave blank.

Block 13. Abstract. Include a brief (*Maximum 200 words*) factual summary of the most significant information contained in the report.

Block 14. Subject Terms. Keywords or phrases identifying major subjects in the report.

Block 15. Number of Pages. Enter the total number of pages.

Block 16. Price Code. Enter appropriate price code (*NTIS only*).

Blocks 17. - 19. Security Classifications. Self-explanatory. Enter U.S. Security Classification in accordance with U.S. Security Regulations (i.e., UNCLASSIFIED). If form contains classified information, stamp classification on the top and bottom of the page.

Block 20. Limitation of Abstract. This block must be completed to assign a limitation to the abstract. Enter either UL (unlimited) or SAR (same as report). An entry in this block is necessary if the abstract is to be limited. If blank, the abstract is assumed to be unlimited.

**Adsorption and Catalysis on Carbonaceous
Adsorbents - Electronic Factors**

by

Edward George Marchand

A DISSERTATION

Submitted in partial fulfillment of the requirements

for the degree of

DOCTOR OF PHILOSOPHY

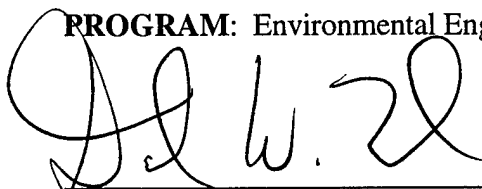
(Environmental Engineering)

MICHIGAN TECHNOLOGICAL UNIVERSITY


1996

This dissertation, "Adsorption and Catalysis on Carbonaceous Adsorbents - Electronic Factors," is hereby approved in partial fulfillment of the requirements for the degree of
DOCTOR OF PHILOSOPHY in the field of Environmental Engineering

PROGRAM: Environmental Engineering

A large, stylized handwritten signature in black ink, appearing to read 'D. W. Hand'.

Dissertation Advisor: Dr. David W. Hand

A handwritten signature in black ink, appearing to read 'John C. Crittenden'.

Chair, Environmental Engineering Ph.D. Committee:
Dr. John C. Crittenden

2/22/96

Date

ABSTRACT

Two carbonaceous adsorbents made from polymeric materials were used in adsorption and catalytic oxidation experiments in the lab and the field. One was a phenol-aldehyde based (Novoloid) fiber, Kuractive, used in a cloth or fabric form. The other was a sulfonated polystyrene divinylbenzene cross-linked polymer adsorbent, Ambersorb® 572. Catalytic oxidation of trichloroethylene (TCE) at 110-250 °C and space velocities of 36,000 to 73 hr⁻¹ (Empty Bed Contact Time, EBCT, 0.1 - 49 s) over plain and transition-metal-oxide impregnated Ambersorb 572 demonstrates the potential for this catalyst/support to convert TCE at low temperatures. The first step in the catalytic process appears to be the addition of a proton from the acid catalysis sites to the TCE, followed by non-specific attacks by the resulting carbenium ion or radical. High conversions were maintained at temperatures as low as 110 °C, although there were numerous by-products. At temperatures above 180 °C the plain adsorbent/catalyst was superior in performance over the metal-impregnated catalysts under the conditions in this study. Water in the feed stream has an immediate, reversible, poisoning effect on the performance of MTU-CAT, a thermally modified Ambersorb 572, and the transition metal-impregnated catalysts used in this study. However, the water poisoning effect was not noticed when the catalyst was the plain support, Ambersorb 572.

Resistive or Joule heating was used to heat both adsorbents. This thermal energy can reduce the local humidity from the incoming gas without heating the entire air stream, regenerate the adsorbent, or provide the activation energy for the oxidation of the desorbing organics on catalyst sites in the adsorbent. At low currents (tens of milliamps at 2-3 V D.C.) the thermal energy applied to the carbon cloth can alter the local relative humidity, favoring adsorption of trichloroethylene over water, increasing the adsorption capacity of the adsorbent by a factor of 4.5 times. However, initial cost estimates favor the use of preheating the air, instead of Joule heating the adsorbent bed, to reduce the relative humidity to maintain high carbon capacities.

Adsorption of organic compounds onto the carbon fibers changes the resistivity of the materials. Different compounds altered the resistance in different ways and at different rates. Methanol, a polar compound, rapidly changed the resistance, while toluene, a non-polar compound, was the slowest to alter the resistance. Trichloroethylene initially decreased the resistivity, and then increased it over time. The change in resistance upon adsorption was found to be concentration dependent. The polarizability of the compound appears to be the key to the rate of change in the resistance. In humidified streams competition for adsorption is evident from the resistance profiles over time. The results of this work lead to the development of an inexpensive analytical device for monitoring the performance of gas-phase adsorption systems.

During a limited study a dynamic electric field (0.5-2 Amps, or 0.4-1.3 W/g) was applied to a catalyst bed of Ambersorb 572 at 180-200 °C. It was found to alter the composition of the effluent of the catalytic oxidation reaction of trichloroethylene (TCE). It is unclear if electrooxidation (transfer of electrons) is responsible or the change is merely a side effect of charging the surface of the adsorbent catalyst under electrodynamic conditions which would impact the stability of the carbenium ion. Under a static electrical field (+1000 V DC) flow-through tests in a lab reactor with TCE and field tests using a contaminated stream from a soil vapor extraction system indicate direct electrooxidation of organics may be occurring.

ACKNOWLEDGEMENTS

First to the U.S. Air Force, for providing the opportunity to participate in the Air Force Institute of Technology Civilian Institute (AFIT/CI) program to obtain a PhD in Environmental Engineering.

The funding for this project was provided by the U.S. Air Force, Environics Division, Tyndall AFB, Florida under the contract No. FO8635-94-00SS (Maj Mark Smith, Project Officer); and Michigan Technological University in the form of waived overhead and graduate student fellowship. In addition, material support was provided by Superior Engineering Technologies, Inc., Houghton MI.

I would like to thank Dr David W. Hand for his guidance and support throughout the project. His willingness to discuss observations from lab tests and implications for applications of the process are especially noteworthy. I would like to thank Dr John C. Crittenden, Dr David J. Chesney (Chemistry), Dr Mike E. Mullins (Chemical Engineering) and Dr Jon A. Soper (Electrical Engineering) who served on my committee, reviewed this work, and put up with many, many questions. Thanks also go to Dr. Howard L. Greene, (Chemical Engineering, Case Western University) for his review and comments on the dissertation. In addition, Dr Anand K. Kulkarni (Electrical Engineering) was instrumental in understanding semiconductors and Dr Sarah Green (Chemistry) on reaction pathways.

I want to thank the students and staff at both the Environmental and Electrical Engineering departments, especially Jeff Schams, Shelle Sandall, Jackie Popko, Mike Dziobak, Dave Perram, Mike Chase, and John Miller, for all their help with equipment and analysis. In addition, thanks go to Volker Selzer for the discussions on conducting polymers.

I thank my wife Gayla, and daughters Sarah, Ann, and Jessica. Without their support, love, and encouragement on the home front, this would have been a most unpleasant undertaking.

Special thanks go to my parents, Geri and George Marchand, for their continued love and support through childhood and over the years, even now that I have a family of my own. Thanks, Dad, for your interest in this work and for our discussions about it.

Finally (why do we save the most important for last?) I wish to thank God for His grace and goodness. With His help I have overcome major obstacles. All praise and honor for this work are to Him who has redeemed my soul.

CONTENTS

ABSTRACT	i
ACKNOWLEDGEMENTS	iii
LIST OF FIGURES	vi
LIST OF TABLES	viii
PREFACE	ix
Chapter 1. Introduction	1
1.1 Background	1
1.2 Targeted Toxic Chemical Sources	2
1.3 Gas Phase Adsorption	2
1.4 Catalysis	3
1.5 Electronic Factors of Gas Phase Adsorption and Catalysis	4
1.6 Joule Heating	5
1.7 Objectives	5
1.8 References	7
Chapter 2. Catalytic Oxidation of Trichloroethylene over Carbonaceous Adsorbents	9
2.1 Introduction	9
2.2 Materials and Methods	11
2.2.1 Catalyst Impregnation Procedures	12
2.2.2 Experimental Reactor Design	13
2.2.3 Ambersorb 572 Characteristics	17
2.2.4 Formation and Characterization of MTU-CAT	17
2.3 Results and Discussion	18
2.3.1 AM 572-P	21
2.3.2 MTU-CAT	23
2.3.3 Metal-Impregnated Ambersorb 572	29
2.3.4 Electric Field Affects Catalytic Oxidation on MTU-CA ...	34
2.3.5 Electric Field Affects Catalytic Oxidation on AM572-P ...	37
2.4 Conclusions	40
2.5 Acknowledgements	41
2.6 References	41
Chapter 3. Adsorption and Destruction of Trichloroethylene on Carbonaceous Adsorbents Under Applied Electric Fields	44

3.1	Introduction	44
3.2	Materials and Methods	47
3.2.1	Adsorbent Characteristics	51
3.2.2	Field Site Description	52
3.3	Results and Discussion	53
3.3.1	Carbon Cloth Capacities for TCE	53
3.3.2	Joule Heating	55
3.3.3	Joule Heating of Activated Carbon Cloth	55
3.3.4	Joule Heating of Amborsorb 572	57
3.3.5	Electric Field Influences on Regeneration	58
3.3.6	Electrostatic Field Affects over Carbon Cloth	61
3.4	Conclusions	62
3.5	Acknowledgements	64
3.6	References	64
Chapter 4.	Electronic Factors of Adsorption on Carbon Fibers	68
4.1	Introduction	68
4.2	Materials and Methods	72
4.3	Results and Discussion	73
4.3.1	Adsorbent Characteristics	73
4.3.2	Resistance Change Upon Adsorption	80
4.3.3	Applications	87
4.4	Conclusions	89
4.5	Acknowledgements	90
4.6	References	90
Chapter 5.	Overall Conclusions and Recommendations	93
Appendix A.	Raw Data from Adsorption/Desorption Analysis from PMI Inc. (Ithaca, NY) for Amborsorb 572 & MTU-CAT	96
Appendix B.	Quattro Pro Spreadsheets with Data for the Figures Used in this Dissertation	144
Appendix C.	Additional Information on Thermal Catalysis of Trichloroethylene over Transition Metal Impregnated Amborsorb 572	174

LIST OF FIGURES

Figure 2-1. System Setup	14
Figure 2-2. Annular Reactor Design	16
Figure 2-3. Gas Volume vs P/Po: (a) AM572-P; (b) MTU-CAT	19
Figure 2-4. BET Adsorption/Desorption Isotherm Data, Delta V/Delta D vs Pore Diameter	26
Figure 2-5. Elemental Analysis of the Materials used in the Oxidation of TCE	28
Figure 2-6. Organic Concentrations vs Time; EBCT=17s, 1 atm, 1500 ppmv Feed	31
Figure 2-7. Hypothetical Micropore in an Electric Field	38
Figure 2-8. CCl ₄ Effluent over AM572-P under Dynamic Electric Field in Annular Reactor	39
Figure 3-1. Annular Reactor Design	49
Figure 3-2. Experimental Setup	50
Figure 3-3. Cloth Isotherms at 38 °C in TCE Flow Cell	54
Figure 3-4. Humidity/Joule Effect on Carbon Cloth, 15 ppmv TCE humid feed, 1 atm, EBCT=0.1s	56
Figure 3-5. Electrostatic Charge on Fiber Induces Charge in Crystallites within Carbon Fibers	63
Figure 4-1. Electron Paths in Graphitic Planes and Crystallites in Cloth Fibers ..	70
Figure 4-2a. Resistance Isotherm Setup for Cloth	74
Figure 4-2b. Dynamic Resistance Isotherm Setup for Cloth	75
Figure 4-3. Resistance vs Temperature for Carbon Materials	77
Figure 4-4. Dynamic Isotherm of TCE with Dry Feed (15, 500, and 1500 ppmv) and Resistance Changes on Activated Carbon Cloth ...	82

Figure 4-5. 1500 ppmv TCE Humid Feed Loading in Flow Cell over Carbon Cloth	83
Figure 4-6. Resistance Change upon Adsorption of Six Compounds on Activated Carbon Cloth	85
Figure 4-7. Resistance Changes in Mixtures of TCE and Water over Carbon Cloth	88

LIST OF TABLES

TABLE 2-1. PHYSICAL PROPERTIES OF AMBERSORB 572	17
TABLE 2-2. OPERATING CHARACTERISTICS OF AM-572-P EXPERIMENTS	22
TABLE 2-3. OPERATING CHARACTERISTICS OF INITIAL MTU-CAT EXPERIMENTS	24
TABLE 2-4. SURFACE AREA ANALYSIS RESULTS FOR VIRGIN AMBERSORB 572 AND MTU-CAT AFTER THE 11 DAY INITIAL EXPERIMENTS	25
TABLE 2-5. GC/MS ANALYSIS OF METHANOL EXTRACT OF MTU-CAT	27
TABLE 2-6. OPERATING CHARACTERISTICS OF COBALT (-Co) AND MANGANESE (-Mn) IMPREGNATED AMBERSORB 572	30
TABLE 2-7. OPERATING CHARACTERISTICS OF TITANIUM IMPREGNATED AMBERSORB 572	33
TABLE 2-8. TEST CONDITIONS DURING ELECTROCATALYSIS RUNS. .	35
TABLE 3-1. ADSORBENT CHARACTERISTICS	52
TABLE 3-2. TEST CONDITIONS DURING JOULE HEATING EXPERIMENTS	59
TABLE 4-1. CHARACTERISTICS OF ACTIVATED CARBON MATERIALS	69
TABLE 4-2. CHEMICAL CHARACTERISTICS OF SIX COMPOUNDS	86

PREFACE

This dissertation was written as a series of papers to be published in appropriate professional journals. As such, Chapters 2, 3, and 4 are written to stand alone and contain duplicative information, especially about the materials and methods used in the experiments.

Appendix A contains the raw data from the nitrogen adsorption/desorption BET done by Porous Materials Inc., (Ithaca, NY). Appendix B contains all the Quattro Pro spreadsheets giving the data supporting the figures. Appendix C contains supplemental information on the catalytic oxidation over the metal oxide impregnated catalysts. The information is summarized in Chapter 2 to keep it to a reasonable length as a publishable paper.

Mention of trademarks and trade names of material and equipment does not constitute endorsement or recommendation for use by the U.S. Air Force, nor can this dissertation be used for advertising the product(s).

This dissertation was written using the following software tools: Harvard Graphics, Quattro Pro, and Word Perfect.

Chapter 1

Introduction

1.1 BACKGROUND

Industrial and remediation processes generate large quantities of air contaminated with organics. The U.S. Environmental Protection Agency (EPA) estimated 1.22 billion pounds of organics were released from point and non-point sources to the air in 1993 from U.S. facilities (US EPA, 1993). Clean Air regulations promulgated by the EPA place limits on the types and amounts of organics that can be released to the environment. Control technologies, especially for dilute waste streams with chlorinated organics, can be expensive and become the major cost involved with the process. At a groundwater contamination site the fuel costs for the catalytic oxidation unit used to treat the air stripper off-gas was almost 80% of the total utilities cost of \$0.36/1000 gallons water treated (Hylton, 1992).

Technologies currently used to limit the release of the organics to the air include gas phase adsorption onto granular activated carbon (GAC) or combustion, either in a direct flame incinerator at high temperatures ($>2000\text{ }^{\circ}\text{C}$) or over a catalyst at moderate temperatures ($200\text{--}500\text{ }^{\circ}\text{C}$). If carbon is used it must periodically be replaced or regenerated, with the resulting stream requiring further treatment/disposal. In combustion systems higher temperatures and/or longer time in the reactor (residence time) allow for complete conversion of the chlorinated organics to water and mineral acids such as HCl. This complete destruction is referred to as mineralization. Partial conversion of the molecules can result in products that are more toxic than the parent compound (such as phosgene from the oxidation of trichloroethylene).

1.2 TARGETED TOXIC CHEMICAL SOURCES

The sources of chemicals are almost as varied as the number of chemicals in existence. The sources targeted for this research work are from the equipment operation/maintenance processes and remediation efforts at a typical Air Force Base. Volatile organic compounds (VOCs) released from these operations require off-gas control. The compounds and the processes include 1) engine cleaning compounds from a cleaning vat, 2) paint booth vapors from an exhaust unit, or 3) chlorinated and non-chlorinated VOCs from remediation processes to clean up contaminated soils and groundwater. Due to the focused regulatory attention on chlorinated organics, trichloroethylene (TCE) was chosen as a representative compound for this research.

1.3 GAS PHASE ADSORPTION

Gas phase adsorption occurs on the surface and in the pores of the adsorbent. The adsorbate (the substance being adsorbed) is held by a combination of Van der Waals and electrostatic forces. The adsorption sites have a wide range of energy and adsorption occurs at the high energy sites first (Sontheimer et al 1988). In small pores the electrostatic fields from the adsorbent overlap and condensation of the gas into the pores is possible. This capillary condensation can dramatically increase the capacity of a given adsorbent. At higher contaminant concentrations (e.g. at higher partial pressures of contaminant, like water at high relative humidity) the adsorbent is more likely to form condensed films as the less energetic sites are filled. In addition, different molecules with different dipole moments and sizes will have different affinities for the various adsorbents.

The adsorbent capacities for the organic of interest are affected by several factors. At increased temperature the capacity is reduced. In fact, thermal processes are the primary way to regenerate adsorbents. Water will also compete for the adsorption sites and reduce the capacity of the adsorbent. A common way to reduce the relative humidity is to pre-heat the incoming air. This has been shown to be a cost-effective option on air stripping operations (Crittenden et al, 1988).

1.4 CATALYSIS

Catalysis is a broad classification for reactions taking place where one of the participating species is not consumed or created, but rather can go on to continue the reaction. In combustion work it is primarily the thermal energy that activates the catalysts. The activated catalyst particles are usually dispersed on supports and the contaminated gas flows over them (similar to a catalyst bed in an automobile).

Other types of catalysis include photocatalysis where the light energy activates the catalyst or electrochemical catalysis (or electrocatalysis) where an applied potential aides in the reaction. Two areas this work focuses on is thermal catalysis and the enhancement (or depression) of the activity and/or selectivity of the catalyst by an external electric field.

In reactors where a catalyst surface is involved, like the car exhaust unit, a term called "heterogeneous" is used to describe the system. This is because the contaminant must diffuse from the bulk gas to the surface, adsorb onto the surface, react on the surface to create the desired end products, desorb the products from the surface, and, finally, diffuse the products away from the catalyst.

Using a carbonaceous-based catalyst researchers (Petrosius and Drago, 1992, Petrosius et al, 1993) effectively destroyed methylene chloride and other chlorinated compounds at temperatures below 300 °C. They found that the activity of the catalyst was enhanced with the addition of transition metal (Mn, Co, Ti) oxides. This research extended their work to include the oxidation of trichloroethylene using the same base material and metal oxides.

1.5 ELECTRONIC FACTORS OF GAS PHASE ADSORPTION AND CATALYSIS

The phenomenon of adsorption and heterogeneous catalysis rely on the molecule coming in contact with the surface. The nature of the electronic states within the surface and the molecules have direct bearing on the outcome of the collision. The electron cloud of the molecule can be distorted by the surface inducing a dipole within the molecule. As the molecule approaches the surface the potential energy of the molecule decreases due to the attraction of the mutually induced dipole moments. The distortion can be sufficient to allow a transfer of electrons, chemisorbing the molecule to the surface. This loss or gain of electrons by the adsorbate increases the reactivity of the adsorbed species. At surfaces with sufficient energy further reactions can occur with these radicals causing a change in the molecular form. The desired change is usually the loss of electrons from the parent molecule, oxidizing it to benign substances. Thus the electron, and its state, are key to these processes whether they are in the molecule or on the surface. With chemisorption of adsorbates over semiconductors, Vol'kenshtein (1963) described the process in terms of band bending. With a "clean" surface the bands of the semiconductor are the same in the bulk as on the surface. When a molecule chemisorbs to the surface, the energy band of the surface bends toward the band of the molecule. Each molecule adsorbed bends the bands an incremental amount until, at equilibrium, the bands are equal and adsorption ceases.

Holder (1970) evaluated the effect of an electrostatic field on the liquid-phase adsorption capacity of a bed of activated carbon. Using potentials from 0 to 25,000 V, he found a range of responses. The capacity of the activated carbon for urea was not altered, while the capacity for n-butyraldehyde increased by 113 percent at 16,000 V. Benzene and phenol capacities increased by 35 percent. Woodard et al. (1986) used flow through carbon fiber electrodes in aqueous streams to evaluate the electrosorption of various charged and neutral compounds. They found the adsorption process to be well described by a Freundlich isotherm and suggest using electrosorption for separating out small, functionalized organic molecules such as amino acids and proteins.

Gas phase electrosorption on semiconductors also occurs. Hoenig and Lane (1968) studied the oxygen uptake onto the n-type semiconductor ZnO. At +150 VDC there was little effect. At +300 V DC there was a drop in oxygen pressure, indicating adsorption onto the surface. Oxygen adsorption onto epitaxial β -HgS films under high fields (10^5 V/cm) was shown by Ivankiv and Muzychuk (1968). As the field increased to 4×10^5 V/cm, the conductivity increased monotonically until saturation of the surface occurred.

Adsorption itself can change the properties of the adsorbent. Researchers (McLintock and Orr, 1968; McIntosh et al. 1947) found that adsorption of gases onto carbon films and rods altered the bulk resistance of the materials. Others (Blackwood and Josowicz, 1991) showed the same effect for conductive polymers. The polymers contain conductive crystallites and non-conductive amorphous regions and the electrical conduction is by hopping from one crystallite to another, even up to 7 Å apart (Thakur and Elman, 1989). No information was available in the literature on the resistance changes upon adsorption for the carbonaceous adsorbents used in this research.

1.6 JOULE HEATING

In electrically conductive materials the electron flow may be impeded by the molecules in the lattice. The energy loss due to this "friction" is converted to heat. The more electrons flowing (i.e. the larger the current) the more collisions and the more heat generated. This heat is generated within the matrix of the material and a bed heated in this manner is heated from the inside out. Irregular shapes and/or impurities in the adsorbent will give rise to preferential pathways in the bed, creating a potential for "hot" spots. Synthetic adsorbents of regular, uniform size, shape, and consistency should be ideal for minimizing these preferential pathways.

1.7 OBJECTIVES

In this research three related areas were focused on to address the control of chlorinated organics from gaseous waste streams. The first was to look at the catalytic

oxidation properties of Ambersorb 572. It has surface areas similar to GAC, but is much stronger than GAC and can be regenerated in-situ. The material was used plain and impregnated with metal oxides of cobalt, titanium, and manganese.

The second area involved electric fields across two different adsorbents, Ambersorb 572 and an activated carbon cloth. The focus was on influencing the adsorption and catalysis reaction to increase capacity or lower the activation energy (operating temperature) of the catalysts, respectively. Dynamic (current flowing) conditions caused the adsorbent beds to heat up due to the Joule heating effect. The last area involved the resistance changes the activated carbon cloth undergoes upon adsorption of organic contaminants.

Specific objectives for this work include:

A) Evaluating the Ambersorb 572 adsorbent, both plain and impregnated, as catalysts in the oxidation of TCE at temperatures below 250 °C.

B) The impact of electric fields on adsorption on activated carbon cloth, and the impact of electric fields on the catalytic reactions over Ambersorb 572 (plain and impregnated).

C) Determine the resistance change upon adsorption on the carbon cloth for seven compounds. Evaluate the impact of concentration on the resistance change for trichloroethylene on the carbon cloth.

D) Field demonstrate a lab-scale system at a contaminated Air Force site.

1.8 REFERENCES

Blackwood, D., and Josowicz, M., "Work Function and Spectroscopic Studies of Interactions between Conducting Polymers and Organic Vapors," *Journal of Physical Chemistry*, 95, pp 493-502, 1991.

Crittenden, J.C., Cortright, R. D., Rick, B., Tang, S-R., and Perram D.L., "Using GAC to Remove VOCs From Air Stripper Off-Gas," *Journal of American Water Works Association*, pp 73-84, May 1988.

Hayes, J.S., "Novoloid Nonwovens," *Nonwoven Symposium*, TAPPI Press, pp. 257-263, April, 1985.

Hoening, S.A., and Lane, J.R., "Chemisorption of Oxygen on Zinc Oxide, Effect of a DC Electric Field," *Surface Science*, 11, pp 163-174, 1968.

Holder, W.D., "The Effect of an Electrostatic Field on the Adsorption Capacity of a Fixed-Bed of Activated Carbon," Masters Thesis, Chemical Engineering, Clemson University, 1970.

Hylton, T.D., "Evaluation of the TCE Catalytic Oxidation Unit at Wurtsmith Air Force Base," *Environmental Progress*, Vol. 11, No. 1, pp 54-57, Feb 1992.

Ivankiv, L.I., and Muzychuk, A.M., "Adsorption on a Semiconductor Surface in an Electric Field," *Russian Journal of Physical Chemistry*, 42, (2), pp 223-225, 1968.

McIntosh, R., Haines, R.S., and Benson, G.C., "The Effect of Physical Adsorption on the Electrical Resistance of Activated Carbon," *The Journal of Chemical Physics*, Vol 15, No. 1, pp 17-27, Jan. 1947.

McLintock, I.S., and Orr, J.C., "The Effect of Oxygen Adsorption on the Electrical Resistance of Evaporated Carbon Films," *Carbon*, Vol 6, pp 309-323, 1968.

Petrosius, S.C., and Drago, R.S., "Decomposition of Chlorinated Hydrocarbons Using Metal Oxides Supported on Carbonaceous Adsorbents," *J. Chem. Soc., Chem. Commun.*, 1992, pp 344-345.

Petrosius, S.C., Drago, R.S., Young, V., and Grunewald, G.C., "Low-Temperature Decomposition of Some Halogenated Hydrocarbons Using Metal Oxide/Porous Carbon Catalysts," *Journal of the American Chemical Society*, 115, pp 6131-6137, 1993.

Sontheimer, H., Crittenden, J.C., and Summers, S., "Activated Carbon for Water Treatment," 2nd Edition, DVGW-Forschungsstelle, Engler-Bunte-Institut, Karlsruhe University, 1988

Thakur, M., and Elman, B.S., "Optical and Magnetic Properties of a Nonconjugated Conducting Polymer," *Journal of Chemical Physics*, **90** (3), pp 2042-2044, 1 Feb 1989.

US Environmental Protection Agency, (EPA) Toxic Release Inventory: Air Emissions of Hazardous Air Pollutants, 1993, found at WWW URL "http://earth1.epa.gov/TRI_93/chap1/".

Vol'kenshtein, F.F., "The Electronic Theory of Catalysis on Semiconductors," translated by Anderson, N.G., translation edited by Birch, E.J. H., A Pergamon Press Book, The Macmillan Company, New York, 1963.

Woodard, F.E., McMackins, D.E., and Jansson, R.E.W., "Electrosorption of Organics on Three Dimensional Carbon Fiber Electrodes," *Journal of Electroanalytical Chemistry*, **214**, pp 303-330, 1986.

Chapter 2

Catalytic Oxidation of Trichloroethylene over Carbonaceous Adsorbents

2.1 INTRODUCTION

Industrial and remediation processes generate large quantities of air contaminated with organics. An estimated 1.22 billion pounds of organics are released to the air each year from U.S. facilities (USEPA, 1993). Clean Air regulations promulgated by the U.S. Environmental Protection Agency (EPA) place limits on the types and amounts of organics that can be released to the environment. Chlorinated organics, specifically trichloroethylene (TCE), were targeted for destruction in this study because of their suspected toxicity and because of the large quantity of TCE being released to the atmosphere (in the top ten, based on quantity released, on the USEPA, 1993 list).

Technologies currently used to limit the release of the organics to the air include gas phase adsorption onto granular activated carbon (GAC) and combustion, either in a direct flame incinerator at high temperatures ($>2000\text{ }^{\circ}\text{C}$) or over a catalyst at moderate temperatures ($200\text{--}500\text{ }^{\circ}\text{C}$). An example of a catalytic unit is one evaluated by Hylton (1992). It utilizes a chromia oxide catalyst in a fluidized bed and operates at an Empty Bed Contact Time (EBCT) of 0.5 s at $370\text{ }^{\circ}\text{C}$ to achieve a 97 percent conversion of trichloroethylene (TCE). Higher temperatures and/or longer time in the reactor (residence time) allows for complete conversion or mineralization of the chlorinated organics to water and mineral acids such as HCl. Partial conversion of the molecules can result in products that are more toxic than the parent compound (e.g. phosgene, COCl_2). By-products of combustion are unwanted but may be tolerable if they are benign.

Destruction of gaseous by-products from automobile exhaust fueled much of the early catalysis research, leading to catalyst beds with mixtures of precious metals finely dispersed on high surface area ceramic supports. High surface area polymer catalysts are

important in industry, especially the fuel additives industry (Al-Jarallah et al, 1988). However, the focus on using them for catalytic oxidation reactions to mineralize organic pollutants has only recently been reported (Petrosius and Drago, 1992, Petrosius et al, 1993).

Petrosius and Drago (1992) evaluated a number of metal oxides on Ambersorb[®] adsorbent supports as well as Ambersorb 563 & 572 alone for oxidation of methylene chloride (250 °C, EBCT=240 s for all experiments). While the supports alone are quite active (68 and 78 percent conversion), a chromium oxide catalyst impregnated onto the surface increases the conversion to 99.9 percent. Titanium dioxide (TiO₂) on Ambersorb 572 showed a 93 percent conversion and a cobalt oxide catalyst also on Ambersorb 572 showed a 75 percent conversion.

In subsequent work the same group (Petrosius et al, 1993) reported the decomposition of several halogenated hydrocarbons over the same types of supports/catalysts at the same conditions (250 °C, EBCT=240 s). They found a 16 percent conversion of tetrachloroethylene (PCE) in humidified air over a chromia oxide impregnated Ambersorb 572 catalyst/support. On plain Ambersorb 563, carbon tetrachloride (CCl₄) conversion in dry air dropped from 73 to 5 percent in 120 hours. By adding water the conversion rose to 47 percent at the 170 hour mark. In other experiments they also noted a 67 percent decrease in the conversion percentage of methylene chloride when the flow was increased by a factor of 5 (EBCT from 240 s to 49 s) with dry feed at 250 °C.

Since the catalytic oxidation process involves electron exchange, it was thought that an applied electric field would alter the process, possibly reducing the activation energy of the reaction. This would in turn reduce the thermal energy requirements for a given conversion. Dynamic fields (current flowing) were passed through beds of reactive Ambersorb 572 to test this hypothesis.

In this research an evaluation was made on the impact of operating the catalysts at low temperatures and short residence times on the catalytic oxidation of TCE from gas streams using transition metal impregnated and non-impregnated Ambersorb 572 adsorbent/catalysts. In addition, the impact of an applied electric field was also evaluated. The impact of the flow rate, catalyst type, and current type (AC or DC) was also evaluated.

2.2 MATERIALS AND METHODS

All chemicals used in the experiments and analyses were reagent grade or better. Reagent grade dichloromethane (99.9+%), titanium (IV) chloride (99.995+%), sodium persulfate, methanol, sodium hydroxide, sulfuric acid, cobalt and manganese nitrates, and potassium permanganate, were purchased from Aldrich Chemical Company (Milwaukee, WI). Water for the bubblers came from a Milli-Q[®] station (Millipore, Molsheim, France) in the lab. TCE in dry nitrogen (500 parts per million by volume [ppmv]) was purchased from Scott Specialty Gas Company (Riverside, CA). TCE in dry air (15 & 1500 ppmv) were purchased from Matheson Gas Products (Joliet, IL). The Ambersorb 572 adsorbent (40x60 mesh, Lot No:923318) was purchased from the Rohm and Haas Company (Philadelphia, PA). All carrier gases including air, argon, helium, nitrogen were ultra-pure and purchased from Interstate Gas Company (Marinette, MI).

On-line gas-phase samples were taken every two hours by an automated sampler and analyzed according to the Environmental Protection Agency's Reference Method 23 (Scott Environmental, 1983) using a Hewlett Packard Model 5890 Series II gas chromatograph equipped with a flame ionization detector (FID) and an electron capture detector (ECD). Compound separation was performed using a stainless steel VOCOL[™] (Supelco, PA) column 60 m long by 0.75 mm diameter with a 1.5 μ m film. The gas samples passed through heated stainless steel lines into a six-port valve (Model RD6P, Valco) that was heated to 160 °C (Valco Instrumentation Temperature Controller). A 0.5 cm³ sample loop attached to the six-port valve provided a gas sample size that yielded a TCE detection limit of about 1 ppm using the FID and about 10 ppb with the ECD. All

reaction efficiencies reported in this study are steady-state conversions, unless otherwise noted.

Two bubblers were used to trap chlorine and sulfur compounds after the 6-port valve. The first in series contained Milli-Q[®] water to trap chloride and sulfate ions and the second trap had sodium persulfate to trap chlorine gas. Chloride and sulfate ions were analyzed using an isocratic elution of anions with a 21mM NaOH solution (flowrate 1ml/min), on a Dionex DX-500 Ion Chromatograph (Dionex Corp., Sunnyvale, CA) equipped with an Ionpac AG11 guard column (4 mm), an Ionpac AS11 analytical column (4 mm), and a Dionex CD20 conductivity detector.

Periodic effluent samples from the gas-phase catalytic reactor were taken to identify by-products, especially chlorinated species not trapped by the water/sodium persulfate bubblers. These were bubbled through dichloromethane (DCM) and the DCM was then analyzed with a Hewlett Packard Model 5970B mass selective detector with electron impact ionization controlled by a Hewlett Packard 5990C Chemstation data system (Hewlett Packard, Minneapolis, MN). A DB1701 (14% cyanopropylphenyl-methylpolysiloxane) capillary column (30 m length, 0.25 mm ID, narrow bore, 0.25 micron film thickness) was used to separate the compounds (J&W Scientific, Folsom, CA). One milliliter per minute of helium was used as the carrier gas. From an initial temperature of 35 °C, the oven temperature was ramped to 230 °C at a rate of 5 °C/min and kept there for a period of six minutes. The injection port and detector temperatures were maintained at 250 °C. The total ion chromatograph plot was generated by scanning masses between 30-800 amu. The fluid from the methanol (solvent) extraction of the exposed catalyst (MTU-CAT) was also analyzed on the HP 5970B under the same program conditions.

2.2.1 Catalyst Impregnation Procedures

The following procedures were used to impregnate oxides of cobalt, manganese and titanium onto plain Ambersorb 572 (AM 572-P). Impregnation of these

metal oxides onto the AM 572-P was carried out using the incipient wetness technique outlined by Petrosius et al. (1993) except as noted below. Solutions of cobalt and manganese nitrate salts or TiCl_4 were added separately to 100 gram lots of the adsorbent. The catalysts were loaded to 14 percent by weight metal/dry gram of adsorbent. The solutions were added from a buret drop-wise until a volume equal to the pore volume of the resin was added. Water and dichloromethane were used to make up the remaining volume requirements for the cobalt/manganese nitrates and TiCl_4 solutions, respectively. The impregnated resin was wet in appearance but there was no separate liquid phase. The titanium tetrachloride impregnated adsorbent was allowed to react with the room humidity to form titanium dioxide. An X-ray diffraction of TiO_2 residue mixed the same way, but allowed to evaporate in a glass vial, indicated over 95 percent of the material was in the anatase crystal form. Therefore, we assume that the TiO_2 on the impregnated adsorbent is anatase which is thought to be more catalytically active. The other materials were heated overnight at 180 °C in an oven (Isotemp Oven Model 655G, Fisher Scientific) under a vacuum supplied by a pump external to the oven. The Co and Mn impregnated adsorbents were then heated in separate batches under nitrogen at 360 °C for 12 hours to remove the nitrates. The catalysts were transferred to 125 ml Erlenmeyer flasks and capped until used.

2.2.2 Experimental Reactor Design

The experimental set-up is displayed in Figure 2-1. TCE in air was metered from pressurized tanks through the reactor followed by a chloride ion trap and exhausted to a fume hood. An optional water bubbler at room temperature was placed before the reactor to provide a humidified air stream (Relative Humidity, R.H., was about 45 percent). Valves were placed before and after the reactor to monitor the TCE concentration. The reactor was wrapped with heat tape to control the temperature of the reactor. A small thermocouple was placed inside the reactor, near the middle of the bed to monitor the temperature. A second thermocouple was placed outside the bed, under the heat tape wrapping to monitor the exterior temperature. Two bubblers were placed at the end of the effluent line, one containing Milli-Q® water for trapping chloride and sulfate

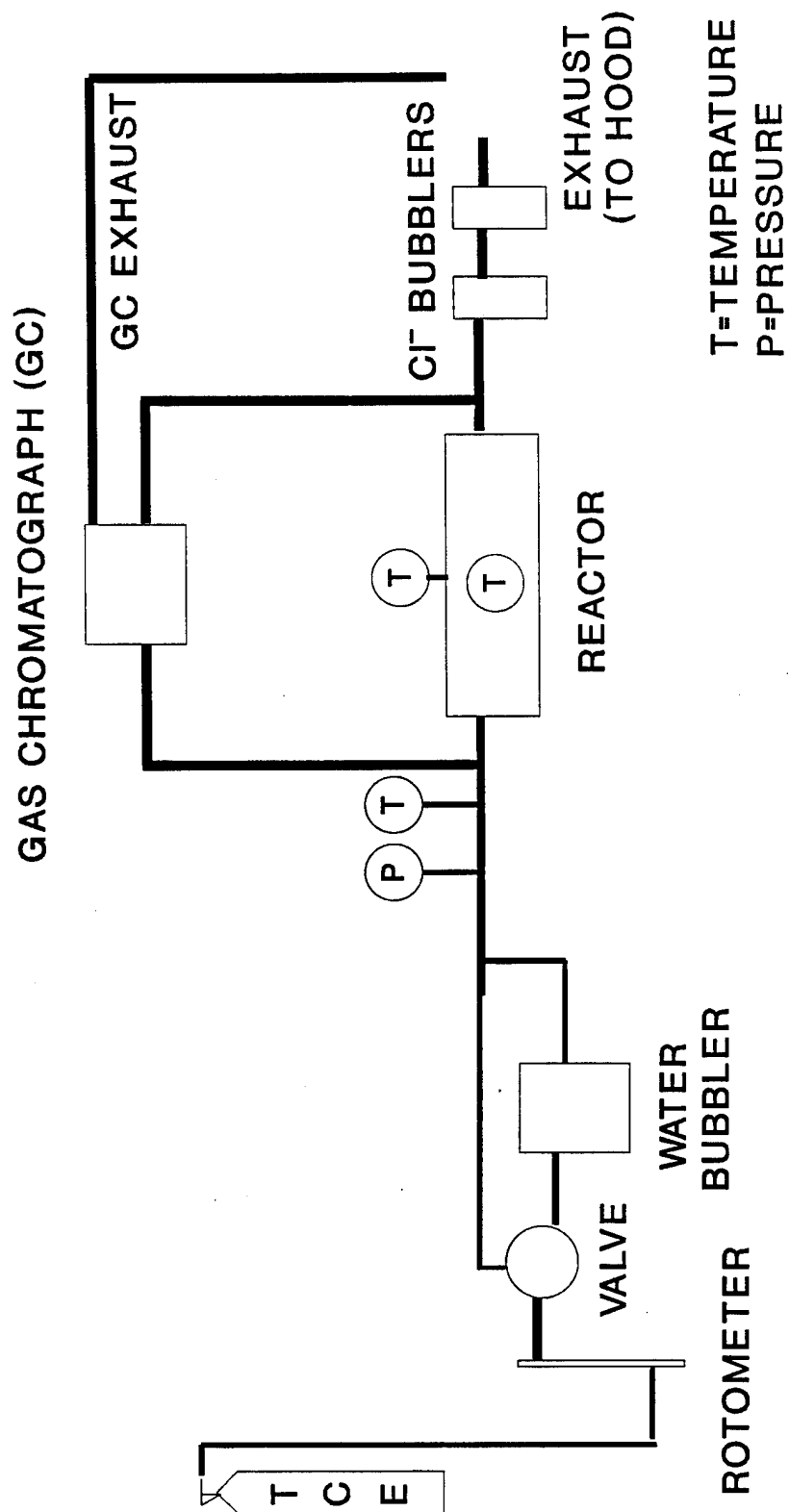


Figure 2-1. System Setup

ions, and the other containing saturated sodium persulfate solution for trapping the chlorine gas. The packed-bed reactor consisted of either a 1.5 inch I.D. by 6 inches long carbon steel column or a glass tube (1/4 inch OD; 1/8 inch ID). Due to the adsorption potential of the catalyst support, some experiments were conducted with materials that were loaded to capacity at room temperature. These are referred to as "pre-loaded" adsorbent/catalysts in this paper.

The oxidation reactor, shown in expanded form in Figure 2-2, was used for all experiments - thermal only and those with an applied electric field. The graphite rod (The Carbide/Graphite Group, Inc., St. Marys, PA; no part or lot number) in the center of the reactor was 1/8 inch in diameter and extended to within 1/2 inch of the bottom. A section of conductive, activated carbon cloth ("Kuractive," FT 200-15, Lot # FK 622096-1B) was used in the bottom of the reactor to keep the adsorbent/catalyst from falling out of the reactor. Electrical isolation was accomplished with Teflon® tape and glass tubing connectors.

All the gas flow rates reported herein are based on 1 atm and 22 °C unless otherwise stated. The empty bed contact times ($EBCT = \text{volume of catalyst bed} / \text{volumetric flow rate}$) or the space velocities ($EBCT^{-1}$) are based on the flow rate at 22 °C. The pressure drop across the bed at the different flowrates used in this study changed by less than 0.5 psi and did not significantly alter the vapor phase concentration.

The term conversion is determined by the amount of TCE in the exit stream as compared to the amount in the feed stream as indicated by the GC. A 100 percent conversion is defined as the complete loss of the TCE in the effluent. Mineralization is defined as the amount of HCl or Cl_2 found in the traps as compared to that which is expected from stoichiometry. A 100 percent mineralization level indicates that all of the available incoming chlorine is accounted for in the traps. Sometimes TCE that is pre-adsorbed on the adsorbent/support will come off and be mineralized in addition to that being fed to the reactor. Under these conditions it is possible to have a mineralization percentage greater than 100 percent.

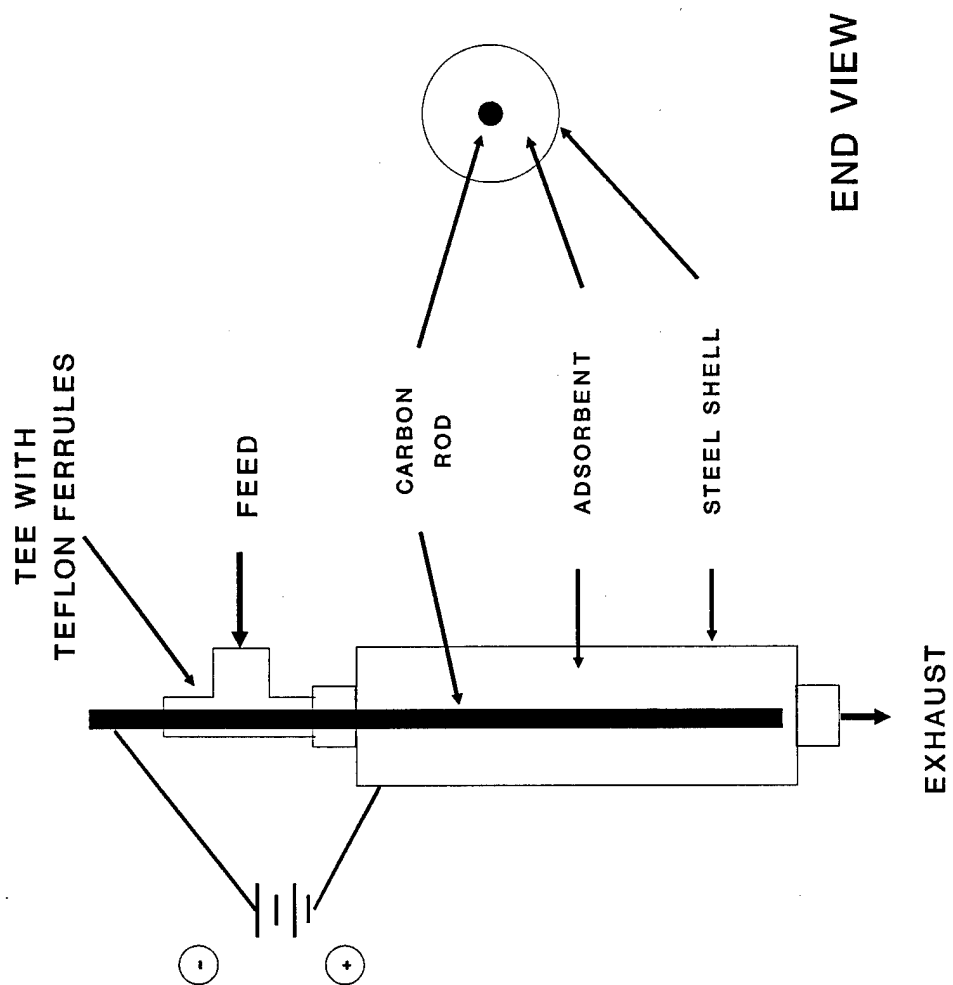


Figure 2-2. Annular Reactor Design

Catalyst support characterizations were evaluated by observing the changes in the surface area as determined by BET analysis and also by direct elemental analysis of the material before and after exposure to the TCE stream to be treated. These support analyses were performed by Porous Materials, Inc. (Ithaca NY) and Huffman Laboratories, Inc. (Golden CO), respectively.

2.2.3 *Ambersorb 572 Characteristics*

The plain Ambersorb adsorbent (AM-572-P) has the characteristics shown in Table 2-1. The material is a highly sulfonated styrene divinylbenzene macroreticular ion exchange resin that is pyrolyzed in a patented process (Rohm and Haas, 1992). An elemental analysis revealed that the material is 1.45 weight percent (± 0.1 percent) sulfur. If each sulfur atom forms a $-\text{SO}_3\text{H}$ group, and if there is a three-dimensional node of seven $-\text{SO}_3\text{H}$ groups forming one catalyst site (Wesley and Gates, 1974), then there are approximately 4×10^{19} sites per gram of material. Turnover numbers (moles reacted per minute/mole of catalyst sites) ranged from 0.2 to 0.002 in this study.

TABLE 2-1. PHYSICAL PROPERTIES OF AMBERSORB 572[†]

Surface Area m ² /g	Microporosity (<20 Å) ml/g	Mesoporosity (20-500 Å) ml/g	Macroporosity (>500 Å) ml/g	Particle Size	Bulk Density g/cc
1100	0.41	0.19	0.24	20 to 50	0.49

[†] - As reported by Rohm and Haas (1992).

2.2.4 *Formation and Characterization of MTU-CAT*

While using an experimental heating process the Ambersorb 572 base material was converted into MTU-CAT. The heating process utilizes electrical energy to resistively (Joule) heat the adsorbent. As the current flows through the bead particles the

electrons impact the lattice of the adsorbent heating it. The current flows around the pores and the actual electron path inside a bead may be quite tortuous. If large currents are used (e.g. using 1.3 Amps/cm² to make MTU-CAT) then areas inside the particles with small cross sections may carry a large current load. This current load may be sufficient to burn away portions of the material, even though the bulk bed temperature remains below the thermal limits of the material.

Evidence for this morphological change in the MTU-CAT material is indicated by the adsorption/desorption BET analysis data shown in Figure 2-3. The hysteresis loop in the plain Ambersorb 572 is a Brunauer, Deming, Deming, and Teller (BDDT) Type IVa isotherm which is indicative that the material possesses straight walled pores (e.g. vertical wells) as the pore shape (Gregg and Sing, 1982). The MTU-CAT shows that these vertical wells still exist, but the separation of the adsorption and desorption lines suggest that slits are formed in the material, similar to a BDDT Type IVb isotherm. One possible way for the slits to form is the electrolytic melting of the material between two adjacent wells. Another possibility is the physical separation of the graphitic planes within the polymer matrix. Additional catalyst sites, differing in performance from the plain material, may have been created in the slits.

2.3 RESULTS AND DISCUSSION

The polymer matrix supports -SO₃H groups on the surface that form acid catalyst sites. These sites can be ion exchanged and the rate of the acid-catalyzed reaction is dependent on the concentration of the -SO₃H sites. When the -SO₃H population is dense then they form clusters. These clusters then behave in a manner similar to catalysis in concentrated acid solution. The polymer would then be able to solvate and stabilize reactive intermediates such as carbenium ions, with the following suggested structure (Wesley and Gates, 1974):

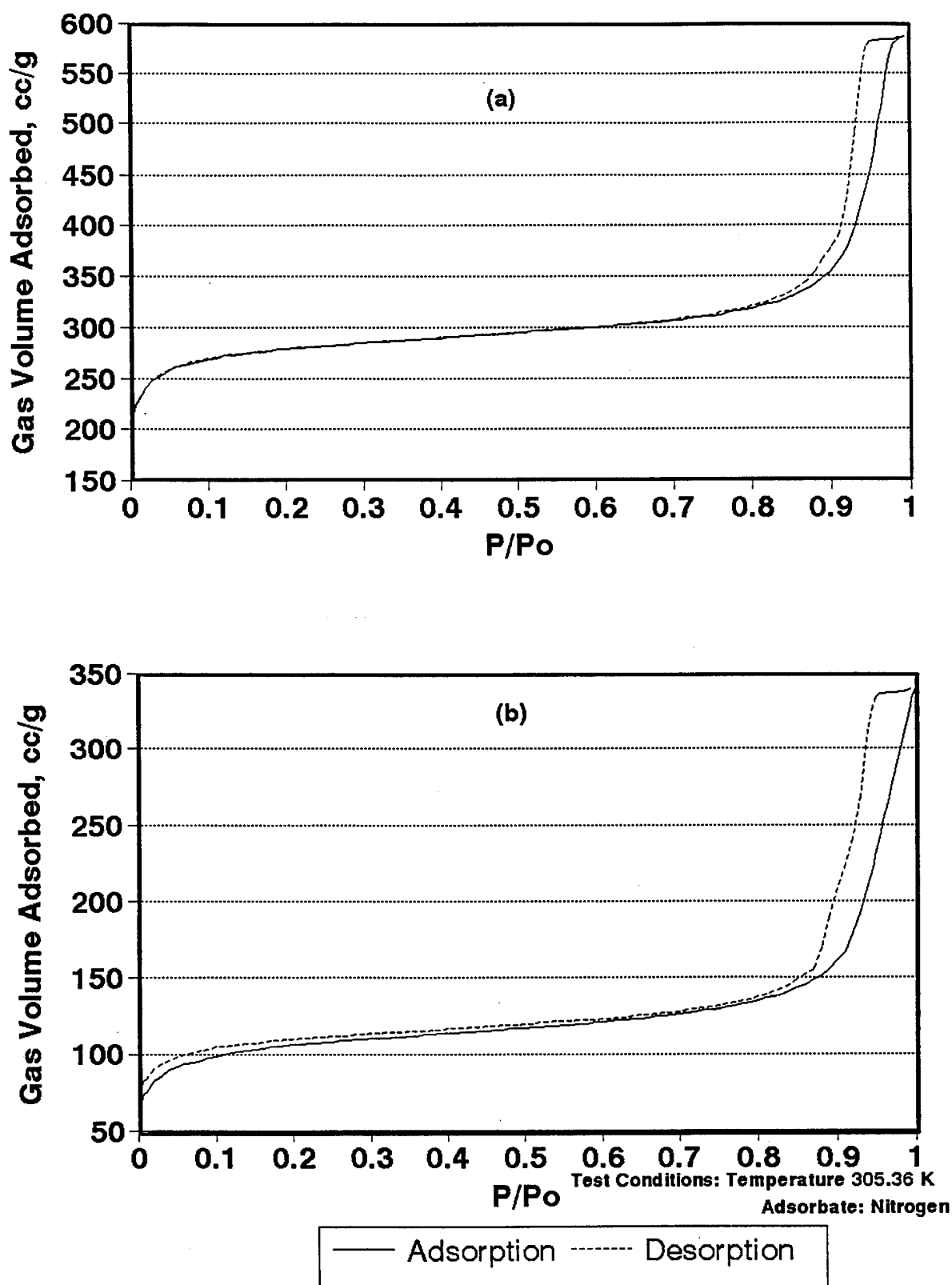
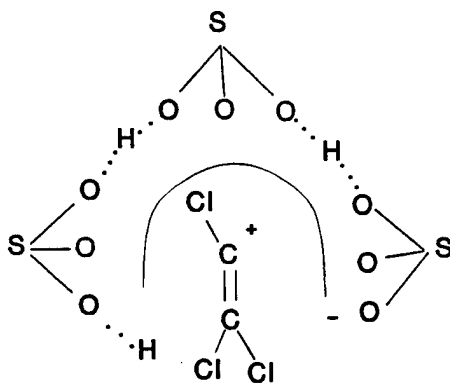


Figure 2-3. Gas Volume vs P/P_o : (a) Virgin AM572-P; (b) MTU-CAT



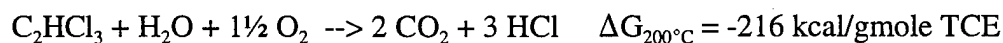
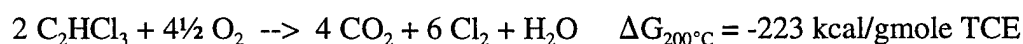
The rate of reaction will be dependent on the number of catalyst sites. Two main factors that would affect the concentration of reactive species at these sites are temperature and the localized TCE concentration. If the temperature is too low then very few reactive species will be formed and coking of the catalyst may occur. If the concentration of TCE is too low in the pores with the capabilities of supporting the reactive species then only a few reactive sites would be formed. If the temperature is too great then the reactive species concentration on the surface will go down. Thus it is possible that there is an optimum temperature to achieve the highest capacity for the reactive species on the surface. This optimum temperature would be dependent on the feed concentration as well as the organic being destroyed because the surface concentration is dependent on the type of organic and its concentration.

The structure of the polymeric adsorbent will dictate how many catalyst sites will be formed and the reactions that occur on them. The $\text{-SO}_3\text{H}$ functional groups must be close enough to interact and form the stabilized center for the reactive intermediate. The rigidity of the polymer dictates how these functional groups are held. If the polymer is too flexible it does not efficiently create the stabilized centers, and fewer catalyst sites are formed. Once formed they are reactive and polar molecules (e.g. water) have a high affinity for the $\text{-SO}_3\text{H}$ groups and exclude reactants and suppress the catalytic activity (Gates, 1992).

Due to the adsorptive nature of the catalyst support, the importance of the adsorption of reactants and products on the surface cannot be over emphasized. Amborsorb 572 was found to have an adsorption capacity of 0.17 ml TCE/g adsorbent at 196 °C when fed a

dry feed stream of TCE (~80,000 ppmv in nitrogen). For this reason chloride analysis of the product stream is the only way to confirm mineralization. The amount of chloride also gives an indication of how the catalyst is performing over time. There is a general decreasing trend in the chlorine content of the effluent, possibly the result of catalyst poisoning with age.

The oxidation of TCE can occur with or without water according to the following reactions:



The conversion of the plain support alone, AM 572-P, was substantial (>99.9 percent at 180 °C). The conversion of the impregnated materials ranged from none to complete conversion. The designations of the catalysts are AM-572-X, where X is the metal oxide code: Mn for manganese; Co for cobalt; and Ti for titanium. Experiments conducted on a thermally modified non-impregnated Ambersorb 572, referred to as MTU-CAT, showed even higher conversion and mineralization levels than the plain support. The following sections outline the experiments of these catalysts. Catalyst aliquots were used in either the "pre-loaded" form or the "as-received" form in the following experiments.

2.3.1 AM-572-P

Experiments using the pre-loaded form (see Table 2-2), were initially performed at 130 °C with no conversion detected. Increasing the EBCT from 1.7 s to 2.7 s by decreasing the gas flow rate did not change the conversion significantly, however chloroform, carbon tetrachloride, and PCE, were detected in the effluent. Increasing the temperature to 180 °C at the same EBCT caused the effluent to drop to below detection limits (>99.9 percent conversion), yet the chloride balance only showed 20 percent Cl

recovery. After 380 hours (approximately 1 gram TCE fed/g catalyst) the catalyst was operating at only 50 percent conversion.

Performance of the as-received (not pre-loaded) catalyst was drastically different. In these experiments the catalyst was maintained at 180 °C at all times. Flow rates varied from 1.1 s to 16.7 s EBCT. Water addition (50 percent RH) to the feed stream had no effect on the catalyst performance. This is a surprising finding since the water reacts so strongly with the polarized -SO₃H catalysis groups. Therefore, either the groups are occupied with something else or they are not responsible for the oxidation occurring on this catalyst.

TABLE 2-2. OPERATING CHARACTERISTICS OF AM-572-P EXPERIMENTS
(1500 ppmv TCE feed).

Temperature (°C)	EBCT (s)	Conversion (%)	Mineralization (%)	Water (Y/N)
		PRELOADED		
130	2.7	0	NT	N
180	2.7	>99.9	20	N
		AS RECEIVED		
180	16.7	>99.9	70	N
180	16.7	>99.9	70	Y
180	1.1	>99.9	NT	N
180	0.5	97	NT	Y
180 [†]	0.15	20	34	Y
180 [†]	0.15	10	14 ^a	Y

NT - Not Taken

^a After 3 days.

[†] Concentration switched to 15 ppmv.

Tabled data is a subset of 192 samples.

Since adsorption is possible, the catalyst was operated until approximately 0.8 g of TCE/g catalyst passed through the system. Chloride samples confirmed the

destruction of TCE as mineralization efficiencies remained high (approximately 86 percent at the end of the experimental sequence). A minimum turnover for the plain, as-received catalyst is approximately 8×10^5 / mole of catalyst sites. It is possible that as the preloaded catalyst heated up, the catalyst sites were exposed to TCE at less than optimum temperatures and fouled by coking of the sites.

2.3.2 MTU-CAT

Table 2-3 summarizes the catalytic oxidation experiments of TCE over the MTU-CAT for a wide range of operating conditions. No "pre-loaded" experiments were performed with MTU-CAT. Exposing MTU-CAT to a dry, 1500 ppmv TCE feed, at a catalyst temperature of 200 °C and an empty bed contact time (EBCT) of 7.7 sec (17.5 ml/min-g catalyst) revealed a very active catalyst. The effluent, as determined by the Flame Ionization Detector (FID) on the GC, remained non-detect for TCE (99.9 percent conversion) and a small amount (approximately 1 ppm) of carbon tetrachloride was detected in the effluent. Approximately 3 g of TCE was fed to the reactor for each gram of catalyst during these initial experiments shown in Table 2-3. The same adsorbent/catalyst charge was used throughout the series of conditions listed in Table 2-3. Some of these early MTU-CAT experiments only used a water bubbler to trap HCl/Cl₂. All remaining experiments reported in this study used an additional sodium persulfate trap for the Cl₂ specifically and increased the chlorine recovery efficiency in the exhaust. Table 2-3 annotates which type of trapping system was used in the initial MTU-CAT experiments. The shift in the effluent from all HCl to greater amounts of Cl₂ suggests the initial reactions reacted with residual water on the adsorbent (desorption studies at 110 °C show approximately 30 mg water/g adsorbent in the "as received" form). As the available water decreased, the reaction shifted to a true dry reaction sequence, but this formed a small amount of water for the "humid feed" reaction to continue.

Additional tests were performed on subsets of the MTU-CAT used in the above experiments. In one experiment (140 °C, 2 s EBCT), a dry TCE feed was used and the effluent dropped to below detection limits on the very sensitive Electronic Capture

Detector (ECD) (>99.999 percent conversion). Analysis of a DCM sample taken while using the dry feed indicated that phosgene, and other by-products (e.g. PCE, hexachloroethane, and possibly some diethoxy ethanes) were being formed in trace amounts.

Water was then added to the dry feed to produce a TCE/air mix with a relative humidity of 45 percent at 22 °C. Within minutes this humidified feed rapidly deactivated the catalyst. Upon removing the water, the catalyst performance slowly recovered. This is in direct contrast to the AM 572-P which showed no effect of added water. This

TABLE 2-3. OPERATING CHARACTERISTICS OF THE INITIAL DRY MTU-CAT EXPERIMENTS (1500 ppmv TCE feed - no water added).

Temperature (°C)	Empty Bed Contact Time (s)	Conversion (%)	Mineralization (%) [†]	Time (hr)
200	7.7	>99.9	104	70
200	7.7	>99.9	80	90
180	24.5	>99.9	127 [†]	
180	9.8	>99.9	NT	
180	4.8	>99.9	NT	
180	3.0	>99.9	62	
150	2.7	>99.9	90	
115	2.9	>99.9	52	190
115	2.9	>99.9	56/(73)	214
110	11.7	>99.9	37/(59)	260

NT - Not Taken

[†] Additional processes evaluated with these experimental runs caused an excess amount of TCE to be desorbed from the adsorbent adding to the chlorine balance.

[‡] Dual trap values are shown in parentheses

Tabled data are a subset of 132 samples.

finding indicates the catalyst sites or the catalytically active species are different from those in the plain material. A minimum turnover number for the dry feed reactions is approximately 8×10^5 /mole of catalyst sites, coincidentally the same as the AM572-P.

In separate experiments the addition of natural gas (CH_4 , 180 °C, concentration approximately 0.15 percent) to the dry TCE/air mix caused a dramatic drop in the TCE conversion. The catalyst performance returned after removal of the natural gas. The formation of water by the oxidation of methane is possible, accounting for the loss in conversion.

BET area analyses, elemental analyses, and a liquid extraction technique were used to elucidate the mechanisms of catalysis and to determine the structural differences of this enhanced catalyst, MTU-CAT. The surface area of MTU-CAT has changed from the parent Ambersorb 572 adsorbent as shown in Table 2-4. There is a shift in the distribution of the pore sizes indicating that the material has indeed changed. However, it is unclear if the change is due to pore blocking/filling from by-products or if the change occurred during the electrolytic activation of the MTU-CAT. Figure 2-4 graphically shows the results of the nitrogen isotherm data.

TABLE 2-4. SURFACE AREA ANALYSIS RESULTS FOR VIRGIN AMBERSORB 572 AND MTU-CAT AFTER THE 11 DAY INITIAL EXPERIMENTS.

SAMPLE ID	Total Surface Area (m^2/g)	Average Pore Diameter (\AA)	Total Pore Volume (ml/g)	Median Pore Diameter (\AA) [†]	Median Pore Diameter (\AA) [‡]
572-P	831	44	0.91	132	56
MTU-CAT	324	65	0.53	296	64

Analysis conditions: Instrument Temperature, 305.36 °K; Room Temperature, 296.7 °K; Adsorbate, Nitrogen.

[†] Based on Pore Volume; [‡] Based on Surface Area

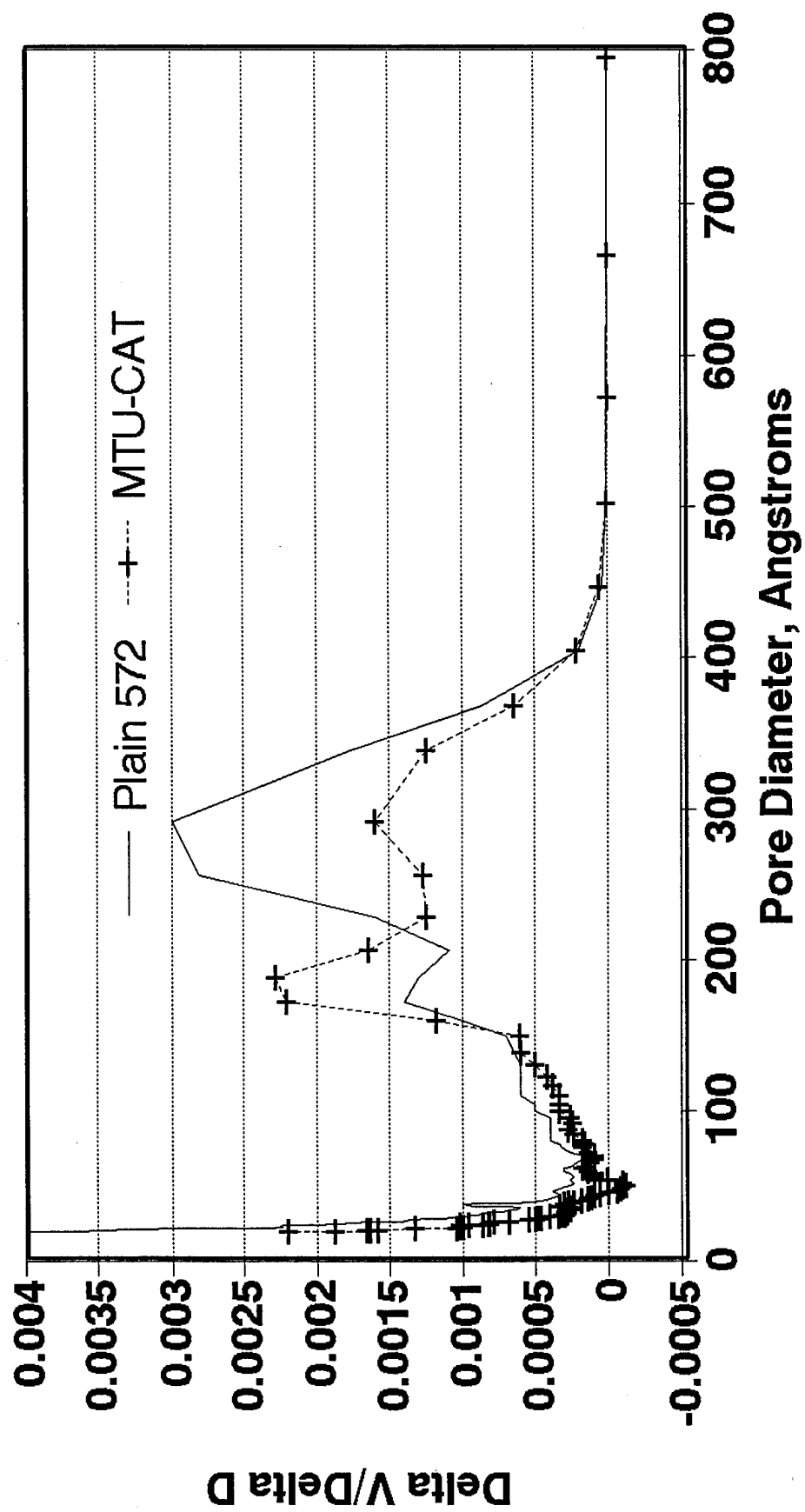


Figure 2-4. BET Adsorption/Desorption Isotherm Data; Delta V/Delta D vs Pore Diameter

The results of elemental analyses on the parent compound (AM-572-P), the enhanced catalyst (MTU-CAT), and a methanol extracted sample of the enhanced catalyst are shown in Figure 2-5. They indicate a dramatic chlorine increase in or on the MTU-CAT. At least some of the chlorine is leachable, as the methanol extracted sample has lost some of the chlorine residual. A GC/MS examination was made of the extracted liquid to identify these compounds (listed in Table 2-5) leached from the catalyst.

TABLE 2-5. GC/MS ANALYSIS OF METHANOL EXTRACT OF MTU-CAT.

Compound	Relative Peak Area (Percentage)
Hexachloroethane	12.4
Pentachloroethane	9.25
Tetrachloroethylene (PCE)	2.54
Trichloroacetic Acid, Methyl Ester [†]	1.47
1,1,2,3,4,4, hexachloro, 1,3 Butadiene	0.39
Dichloroacetic Acid, Methyl Ester [†]	0.29

[†] The methylated ester of the parent acid was probably created when the methanol reacted with the acid over the -SO₃H groups (Morrison and Boyd, 1980).

The existence of the dichloroacetic and trichloroacetic acids on the catalyst surface, and the phosgene noted earlier, suggest a radical mechanism similar to the photocatalysis of TCE in the gas phase over titanium dioxide. Nimlos et al (1993) identified these compounds as by-products when the hydroxyl radical ($\bullet\text{OH}$) attacks the TCE. They report that the reactive chlorine atom, $\bullet\text{Cl}$, is formed, then this in-turn attacks the organics to make the dichloroacetic acid. In addition, they suggest that the same reaction mechanisms would occur if PCE was the target organic instead of TCE. Under these conditions trichloroacetic acid would be formed.

It is also possible that the radical in this catalyst could be $\bullet\text{C}_2\text{Cl}_3$ based on the recovery of 1,1,2,3,4,4 hexachloro butadiene (radical:radical recombination) from the surface. Other species could also exist, such as the carbenium ion $\text{C}_2\text{H}_2\text{Cl}_3^+$, that could be

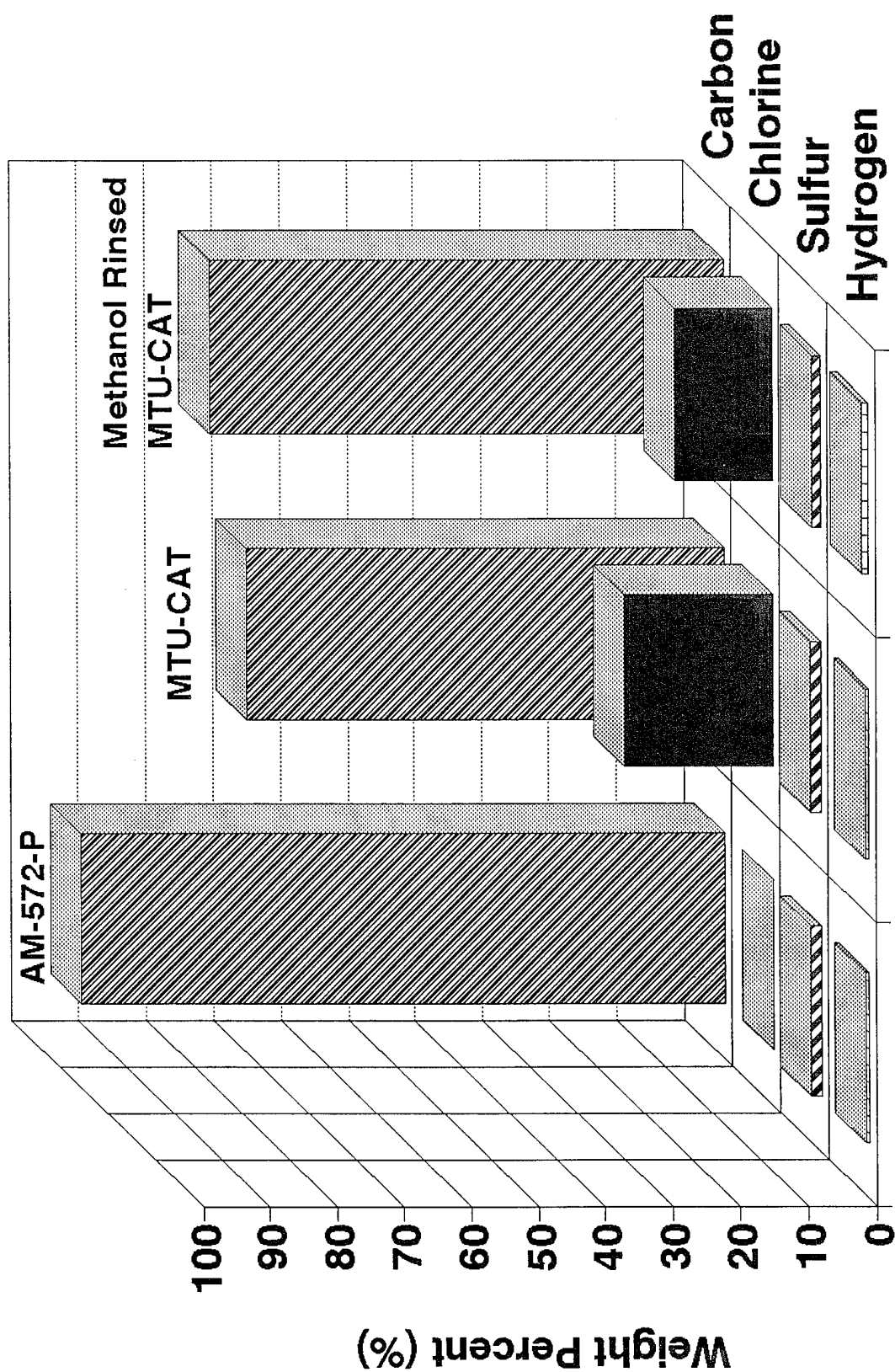


Figure 2-5. Elemental Analysis of the Materials used in the Oxidation of TCE

stabilized by the sulfonate groups on the polymeric support. No matter how these surface adsorbed by-products are created, they do increase the chlorine loading of the catalyst. These and potentially other polymerized, chlorinated by-products, are on the catalyst surface.

It was expected that the hydrogen levels would be depleted in the catalyst due to the hydrogen interactions noted earlier, however there is no statistical difference between the amount of hydrogen in the samples. This suggests that the hydrogen is protected within the matrix of the polymer and not exposed to the reaction sequence. Unfortunately the same cannot be said of the carbon matrix itself as there is a loss of carbon in the MTU-CAT material. It is unclear if this is due to the structural damage noted above (which may account for some of the loss in surface area). Whatever the cause, the enhanced catalyst has lost the volume equal to that contained in the micropores of Ambersorb 572 (0.4 ml, [Rohm and Haas, 1992]). If the micropores are blocked off, this suggests that the $\text{-SO}_3\text{H}$ groups in the mesopores are in sufficient proximity and numbers to support the reactive intermediate species (e.g., carbenium ion/radical) to oxidize TCE. However, Figure 2-4 indicates that only about two thirds of the micropores are lost.

2.3.3 Metal-Impregnated Ambersorb 572

The experimental results with AM-572-Mn and AM-572-Co, shown in Table 2-6, were conducted with a dry feed. As shown in Figure 2-6, the catalysts appear to have induction times before they become active. This possibly occurs in two steps. First, is the loading of the high-energy sites in the pores (adsorption). Second, building up concentrations of reactive intermediates supported in the $\text{-SO}_3\text{H}$ groups in the pores. Once a critical loading of reactive intermediates occurs, then the reaction consumes the excess TCE shown exiting the reactor in Figure 2-6, in addition to removing the influent TCE. Water shows a fouling trend in both of these catalysts as well indicated by the increase in TCE concentration shown in Figure 2-6. No chloride samples were taken to determine mineralization efficiencies, nor were the experiments continued to evaluate the

reversibility of the water poisoning. The AM 572-Mn experiments (210 and 180 °C at 3.8 and 7.6 s EBCT) which started with humid feeds showed little conversion (0-12 percent) as shown in Table 2-6, again showing the deactivation effect water has on the catalysts.

TABLE 2-6. OPERATING CHARACTERISTICS OF COBALT (-Co) AND MANGANESE (-Mn) IMPREGNATED AMBERSORB 572 (1500 ppmv TCE feed).

CATALYST	Temperature (°C)	EBCT (s)	Conversion (%)	Mineralization (%)	Water (Y/N)
-Mn	175	16.9	>99.9 ^a	NT	N
	175	16.9	80-88	NT	Y
	210	3.8	0	NT	Y
	210	7.6	12	NT	Y
	180	7.6	5	NT	Y
-Co	140	6.7	0	NT	N
	140	10.3	0	NT	N
	140	49	0	NT	N
	190	24	80	17	N
	190	24	>99.9	NT	N
	190	9.6	>99.9	47	N
	190	2.8	>99.9	NT	N
	130	32	>99.9	27	N
	130	9.6	>99.9	20	N
	130	9.6	99.9	NT	N
	130	3.0	40	NT	N

^a After induction period - see text.

Tabled data are a subset of 102 samples (Mn) and 133 samples (Co).

Heat treatment of the cobalt impregnated catalyst was done to ensure the oxides were sufficiently formed prior to exposure to the TCE. The heating was done by taking an aliquot of the initial 100 g batch of AM572-Co and placing it in a tube furnace

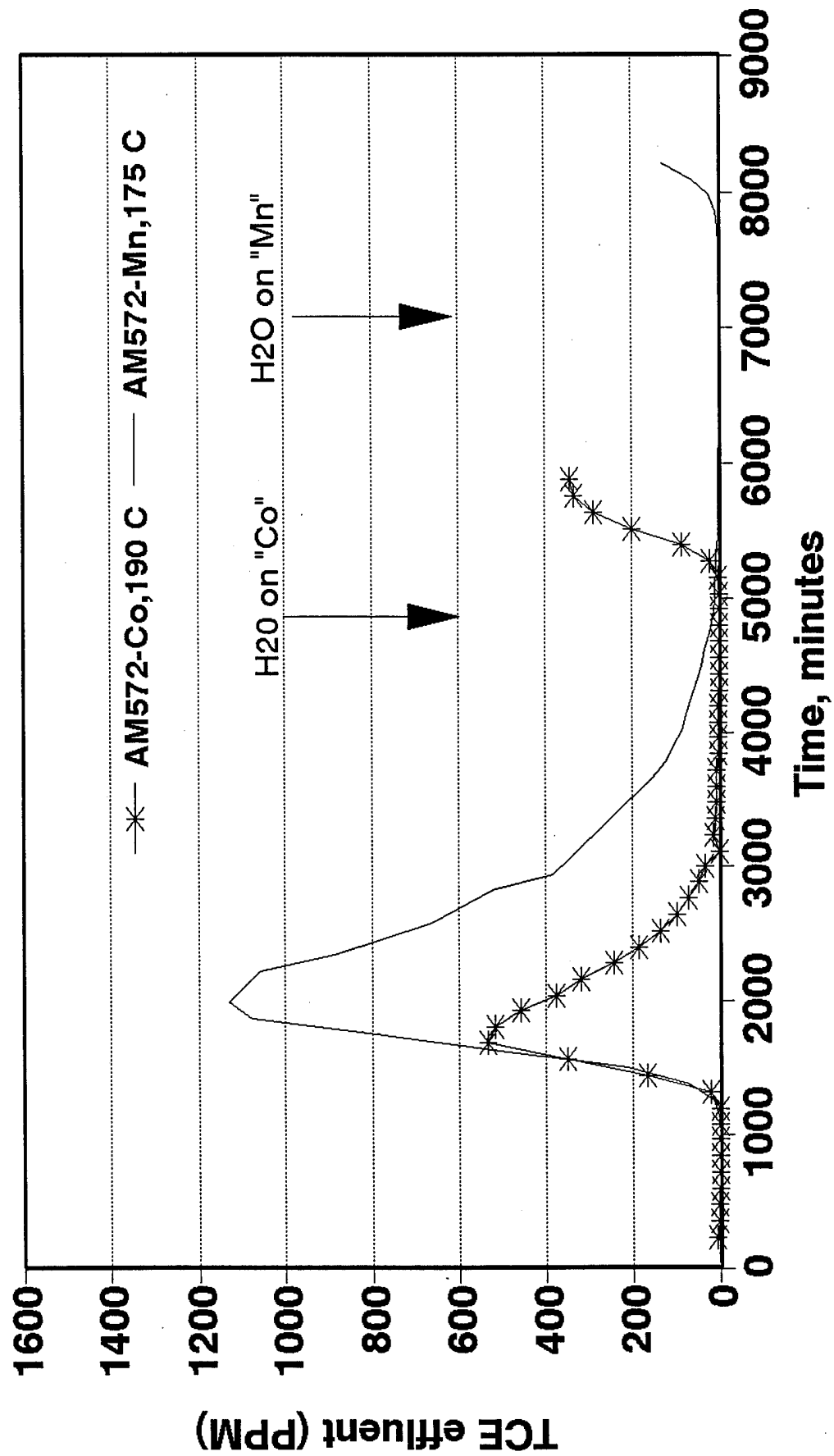


Figure 2-6. Organic Concentration Vs Time; EBCT=17 s, 1 atm, 1500 ppm TCE feed

and heating to 250 °C in air over night. Some of this material, AM572-Co(H), was put into the steel reactor (25 s EBCT; 280°C). Only a 67% conversion was obtained, with chloroform and PCE as the major by-products. The catalyst suffered a 12 percent weight loss during the experiment.

In an attempt to specifically target the oxides onto the sulfonic functional groups, cobalt was ion exchanged with the hydrogen in the -SO₃H groups. This new batch of catalyst was made by passing cobalt nitrate (1 M) through a bed of plain Ambersorb 572. As expected the rigid, pyrolyzed adsorbent has a low exchange capacity (less than 1/6th that of IRN 77) because of the inability of the adsorbent to swell to accommodate the larger cobalt cation. This catalyst, AM 572-Co(e), at 180 °C (1 s EBCT) also had an induction period, after which complete conversion (>99.9 percent) is achieved, but the mineralization is only 7 percent. Shortly afterwards the catalyst completely deactivates. Heat treating an aliquot of the AM-572-Co(e) using the same procedures as the AM572-Co above to make AM 572-Co(e)/H resulted in a non-active catalyst. The experiments showed a typical adsorption curve (short loading with breakthrough) and no conversion.

The results of experiments with a pre-loaded AM-572-Ti are shown in Table 2-7. Early high mineralization efficiencies may be the result of excess TiCl₄ conversion and not destruction of TCE. Adding Milli-Q water to the AM-572-Ti in a glass vial causes it to get very hot, confirming the existence of residual TiCl₄ in the pores. To remove this effect the catalyst, referred to as AM-572-Ti(W), was washed, dried, and preloaded before use. As the catalyst heated up to 200 °C, approximately 1/3 of the preloaded TCE exited the reactor along with other by-products, including PCE. Other by-products detected (typically found in this work) during the remainder of the experiments with this catalyst include carbon tetrachloride, chloroform, hexachloroethane and possibly pentachloroethane. The product spectrum shifted over time with the hexachloroethane concentration decreasing while the TCE concentration in the effluent was increasing. These excessive by-products do not favor the use of AM-572-Ti.

The product spectrum between the metal-impregnated and the plain catalysts are similar. In addition, there does not seem to be any enhancement of the catalyst performance with the addition of the metal oxides. It is possible that these temperatures are too low to activate the reactions over these metal oxides.

TABLE 2-7. OPERATING CHARACTERISTICS OF TITANIUM IMPREGNATED AMBERSORB 572 (1500 ppmv TCE feed).

CATALYST	Temperature (°C)	EBCT (s)	Conversion (%)	Mineralization (%)	Water (Y/N)
-Ti	105	12.7	>99.9	90	N
	105	12.7	>99.9	77	N ^a
	105	12.7	>99.9	28	N ^b
	150	23	>99.9	20	N
	175	35	>99.9	50	N
	175	10	>99.9	30	N
	175	3.7	>99.9	50	N
-Ti(W) [†]	200	3.3	see text		
	200	31	>99.9	NT	N
	200	11	<99.9	58	N
	200	11	>99.9	35	N
	200	11	>99.9	20	N
	200	3.0	50	36	N

NT - Not Taken

[†] Washed - see text.

^a After 1300 minutes.

^b After 1600 minutes.

^c 16 hours later.

^d 30 hours later.

Tabled data are a subset of 320 samples

An experimental catalyst, XE-706, based on the same technology presented here but using a proprietary metal oxide mix on Ambersorb 572, was provided by the Rohm and Haas Company. At 260 °C, with a dry 1500 ppmv TCE feed, a >99.9 percent

conversion at an EBCT of 11 s was observed after an induction period of approximately 2 days. Small amounts of chloroform and PCE were noted in the effluent. When the feed stream was humidified the catalyst rapidly, but not completely, deactivated (although it was still losing activity when the water was removed) resulting in a TCE effluent concentration of about 400 ppmv. Within 12 hours after removing the water the catalyst had regained the >99.9 percent conversion level before water was added. No chloride analyses were done to confirm mineralization.

2.3.4 Electric Field Affects Catalytic Oxidation on MTU-CAT

Electric fields were observed to alter the by-product spectrum of TCE oxidation over MTU-CAT. The conditions of the experiments are listed in Table 2-8 and are interspersed with the experiments shown in Table 2-3. That is, thermal-only operations were performed (heat tape designation in Table 2-8) and then the Joule heating work was performed at the same temperature and flow conditions prior to changing to the new temperature and flow conditions were evaluated.

As discussed in section 2.3.2, the 1500 ppmv TCE dry feed (EBCT varied from 43 to 2.9 s) was converted by over 99.9 percent to mineralization products (HCl and Cl_2) and a small amount of carbon tetrachloride (CCl_4) at 200 °C. The heat-tape, used to initially heat the bed, was turned off and Joule heating maintained the bed temperature. An application of 2.5 V DC across the annular reactor containing 8.8 gm of catalyst caused the small CCl_4 peak to disappear from the effluent and no new peaks appeared. The cell potential was increased to 6.0 V DC to maintain the reactor at 200 ± 10 °C. Despite the continued >99.9 percent conversion, the chloride results showed an 80 percent decrease in the mineralization occurring in the system with the applied electric field. Changing back to heat-tape and turning off the electric field resulted in two things: 1) the mineralization levels, as determined from the chloride mass balance, returned to >99 percent, and 2) the CCl_4 peak returned to the effluent.

A repeat of the experiment on the following day did not show this change in the mineralization as the chloride levels remained high under the 3-7 V DC applied potential, but the CCl_4 disappeared as before. Increasing the potential further to 9.0 V DC brought the CCl_4 peak back. Reducing the potential to 7.0 V DC caused the CCl_4 peak to disappear again. The zero-field mineralization levels had dropped overnight to 80 percent, which remained stable under the applied voltages. Alternating current (60 Hz), used both days, also showed the same trends as the DC.

TABLE 2-8. TEST CONDITIONS DURING ELECTROCATALYSIS RUNS (1500 ppmv TCE feed).

Heat Source	Temp (°C)	Cl (%)	CCl_4	EBCT (sec)
Heat Tape	200	>99	Yes	43
2.5-4 V DC	199-204	16	No	43
4-5 V DC	198-205	NT	No	43
5-5.5 V DC	201-207	5	No	43
5.5-6 V DC(R) [†]	199-206	NT	No	43
6 V AC	194-197	NT	No	43
10.5-11 V AC	198-210	5	No	43
Heat Tape	200	NT	Yes	43
Heat Tape	199	78	Yes	7.5
1.5-4.5 V DC	199-200	NT	‡	7.5
4.5-7 V DC	196-202	76	No	7.5
9-10.5 V DC	192-210	NT	Yes	7.5
7 V DC	202	NT	No	7.5
Heat Tape	200	76	Yes	2.9
2.7-5.2 V DC	197-204	NT	Yes°	2.9
5.2-7 V DC	195-205	67	Yes°	2.9
Heat Tape	183	>99	Yes	27

2.7-4 V DC	177-190	NT	No	27
4 V DC	184-186	40	No	27
4 V DC	183-185	NT	No	9.8
4 V DC	182-183	NT	No	4.8
4 V DC	180-182	59	No	3
Heat Tape	179-185	NT	Yes	3
Heat Tape	149	NT	Yes	2.9
2.7-16.5 V DC	141-159	NT	Yes	2.9
7.5-10.5 V DC	153-161	59	Yes	2.9

† Reversed polarity on cell.

‡ Initially yes, but went away.

□ Initial switch to AC resulted in a temperature rise to 231 °C in less than 1 minute. Temperature was back to 209 °C within 4 minutes.

○ CCl₄ concentration reduced by ½ based on GC areas.

Tabled data are a subset of 192 samples.

The trend repeats itself when the experiments were run at 180 °C; complete conversion (>99.9), but mineralization drops by 74 percent with an applied electric field. In addition, the CCl₄ peak disappears with the applied potential, unless very high flow rates (0.5 s EBCT) are utilized and then it is only reduced in size. At 140 °C the catalyst remained active and had complete conversion, but mineralization under the applied potential was only 59 percent.

The effect of the electric field on the CCl₄ is dependent on flow rate. At the highest flow rate (EBCT 2.9s), under zero-field conditions, the TCE effluent concentration remained below detectable limits (>99.9 percent conversion) but the small CCl₄ concentration approximately doubled based on the areas from the gas chromatograph. Applying a potential of 2.7-7 V DC only decreased the CCl₄ concentration, not eliminating it entirely while the TCE concentration remained below detection limits.

The changes in the CCl_4 and chloride ion concentrations over these experiments is most perplexing. No definitive conclusion can be made based on the limited data. Uneven heating, causing hot and cold spots in the catalyst material may be one reason, another may be the how the electrons flow in the MTU-CAT catalyst.

The structure of the electrically modified Ambersorb 572, MTU-CAT, may suggest how an applied electric field alters the by-product spectrum of the TCE oxidation reaction. The catalyst still contains sulfonate groups and a hypothetical catalytic site in an electric field is shown in Figure 2-7. The electron flow path differs from the bulk by traveling one of three options: 1) around the micropore (path "A"); 2) through the micropore via the sulfonic groups (path "B"); or 3) under the micropore (path "C"). The path traveled will, of course, be determined by the resistance of the different choices. If the path is through the sulfonic groups, then the electron may pass from one polymer section to another as the sulfonic groups are probably on different polymer sections. The micropore is a block to the flow of electrons and a slight electrostatic charge may build up on the sides. The potential drop across one micropore due to the overall applied electric field would be insignificant (at a bed potential of 5 V; assuming 40 beads between electrodes, no loss at electrode:bed interface with a linear drop across the beads, and a pore diameter of 10 nm would give a potential difference of 3×10^{-6} V).

2.3.5 Electric Field Affects Catalytic Oxidation on AM572-P

Using heat tape to heat the plain adsorbent/electrocatalyst, AM 572-P, to 180 °C in the annular reactor resulted in complete conversion of the 1500 ppmv TCE feed, while mineralization was approximately 70 percent, with CCl_4 just above detection limits as the only peak in the effluent. Applying an electric potential of 5-17 V DC had no effect on conversion. In direct contrast to the MTU-CAT performance, the CCl_4 desorbed from the surface increasing its effluent concentration by a factor of about 6 at the peak of the desorption (see Figure 2-8). While the external thermocouple registered a lower temperature, the resistance change in the bed indicates an increased temperature in the

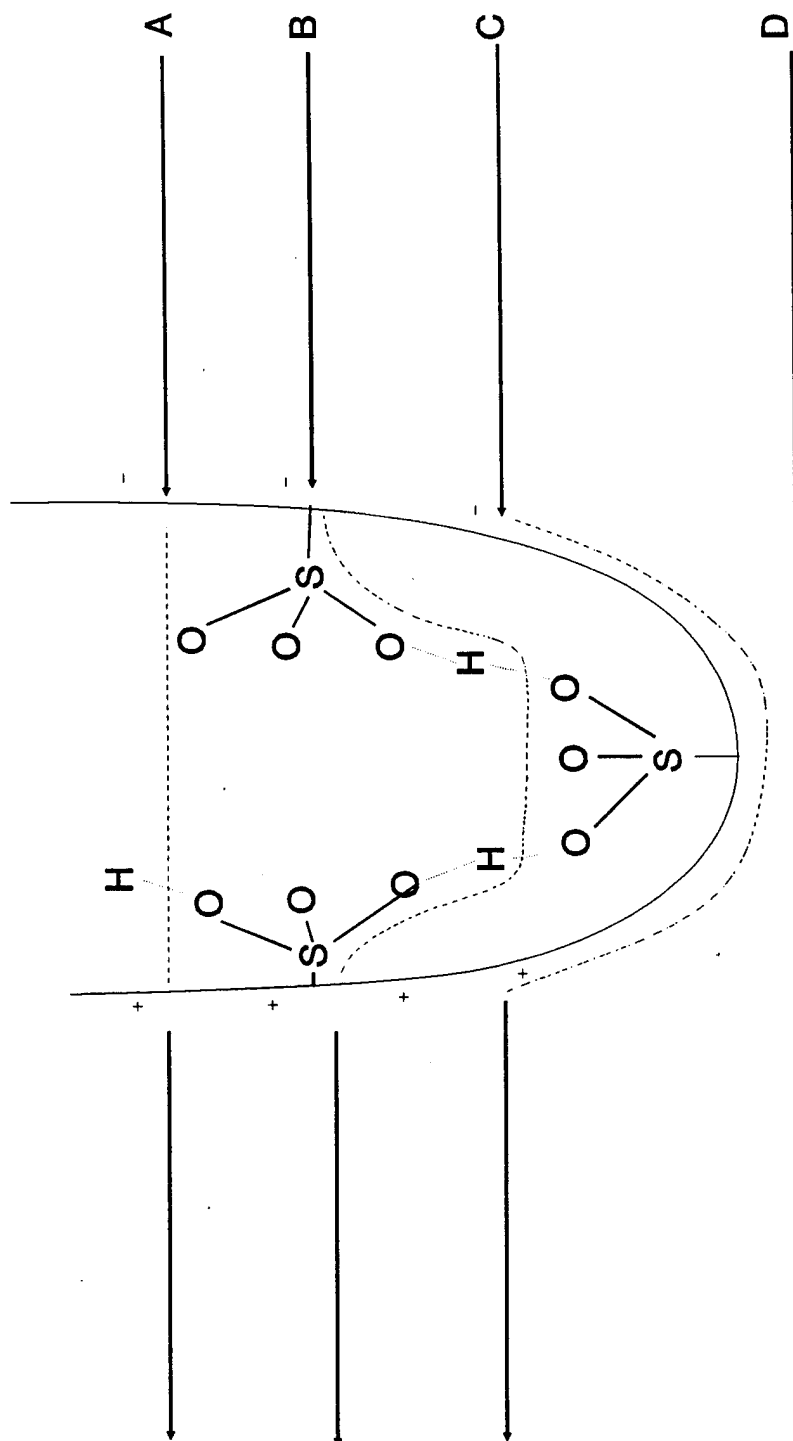


Figure 2-7. Hypothetical Micropore in an Electric Field.
 Electron paths: "A" behind pore; "B" through sulfonic groups; "C" under pore; and "D" bulk flow.

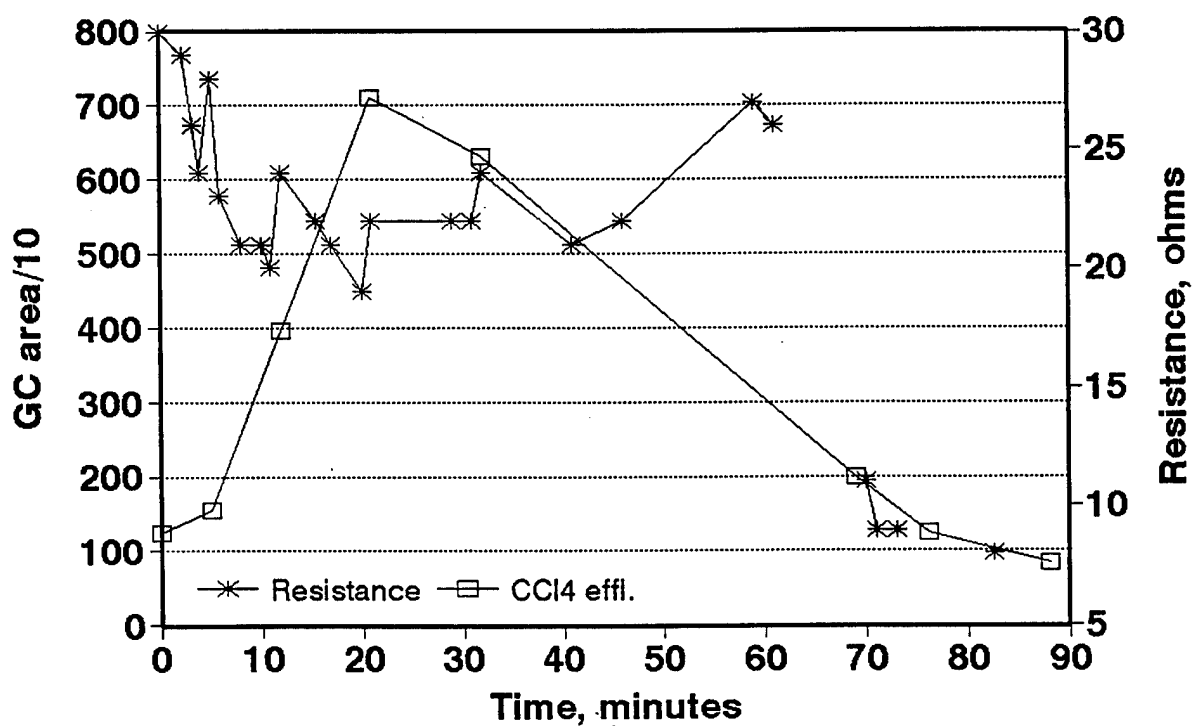
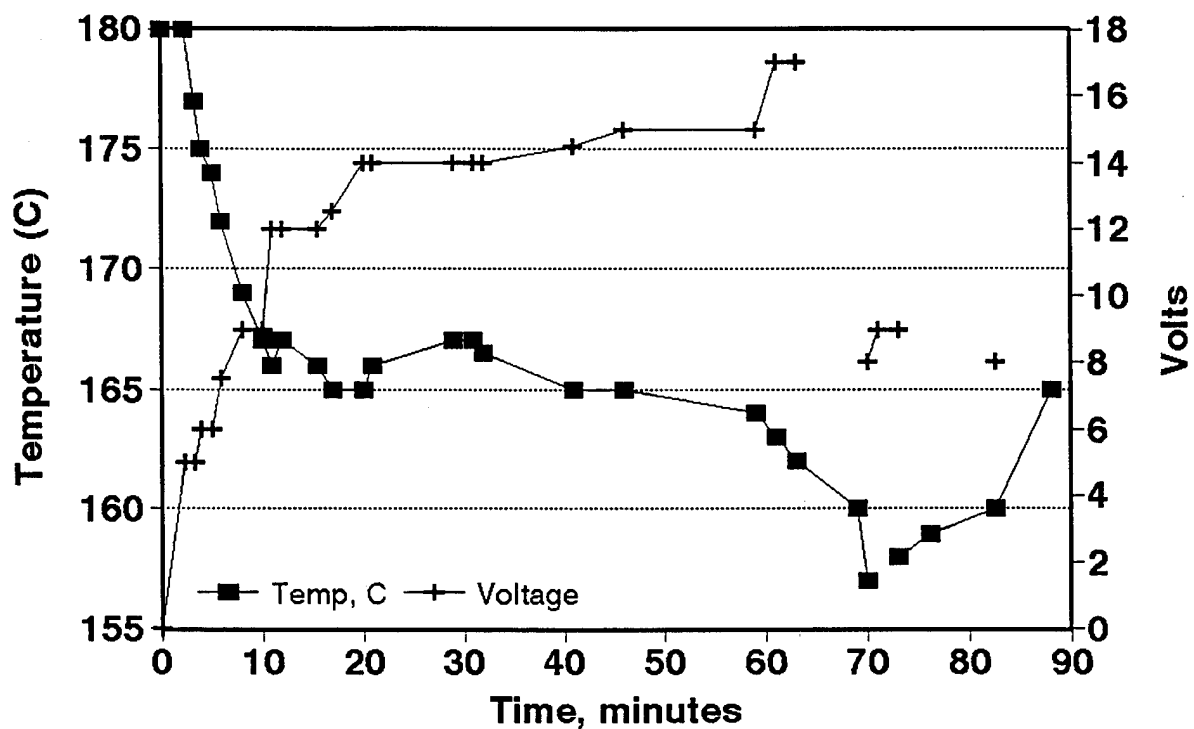


Figure 2-8. CCl₄ Effluent over AM572-P under Dynamic Electric Field in Annular Reactor; EBCT = 16.7s, 1 atm (no heat tape)

bed, suggesting a thermal gradient was set up in the reactor. Unfortunately this means the true temperature at the adsorbent surface is unknown.

Ambersorb 572 was impregnated with a series of transition metal oxides (titanium, cobalt, and manganese) to create catalytic oxidation sites inside the polymer matrix as described earlier. The titanium oxide catalyst was initially non-conductive but became conductive upon washing with Milli-Q water. An applied electric field over these catalysts in the same annular reactor did not alter the performance of the thermal-only catalysis. Cation migration of the metals in the bed is possible though. After the cobalt oxide electrolytic experiment the center graphite rod had a bluish coating that was assumed to be cobalt.

2.4 CONCLUSIONS

Low temperature catalysis of TCE over polymeric adsorbents is possible, even down to 110 °C in dry air. Water, and possibly methane, fouls the MTU-CAT catalyst, but water has no effect on the plain Ambersorb 572 catalyst. The fouling that does occur is reversible. Impregnation of metal oxides do not enhance the mineralization or conversion of the parent material to oxidize TCE under the conditions of this study. Sulfonic-group supported carbenium ions or radicals potentially exist and are probably the catalyst responsible for the low temperature conversion of TCE. By-products vary slightly and are chloroform, carbon tetrachloride, perchloroethylene, hexachloroethane, and, under extremely dry conditions, phosgene.

While this work points to the possible operation of this catalyst at temperatures of 110 °C, it should be realized that there are extensive by-products formed and complete mineralization is not realized. In addition, the operation time of the catalyst is severely shortened as the temperature is decreased as indicated by the significant increase in by-products detected by the gas chromatograph. However, if the suspected radical/carbenium ions are present and acting as the reactive intermediate species, then

increasing the temperature too far may either destabilize the $\text{-SO}_3\text{H}$ system or simply desorb the oxidizing intermediates.

An imposed electric field can minimize or eliminate, depending on flow and potential, carbon tetrachloride (a by-product from the catalytic oxidation of TCE) over an Amborsorb 572-based catalyst. At high flow conditions the by-product is merely reduced and not eliminated. Impregnation of Amborsorb 572 by transition metal catalysts did not demonstrate any impact from an applied field. At potentials above 7 V DC the effect is reversed and carbon tetrachloride returns to the effluent.

2.5 ACKNOWLEDGEMENTS

This work was funded jointly by Superior Engineering Technologies, Inc., Houghton MI 49931, and the Environics Directorate of the U.S. Air Force's Armstrong Laboratory, Tyndall AFB FL 32403, Maj Mark Smith, Project Officer. Mention of trademarks and trade names of material and equipment does not constitute endorsement or recommendation for use by the U.S. Air Force, nor can this article be used for advertising the product(s). Support from Michigan Technological University is greatly appreciated. Appreciation is also expressed to the Rohm and Haas Company for providing the XE-706 catalyst sample for comparison.

2.6 REFERENCES

Al-Jarallah, A.M., Siddiqui, M.A.B., and Lee, A.K.K, "Kinetics of Methyl Tertiary Butyl Ether Synthesis Catalyzed by Ion Exchange Resin," *Can. J. Chem. Engr.*, 66, 802-807, (1988).

Gates, B.C., "Catalytic Chemistry," John Wiley & Sons, Inc., New York, 1992.

Gregg, S.J., and Sing, K.S.W., Adsorption, Surface Area, and Porosity, 2nd ed., Academic, London, 1982.

Hylton, T.D., "Evaluation of the TCE Catalytic Oxidation Unit at Wurtsmith Air Force Base," *Environmental Progress*, Vol. 11, No.1, pp. 54-57, 1992.

Morrison, R.T., and Boyd, R.N., "Organic Chemistry," Allyn and Bacon, Inc., Boston, pp. 592-614, 1980.

Nimlos, M.R., Jacoby, W.A., Blake, D.M., and Milne, T.A., "Direct Mass Spectrometric Studies of the Destruction of Hazardous Wastes 2. Gas Phase Photocatalytic Oxidation of Trichloroethylene over TiO_2 : Products and Mechanisms," *Environmental Science and Technology*, 27, pp 732-740, 1993.

Petrosius, S.C., and Drago, R.S., "Decomposition of Chlorinated Hydrocarbons Using Metal Oxides Supported on Carbonaceous Adsorbents," *J. Chem. Soc., Chem. Commun.*, 1992, pp 344-345.

Petrosius, S.C., Drago, R.S., Young, V., and Grunewald, G.C., "Low-Temperature Decomposition of Some Halogenated Hydrocarbons Using Metal Oxide/Porous Carbon Catalysts," *Journal of the American Chemical Society*, 115, pp 6131-6137, 1993.

Rohm and Haas, "Technical Notes: Amborsorb[®] Carbonaceous Adsorbents, Specialty Purifications," Philadelphia, PA, August 1992.

US EPA, 1993 Toxic Release Inventory, Air Emissions of Hazardous Air Pollutants, 1993, at WWW URL "http://earth1.epa.gov/TRI_93/chap1/".

Vol'kenshtein, F.F., "The Electronic Theory of Catalysis on Semiconductors," translated by Anderson, N.G., translation edited by Birch, E.J. H., A Pergamon Press Book, The Macmillan Company, New York, 1963.

Wesley, R.B., and Gates, B.C., *Journal of Catalysis*, 34, 288, 1974.

Ambersorb® is a trademark of the Rohm and Haas Company, Philadelphia, PA.

Milli-Q® is a trademark of the Millipore Company, Molsheim, France.

Chapter 3

Adsorption and Destruction of Trichloroethylene on Carbonaceous Adsorbents Under Applied Electric Fields

3.1 INTRODUCTION

Technologies used to control off-gas emissions are typically adsorption onto activated carbon or oxidation, either in a high temperature ($>2000\text{ }^{\circ}\text{C}$) flame combustor or at lower temperatures ($200\text{--}500\text{ }^{\circ}\text{C}$) over a catalyst. Adsorption capacities of carbon can be severely limited due to high humidities entering the carbon bed. At high water vapor pressures, that is, high relative humidities, capillary condensation occurs inside the carbon, drastically reducing the adsorption capacity of the bed. Crittenden, et al (1988) demonstrated that heating the off-gas to lower the relative humidity (RH) was cost effective to maintain the full carbon bed capacity.

Once the carbon is loaded with organics it must be regenerated, usually with steam, and the resulting liquid requires further treatment such as incineration or catalytic oxidation although there is increased interest in reuse and recovery of the organics. Fuel costs for the high temperature oxidation systems usually limit this technology to the most recalcitrant organics (e.g. PCBs). Even catalytic oxidation units operating at moderate temperatures consume energy, increasing operating costs.

Research continues to focus on energy efficient alternatives to regenerate carbon and also on catalysts (or other organic destruction processes) that operate at lower temperatures ($<300\text{ }^{\circ}\text{C}$). The alternatives focused on here relate to using electric fields to regenerate adsorbents, to utilize a novel RH swing process that efficiently adsorbs and concentrates organics, to drive low-temperature ($140\text{--}200\text{ }^{\circ}\text{C}$) catalytic oxidation reactions, and even to directly electrooxidize organics.

Lordgooei, (1995) and Petkovska et al, (1991) utilized electrical energy regenerate adsorbents. The process thermally heats a bed of carbon fibers while using a low-flow purge rate to remove the organics. This concept was originally used by Economy and Lin (1976) when the carbon fiber adsorbent was first introduced into the marketplace. The resistive, or Joule, heating drives the organic off the adsorbent and into the surrounding air where it is swept away by the purge gas. Joule heating occurs when the electrons flowing through the material collide with the lattice structure. The kinetic energy is converted to heat upon impact. The greater the number of electrons flowing (larger current) the more collisions occur causing the adsorbent to increase in temperature. Accordingly, increasing the irregularities in the lattice structure increases the resistance, reducing the current needed to obtain a given desorption temperature.

Petkovska et al (1991) regenerated a stack of 20 carbon cloth sections that were loaded with 1,1,1 Trichloroethane using electrical energy at a maximum temperature of 150 °C. Using direct current (3.5-5.4 V; 0.13-0.17 V/cm²) he found that a high voltage (that is, high temperature) and low purge rate are the best combination to concentrate the organics for further treatment either by condensation or destruction, which concurs with the findings of Davis (1987) for thermal treatment of adsorbents. Petkovska went on to develop a one-dimensional model (Petkovska and Mitrović, 1992) to describe the electrothermal desorption process. Unfortunately the irregularities of the material cause the bed to be non-uniformly heated, a requirement for the Petkovska model. Lordgooei (1995), cognizant of the three dimensional temperature variation in the carbon bed that develops during the heating cycle, is working on a numerical model to describe the adsorption/regeneration system. The Joule heating technology is also applicable to granular activated carbon (GAC), and others (Katsura, 1991; Ozawa, 1978; and Stankiewicz, 1990) have pursued that process.

The water vapor isotherms on the activated carbon cloth used in this study mimic granular activated carbon, resulting in capillary condensation starting around 50 percent RH (Cal, 1995). Competitive effects between water and the organics studied was also reported. He found that benzene adsorption (500 ppmv) was not affected by water until

the feed stream reached 65 percent RH, when a rapid decrease in the benzene capacity was noted with increasing RH. The water condensed in the micropores blocking the pores to the gas phase benzene. However, increased benzene concentrations decreased the amount of water adsorbed at a given RH (at 86 percent RH and 500 ppmv, 284 mg water/g adsorbent was adsorbed - at the same RH but at 1000 ppmv benzene, only 165 mg water/g adsorbent was adsorbed).

Since the cloth adsorbent behaves like a semiconductor (Petkovska et al, 1991) it would be expected that the material would behave uniquely in an electric field. Vol'kenshtein (1963) predicted that the adsorption properties of semiconductors could be altered by an electric field that changed the Fermi level of the semiconductor. This electrical-field-induced adsorption, or electrosorption, has been reported in the literature over different materials in aqueous phases, including activated carbon, when high potentials are used (up to 25,000 V) (Woodard et al, 1986; Holder, 1970; Hoenig and Lane, 1968).

Static electric fields can also be utilized to directly alter reactions. Since gas phase electrocatalyst reactions occur (e.g., ammonia synthesis occurs over metal electrodes at high potentials [Yeh, 1968]), it was thought that trichloroethylene (TCE) may be directly oxidized over the carbon cloth. There is no literature on the electrooxidation of halogenated organics over any surface, metal or carbonaceous.

In this work electric fields were applied to adsorbent beds. Dynamic fields, causing Joule heating, were applied to adsorbents at low and moderate levels. The low level heating changed the local relative humidity reducing the competitive interaction of the water which resulted in an increased organic capacity in the carbon cloth. Isotherms on the cloth at elevated temperatures were conducted with and without applied electrical energy to determine the capacities of the various systems. At higher current densities the adsorbent was heated to the point of regeneration, or in the case of the Ambersorb 572®, to the point of catalytic oxidation of trichloroethylene. Static fields (+1000 V DC) were

applied to the carbon cloth to determine if direct electrooxidation of TCE is possible under lab and field conditions.

3.2 MATERIALS AND METHODS

Water for the humidity bubblers came from a Milli-Q[®] station (Millipore, Molsheim, France) in the lab. TCE in dry nitrogen (500 parts per million by volume [ppmv]) was purchased from Scott Specialty Gas Company (Riverside, CA). TCE in dry air (15 & 1500 ppmv) were purchased from Matheson Gas Products (Joliet, IL). The Amborsorb 572 adsorbent (40x60 mesh, Lot No:923318) was purchased from the Rohm and Haas Company (Philadelphia, PA). The carbon cloth ("Kuractive," FT 200-15, Lot # FK 622096-1B, Kuraray Company, Bizen, Okayama, Japan) was provided, as were the graphite rods (The Carbide/Graphite Group, Inc., St. Mary's, PA). All carrier gases including air, argon, helium, and nitrogen were ultra-pure and purchased from Interstate Gas Company (Marinette, MI).

General lab equipment items are: a mass flow controller 5850 E (Brooks Instrument Division, Emerson Electric Co., Hatfield PA), a low voltage/medium amperage (0-42 V/3 A) DC source 6290A (Hewlett Packard), an Alnor Type 7000 Dew Pointer (Alnor Instrument Company, Chicago, IL) and a Fisher Scientific temperature/humidity monitor (Pittsburgh, PA) to determine relative humidities, and Variac controllers for external heating of the system. The Fisher Scientific humidity meter was calibrated using sulfuric acid solutions at known concentrations yielding constant relative humidities as listed in the CRC Handbook of Chemistry and Physics, 1980.

The lab bench contained a dual AC/DC power supply (Lab-Volt, model 194, Buck Engineering Co, Farmingdale NJ) with an output of 0-36 V at 0-5 Amps (AC frequency was 60 Hz). The HP DC source mentioned above could be operated in two modes: constant current or constant voltage. The Lab-Volt could only be operated in the constant voltage mode.

Sampling procedures to determine the influent and effluent concentrations of TCE, measurement of by-products, and chloride/sulfate production are reported in Chapter 2.

The adsorbent/catalyst materials were used in two different packed-bed configurations. All of the catalytic oxidation reactions were over Ambersorb 572 beads that were in an annular reactor as shown in Figure 3-1. The graphite rod (The Carbide/Graphite Group, Inc., St. Marys, PA; no part or lot number) in the center of the reactor was 1/8 inch in diameter and extended to within 1/2 inch of the bottom. A section of conductive, activated carbon cloth ("Kuractive," FT 200-15, Lot # FK 622096-1B) was used in the bottom of the reactor to keep the adsorbent/catalyst from falling out of the reactor. Electrical isolation was accomplished with Teflon[®] tape and glass tubing connectors.

The carbon cloth was used in a flow through system where the bed was sandwiched between two porous stainless steel electrodes as shown in Figure 4-2b. The flows were metered and inlet and effluent concentrations could be taken as shown in Figure 3-2. The reactors could be heated externally with heat tape, internally with Joule heating, or both. The larger reactor (1.5 inch I.D. by 6 inches long carbon steel column) was used in the annular configuration with thermocouples inside and outside the reactor. The flow-through reactor (quartz glass tube 1/4 inch OD; 1/8 inch ID) only had a thermocouple on the outside of the reactor.

The isotherms were conducted by passing contaminated air at a given flow rate over the adsorbent while monitoring the effluent. When the effluent reached the influent and stabilized for 10 or more hours, the feed was changed to the next higher concentration. The process was repeated until all three concentrations (15,500, and 1500 ppmv) of TCE had been fed through the adsorbent bed. The area under each of the three breakthrough curves was calculated and summed up to give the reported capacities.

The reactor beds for the static electric field experiments were made out of the same glass and screen materials as the flow through cells noted above. The field unit consisted

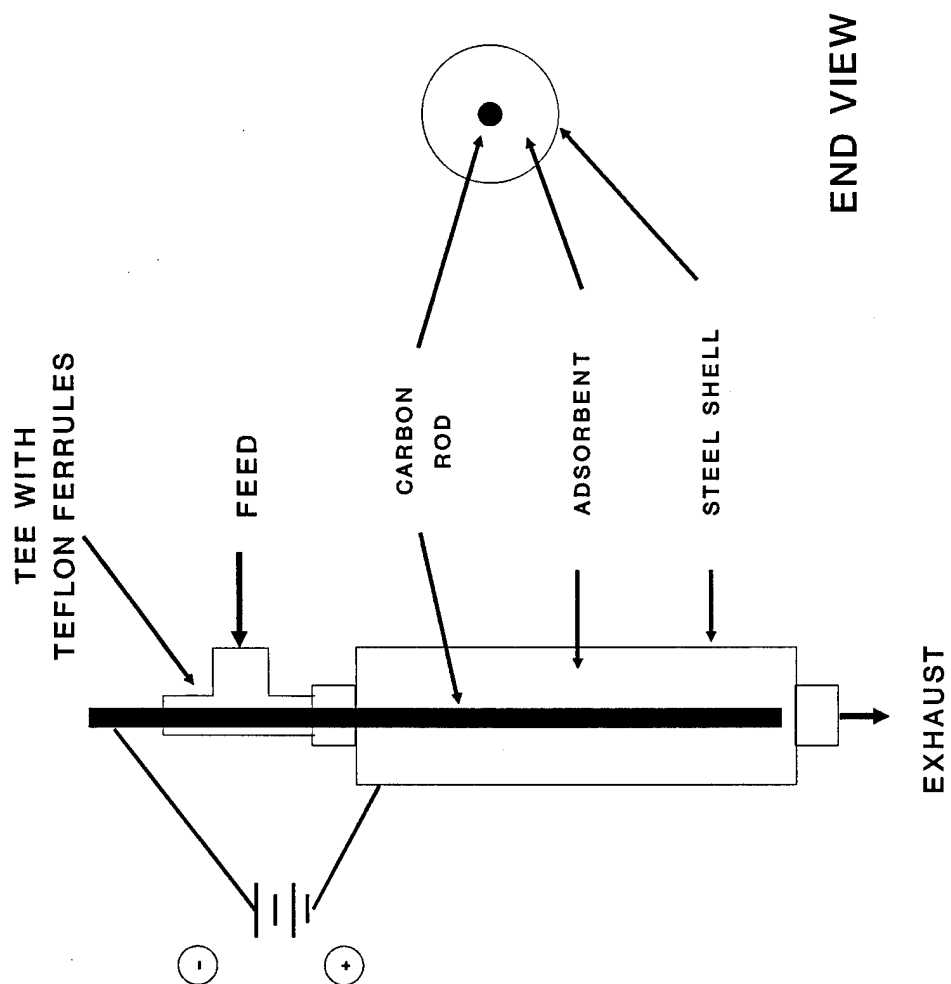


Figure 3-1. Annular Reactor Design

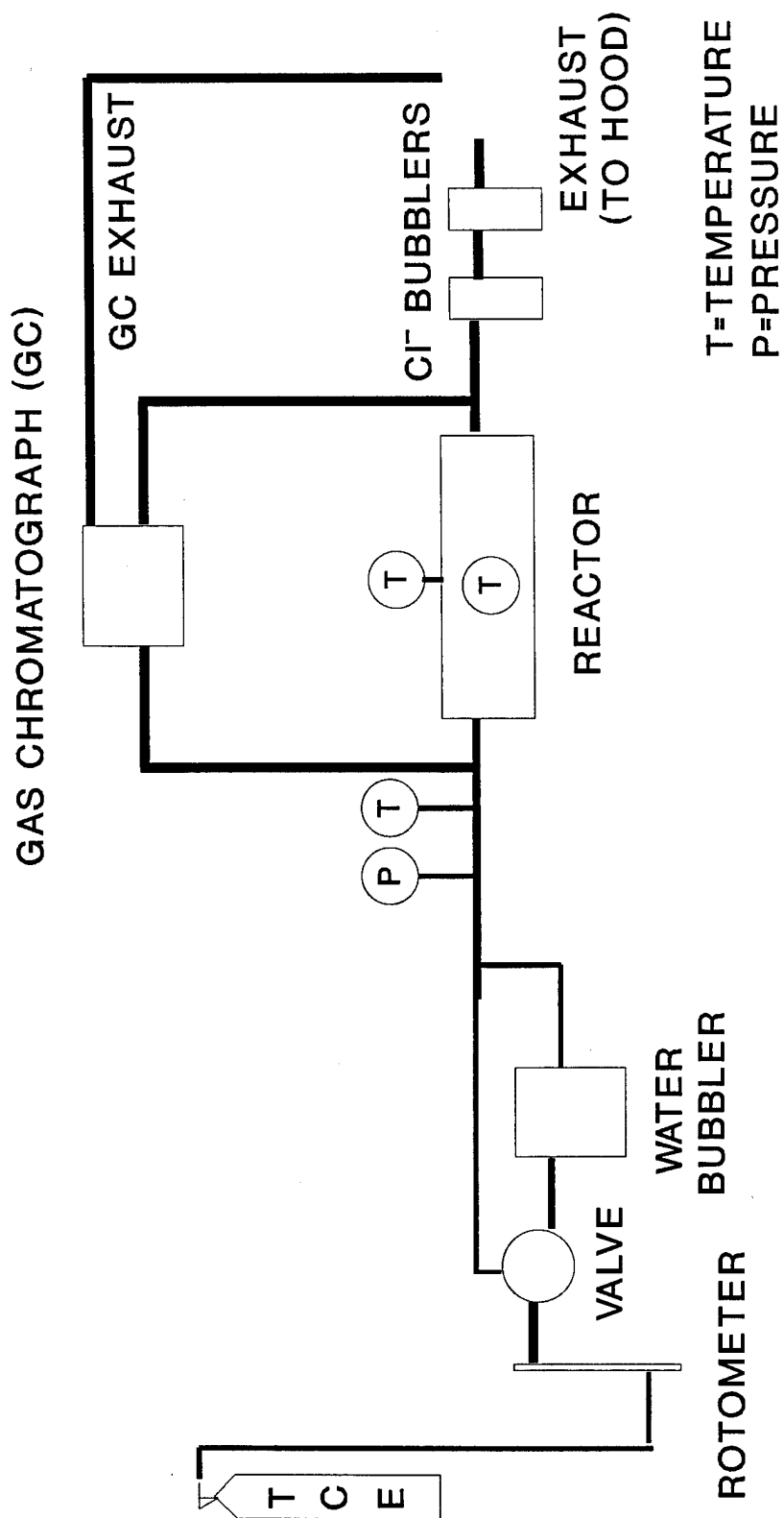


Figure 3-2. Experimental Setup

of a support/electrode stainless steel screen, with two layers of carbon cloth setting upon it with no second screen (unit was vertical with gas flowing from below, past the screen and the cloth sections before exiting). The lab reactor was a flow cell with both stainless steel screens, but the second electrode was not connected.

All the gas flow rates reported herein are based on 1 atm and 22 °C unless otherwise stated. The empty bed contact times (EBCT = volume of catalyst bed/volumetric flow rate) are based on the flow rate at 22 °C. The pressure drop across the bed at the different flowrates used in this study changed by less than 0.5 psi and did not significantly alter the vapor phase concentration.

The term conversion is determined by the amount of TCE in the exit stream as compared to the amount in the feed stream. A 100 percent conversion is defined as the complete loss of the TCE in the effluent. Mineralization is defined as the amount of HCl or Cl₂ found in the traps as compared to that which is expected from stoichiometry. A 100 percent mineralization level indicates that all of the available incoming chlorine is accounted for in the traps.

3.2.1 Adsorbent Characteristics

The plain Ambersorb 572 (AM 572-P) is a sulfonated polystyrene divinylbenzene cross-linked polymeric adsorbent (ion exchange resin) that has been pyrolyzed in a patented process. This adsorbent comes in the form of uniform spherical beads with the characteristics shown in Table 3-1. The material contains micropores, mesopores, and macropores. Inside the pores the sulfonate groups are attached to the polymer material, probably attached as functional groups off the ends of the planar structures shown by Neely and Isacoff (1982). In the micropores, and possibly the mesopores, the sulfate groups are in close enough proximity to interact with one another to hydrogen bond and create strong acidic sites (Gates, 1992).

The carbon cloth (K-cloth), also listed in Table 3-1 for comparison, is essentially phenolic (Novoloid) fibers in a needled felt form that have been pyrolyzed and activated at high temperatures. Thus, heating the cloth to high temperatures to regenerate the adsorbent is not a problem. Unfortunately the AM 572-P is limited to 325 °C in air or breakdown of the adsorbent begins to occur. This limits the operational range of the Joule heating process for the adsorbent.

The thermal conductivity of the AM 572-P is poor and thermal gradients can develop in the beds. Using the AM 572-P in the annular reactor with thermocouples inside the bed and on the outside edge, thermal gradients of 10 degrees Celsius per centimeter (10 °C/cm) were observed during initial heating with heat tape. This points to the use of short electrode spacing in the final reactor design. The carbon cloth has a thermal conductivity of 0.7 mW/cm °K (Hayes, 1993), approximately that of platinum (Robinson, 1987).

TABLE 3-1. ADSORBENT CHARACTERISTICS

ADSORBENT	SURFACE AREA m ² /g	DENSITY g/cc	PORE VOLUME ml/g
Ambersorb 572 [†]	1100	0.49	0.84
Kuraray FT 200-15 ^{††}	730-900	1.27	0.38

[†] Data from Rohm and Haas (1992).

^{††} Data from Cal (1995) and Kuraray Chemical Co.

3.2.2 Field Site Description

The field site (IC-1) is at McClellan Air Force Base (McAFB), an active installation located north of Sacramento in the Central Valley of California. Soil vapor extraction is in use at the site to remove TCE, tetrachloroethylene (PCE), and Freon 113 contamination in the vadose zone. The contaminated vapors are treated in a fluidized-bed catalytic oxidation unit utilizing a chromia oxide catalyst operating at 1100 °F and 630 cfm (Empty Bed Contact Time [EBCT]= 0.8 s). The effluent air goes to a caustic scrubber to remove any HCl or HF that may have formed in the reactor. During the field

study the incoming air concentrations varied but were typically around 15 ppmv TCE and 55 ppmv PCE (Freon 113 was undetectable on the field gas chromatograph [GC]). The feed stream relative humidity also varied from 35 to 60 percent. In the field a Scentoscreen portable GC (Sentex Systems, Inc., Ridgefield, New Jersey) was used that had an argon ionization detector in it. A mixed gas tank of TCE (100 ppmv), PCE (200 ppmv), and Freon 113 (50 ppmv) in dry air was purchased from Matheson Gas (Joliet, IL) to mimic field site conditions. This standard gas was used in the field to calibrate the GC on-site.

3.3 RESULTS AND DISCUSSION

3.3.1 Carbon Cloth Capacities for TCE

Isotherms were performed on the cloth to evaluate the impact of applied electrical potential on the adsorption capacity and relative humidity. Figure 3-3 shows the TCE (15, 500 and 1500 ppmv) isotherm results at 38 °C with dry and humid feeds; with and without electric potential. Heat tape, controlled by a temperature controller, was used to keep the bed at isothermal conditions. As the amount of Joule heating increased, the heat input from the heat tape automatically reduced, maintaining the temperature of the bed at 38 °C (± 0.3 °C). As shown in Figure 3-3, no increase in capacity was noted with an applied potential. Indeed, there appears to be a negative influence, however the difference is within experimental error. This indicates that the effect at these potentials is due to the changes in the relative humidity and not due to electrosorption occurring on the surface. As can be seen, the capacity is reduced at the 1500 ppmv level with water addition, regardless whether the electrical potential is there or not.

Humidity (80 percent RH) has a much larger impact on the capacity than temperature. A 15 ppmv TCE dry feed at 25 °C (not shown in Figure 3-3) resulted in essentially the same capacity as the dry 38 °C loading. However, the difference between the dry and humid 25 °C loadings (a factor of about 9) is due to the loss of capacity from relative humidity effects. Localized Joule heating of the bed decreases the RH and

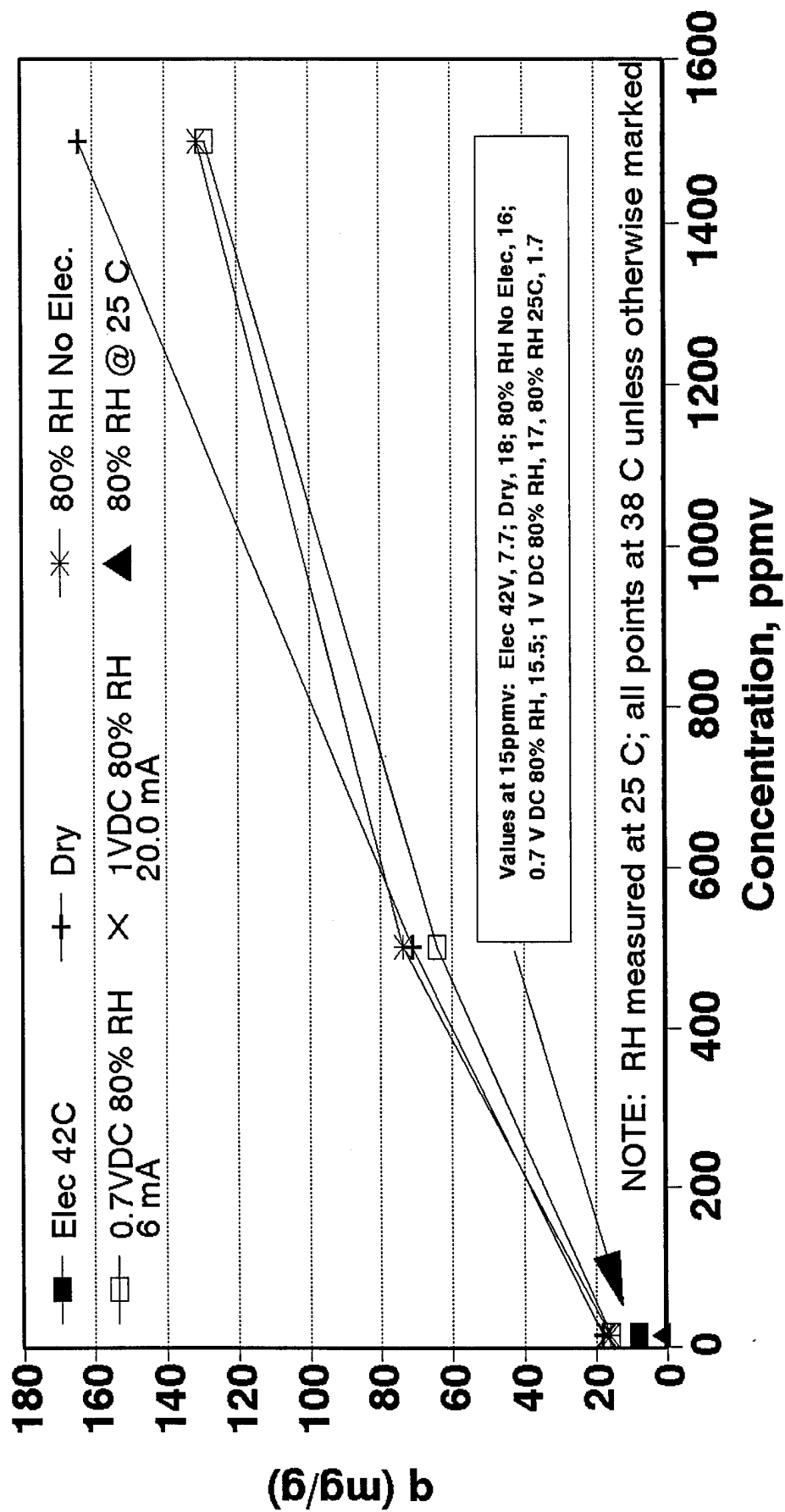


Figure 3-3. Cloth Isotherms at 38 C in Trichloroethylene Flow Cell

dramatically increases the capacity of the bed over the non-heated capacity. However, heating the bed too much results in a decreased adsorption capacity (see Figure 3-3; 42 °C, 15 ppmv, isotherm point)

3.3.2 Joule Heating

When discussing Joule heating it is important to address the type of electrical energy used (AC or DC), the magnitude of the applied potential, and the reactor design (packed bed or annular). Another factor is the distance between electrodes (length of resistor). Increased resistance is desirable to keep the power requirements low for a given heating cycle, however hot and cold spots can develop in a large bed with large distances between electrodes.

3.3.3 Joule Heating of Activated Carbon Cloth

Low level Joule heating of the carbon cloth in humid feeds showed an increased capacity with the application of a small potential over the initial room-temperature capacity. Figure 3-4 illustrates this effect. The initial short breakthrough is at 25 °C and 80 percent RH. An applied potential of 4 VDC (30 mA) raised the bed temperature to 42 °C and caused the effluent to drop, an indication that the bed was adsorbing more TCE. At an EBCT of 0.1 s the exiting air temperature was only 0.5 to 1 °C warmer than the inlet air temperature. The increase in capacity is approximately 4.5 times (the capacities are also shown in Figure 3-3 as the humid feed at 25 °C and electroheated capacity at 42 °C). This is not an optimized system and capacities greater than this are expected. Based on the data in Figure 3-3 at 38 °C the capacity increase could be as much as 9 times greater than the non-heated capacity. This increase in capacity is due to the competing effects within the adsorbent. As the adsorbent gets hotter, the overall capacity is reduced due to thermal interactions, however the relative humidity is also reduced and the capacity for the organic increases.

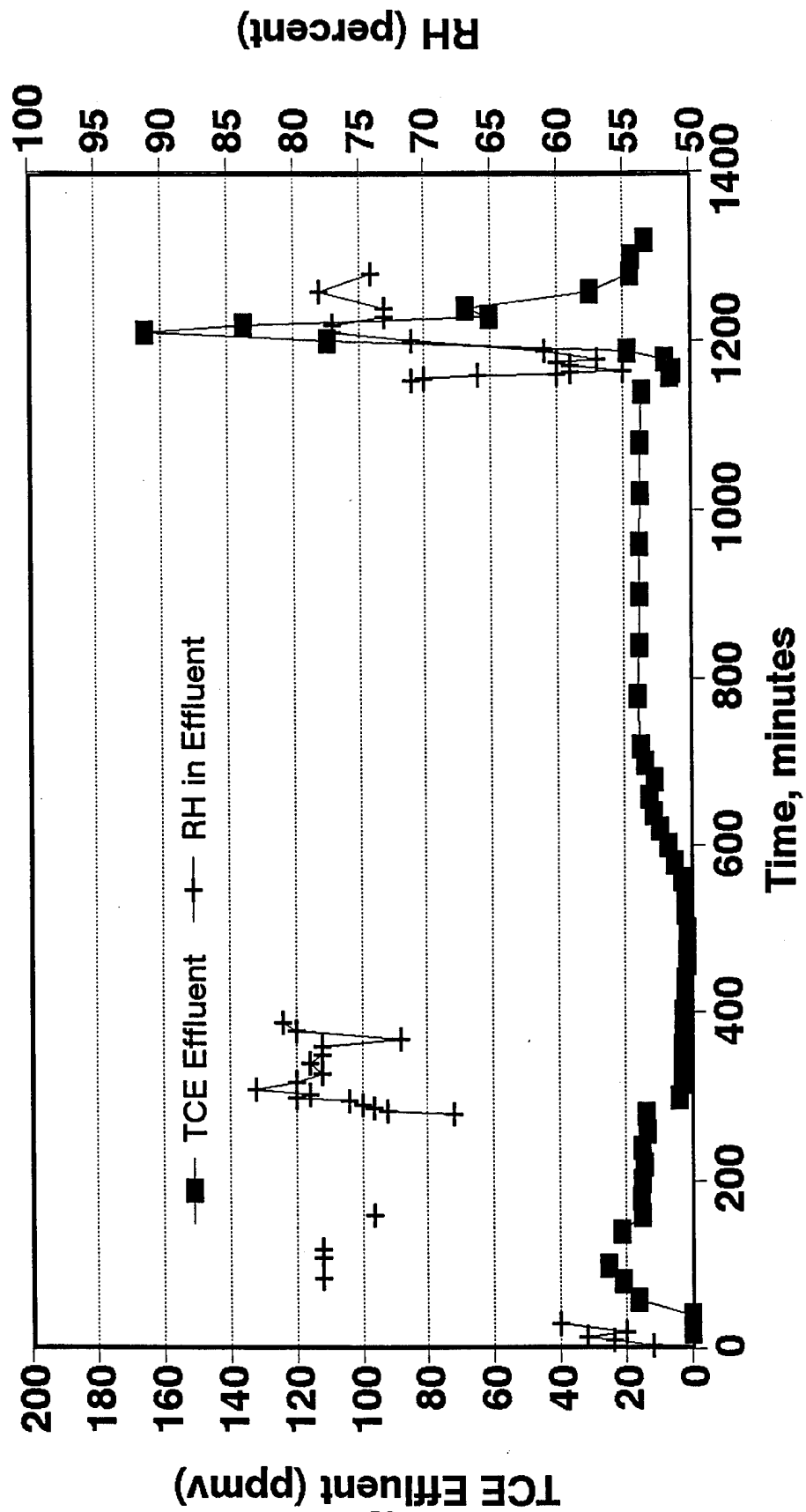


Figure 3-4. Humidity/Joule Effect on Carbon Cloth, Humid 15 ppmv TCE Feed,
0.1 s EBCT, 1 atm

When the applied potential is removed the excess adsorbed TCE is rapidly desorbed with a peak maximum concentration of 160 ppmv, or about a ten fold increase in concentration. The cycle is repeatable, with the same capacity and desorption curves resulting. The power input to create this additional capacity is 0.6 w-hr (36 w-hr/gram adsorbent). An alternative process (Crittenden et al., 1988) would heat the incoming air to reduce the humidity, instead of locally reducing it at the adsorbent surface. The incoming air has an enthalpy at saturation of 36.3 Btu/lb dry air. At 42 °C the RH would have dropped to 33 percent and the enthalpy at saturation would be 45.3 Btu/lb dry air. Heating to 42 °C the same volume of air that passed over the adsorbent during the increased capacity time would have required 0.1 w-hr of power, or 1/6th the amount from the Joule heating. The system is not optimized as to design or materials and the factor of six difference may be a conservative estimate.

The heating input to raise the bed to 42 °C is not factored in the above numbers for the air-heating option, but is estimated to be 0.05 cal, based on a Specific Heat of carbon at 0.168 cal/g-°C (Robinson, 1987). Based on the small thermal increase of the incoming air over the Joule heated bed, it is expected that the heat transfer to the bed would be slow and it would take some time to heat the bed initially. Therefore, an optimized system would utilize Joule heating to rapidly heat the bed initially to the desired temperature and then utilize incoming air that was preheated to maintain the desired bed temperature to reduce the RH over the adsorbent.

3.3.4 Joule Heating of Amborsorb 572

The electron flow within the bed of Amborsorb beads is expected to flow radially through a given cross section of the bed. Due to the design of the reactor the actual electron density will be higher at the center graphite rod, however. Inside the individual particles variations in current density are also probable. Due to the porous nature and physical makeup of the polymer, the electron flow inside the particle may take a tortuous path within the bead, traveling from one pyrolyzed polymer section to another, possibly even by way of the sulfonate groups (if those groups are in close enough

proximity to allow electron transfer). If the adsorbent is heated too rapidly these electron flow paths may heat portions of the bead beyond safe limits, even though the bulk bed temperature is well below the temperature limit of the material. Indeed, MTU-CAT, a Joule-heated catalyst created from plain Ambersorb 572, was heated rapidly changing the pore shape and catalytic performance as discussed in Chapter 2.

Joule heating, at sufficiently high potentials, can provide the thermal energy of activation for the catalytic oxidation of TCE. Plain Ambersorb 572 has been shown to have catalytic properties (Chapter 2, this work; Petrosius et al, 1993; and Petrosius and Drago, 1992) for the oxidation of chlorinated organics.

As discussed in Chapter 2, heat tape was used on an annular reactor to provide the initial 200 °C heating input to drive the oxidation reaction with TCE. This reduced the incoming, dry, 1500 ppmv feed, to less than 1 ppmv (detection limit on gas chromatograph). Joule heating, both AC (60 Hz) and DC, was used to replace the heat tape and the TCE effluent concentration remained below detection limits over multiple testing sequences. Reducing the temperature of the reaction to 180 °C and repeating the multiple testing sequences gave the same result: complete conversion of TCE in the reactor. A limited number of experiments were done even as low as 140 °C, with no detectable TCE in the effluent. A summary of the conditions used are shown in Table 3-2.

3.3.5 Electric Field Influences on Regeneration

Regeneration of adsorbents can be done with Joule heating alone, or in combination with steam. Hand, et al (1995) showed effective regeneration by using a combination of electricity and steam to clean samples of Ambersorb 572 which had been loaded with TCE in the liquid phase. The steam-alone process had broader peak effluents and longer tails, while the electroenhanced process had higher, sharper effluent profiles and almost no tailing. This is due to the internal heating of the bed by the Joule heat, increasing the internal thermal energy of the bed. This may have kept the steam from condensing in the pores and slowing mass transfer out of the adsorbent.

TABLE 3-2. TEST CONDITIONS DURING JOULE HEATING EXPERIMENTS
(1500 ppmv TCE feed).

Voltage Applied	Temperature (°C)	EBCT (sec)
2.5-4 V DC	199-204	43
4-5 V DC	198-205	43
5-5.5 V DC	201-207	43
5.5-6 V DC(R) [†]	199-206	43
6 V AC	194-197	43
10.5-11 V AC	198-210	43
1.5-4.5 V DC	199-200	7.5
4.5-7 V DC	196-202	7.5
9-10.5 V DC	192-210	7.5
7 V DC	202	7.5
6-10 V AC	198-209 [□]	7.5
2.7-5.2 V DC	197-204	2.9
5.2-7 V DC	195-205	2.9
2.7-4 V DC	177-190	27
4 V DC	184-186	27
4 V DC	183-185	9.8
4 V DC	182-183	4.8
4 V DC	180-182	3
2.7-16.5 V DC	141-159	2.9
7.5-10.5 V DC	153-161	2.9

[†] Reversed polarity on cell.

[□] Initial switch to AC resulted in a temperature rise to 231 °C in less than 1 minute. Temperature was back to 209 °C within 4 minutes.

In regeneration experiments with the liquid-loaded AM 572-P using Joule heating alone, the process did not work very well. As the adsorbent dried it clumped

together, pulling itself away from the electrodes in the annular reactor. This loss of electrical contact caused problems of uneven heating. This problem could be avoided by switching to a different reactor design, using different materials, or both. For example, if the reactor was agitated by an air blast to break up the clumps, this would allow the current to flow again. The liquid-loading work of Economy and Lin (1976) with phenol showed that the cloth fibers do not show this tendency and could be effectively regenerated from liquid loadings.

There is a more important drawback to regenerating these adsorbents with Joule heating however. The resistance of the carbon cloth decreases when the material is heated (the semiconductor behavior noted by Petkovska, 1991). As the adsorbent heats, the hot areas become more conductive and more current flows through that section of the bed. Of course, as more current flows, the hotter that section becomes and the process is in a vicious cycle until the adsorbent is red hot and glowing. Indeed, in one early experiment a copper electrode end was melted (mp 1083 °C) during a rapid heating cycle. In addition, as discussed in the next chapter, when an organic adsorbs to the cloth the resistance increases. Thus, the areas that need the regeneration the most are also the most resistive and the electron path will favor "clean" adsorbent sections since they are more conductive.

Care can be used to minimize this effect by proper electrode configuration, spacing, and heating rates. For example annular heaters can be used to evenly distribute the charge along the length of the bed, obtaining a radial direction of electron flow and heating. However, the adsorbent in the interior would experience a higher current density and a thermal gradient in the radial direction would develop. A better alternative would be to have large flat plates or flow through screens to get an even distribution of current prior to going through the adsorbent bed. In preliminary experiments it is anticipated that the electrical costs for regeneration are 16 \$/m³, based on a 200 °C heating cycle for 10 hours. This is in comparison to 110 \$/m³ for steam regeneration (assuming 20 Kg steam/Kg adsorbent, and \$5/1000 lb steam [Rick et al, 1987])

3.3.6 Electrostatic Field Affects over Carbon Cloth

Laboratory and field experiments were performed to evaluate the impact of Joule heating on the catalytic oxidation of TCE over carbonaceous adsorbents. The static fields are applied at ambient temperatures, however, some current flows during the experiments as indicated by the small increase in bed temperature. The laboratory feed consisted of just trichloroethylene (TCE), whereas the field feed stream has TCE, tetrachloroethylene (PCE), and Freon 113.

Using 4 sections (0.007 g) of the carbon cloth in a 1/4" OD flow-through reactor, the effects of a static electric field were first investigated in the laboratory. A stream of humidified TCE in air (15 ppmv; EBCT = 0.1 s) was passed through the bed. Sufficient volume was used to reach capacity loading at room temperature (effluent=influent). A static potential of +1000 V was applied to the effluent-end stainless steel screen holding the cloth in position. The temperature of the bed rose 6 °C above room temperature within 20 minutes and remained stable. The effluent decreased due to the relative humidity shift described above. After 15 hours the effluent TCE concentration was about 60 percent of that coming in. In addition, there were 4 new peaks on the chromatogram output. Based on retention times three of them were tentatively identified as carbon tetrachloride, chloroform, and PCE. The fourth peak was an unknown. Unfortunately, when attempting to get a chloride sample the reactor broke losing any other confirmatory information on the reaction. Time constraints for the field work did not allow for a repeat experiment.

Direct electrooxidation of TCE was attempted again under field conditions at McAFB, Site IC-1. Two sections of the carbon cloth were supported on a stainless steel screen that was charged to +1000 V DC. The contaminant stream varied from 35-55 percent relative humidity and flowed up through the screen, through the bed and to chloride traps (two in series). No heat control was used on the bed, and ambient temperatures ranged from 17-38 °C. Field results showed no difference between influent and effluent TCE/PCE concentrations. Chloride analysis of the traps verified this, but also

showed fluoride in the effluent. Thus, while TCE and PCE were not being affected, the Freon 113 was at least partially oxidized.

Under these electrostatic conditions the carbon cloth individual fibers would have been charged on the outer surfaces of each rod-shaped fiber. Some electron flow did occur, based on the Joule heating that was noted. The barriers between two graphitic-ordered domains, separated by an amorphous sea, would have caused induction of the charge as shown in Figure 3-5. These charge separations at the boundaries may have had some impact on the reaction.

Under electrodynamic conditions the charges would have been spread throughout the rod not just on the outer shell of the fiber. In order to take advantage of the high surface area for catalysis (and the sulfonated groups in the Amborsorb-based catalysts) electrodynamic conditions need to be used. However, when this is done, there is Joule heating that also occurs and separating the thermal vs. electrolytic effects are not possible.

3.4 CONCLUSIONS

Joule heating can rapidly heat the adsorbents used in this study as well as enhance the desorption rate during steam regeneration. However, hot spots can occur in an adsorbent bed and controls (bed design, electrode spacing, heating rate) are critical to limiting their effects. Regenerating liquid loaded Amborsorb 572 with Joule heating is problematic and a final design will require special agitation tools. Low level Joule heating can increase the capacity of the carbon cloth for TCE in humid streams. However, once the bed is hot, the energy costs indicate that heating the incoming air would be cheaper than heating the bed with Joule heating. In addition, cooling the bed back down in a humid stream removes TCE from the surface, not completely regenerating it but rather releasing the excess adsorbed under reduced RH conditions. Thus an adsorption/regeneration cycle could be used for just the increased capacity of the adsorbent due to the RH shift to concentrate the organics in the air stream. In strong electrostatic fields (+1000 V DC) direct

Charged Carbon Fiber
(not to scale)

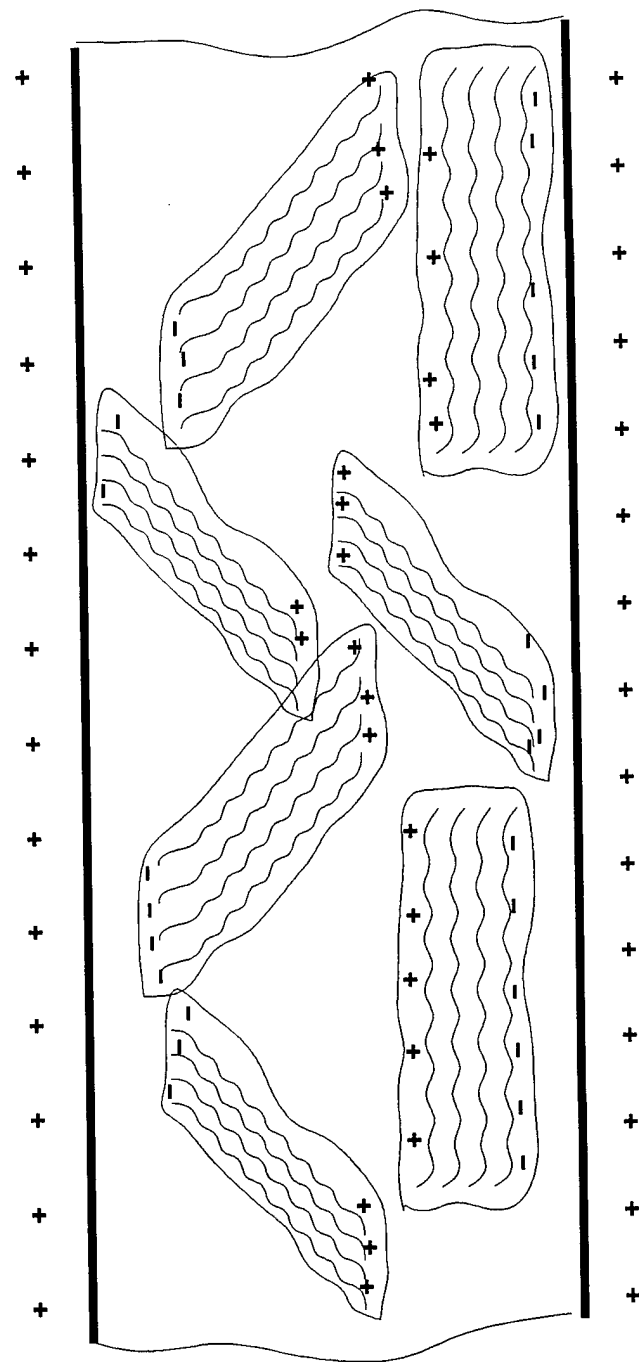


Figure 3-5. Electrostatic Charge on Fiber Induces
Charge in Crystallites Within Carbon Fibers

electrooxidation of TCE in the lab, and Freon 113 in the field, is suggested based on the limited data. Further work is needed to verify the finding.

3.5 ACKNOWLEDGEMENTS

This work was funded jointly by the Superior Engineering Technologies, Inc., Houghton MI 49931, and the Environics Directorate of the U.S. Air Force's Armstrong Laboratory, Tyndall AFB FL 32403, Maj Mark Smith, Project Officer. Support from Michigan Technological University is greatly appreciated. Mention of trademarks and trade names of material and equipment does not constitute endorsement or recommendation for use by the U.S. Air Force, nor can this article be used for advertising the product(s).

3.6 REFERENCES

Cal, M.P., "Characterization of Gas Phase Adsorption Capacity of Untreated and Chemically Treated Activated Carbon Cloths," Environmental Engineering in Civil Engineering PhD Dissertation, University of Illinois at Urbana-Champaign, 1995.

Crittenden, J.C., Cortright, R. D., Rick, B., Tang, S-R., and Perram D.L., "Using GAC to Remove VOCs From Air Stripper Off-Gas," *Journal of American Water Works Association*, pp 73-84, May 1988.

Davis, M.M., "Studies on the Optimal Thermal Regeneration of Adsorption Beds," Chemical Engineering PhD Dissertation, University of Virginia, 1987.

Economy, J., and Lin, R.Y., "Adsorption Characteristics of Activated Carbon Fibers," *Applied Polymer Symposium*, No. 29, pp. 199-211, 1976.

Gates, B.C., "Catalytic Chemistry," John Wiley and Sons, 1992.

Hand, D.W., Crittenden, J.C., and Perram, D.L., "Electrocatalytic Oxidation of Trichloroethene", SBIR Final Report, Jan 1995, in publication.

Hayes, J.S., "Novoloid and Related Fibers in Nonwoven Structures," INDEX 93 CONGRESS, Session 2C - Fibres, Geneva, 20 April 1993.

Hoenig, S.A., and Lane, J.R., "Chemisorption of Oxygen on Zinc Oxide, Effect of a DC Electric Field," *Surface Science*, **11**, pp 163-174, 1968.

Holder, W.D., "The Effect of an Electrostatic Field on the Adsorption Capacity of a Fixed-Bed of Activated Carbon," Masters Thesis, Chemical Engineering, Clemson University, 1970.

Katsura, Shinro, "Activated Carbon-Based Adsorbents for Air Purification," Jpn. Kokai Tokyo Koho, 7 pp., 1991.

Lordgooei, M., Kelly, T., Covington, B., Carmichael, K., Rood, M., and Larson, S., "Development of an Activated Carbon Cloth (ACC) Cryogenic system to Recover and Reuse Toxic Organic Vapors," presented in Section: Carbon-Based Materials for Gas Separations, Purification & Cleanup, American Institute of Chemical Engineers Spring National Meeting, Houston, TX, March 20, 1995.

Ozawa, Tateki, "Adsorption Apparatus for Treating Foul Smelling Gases," Japan. Kokai, 3 pp., 1978.

Neely, J.W., Isacoff, E.G., "Carbonaceous Adsorbents for the Treatment of Ground and Surface Waters," Marcel Dekker, Inc., New York, p. 61, 1982.

Petrosius, S.C., and Drago, R.S., "Decomposition of Chlorinated Hydrocarbons Using Metal Oxides Supported on Carbonaceous Adsorbents," *J. Chem. Soc., Chem. Commun.*, 1992, pp 344-345.

Petrosius, S.C., Drago, R.S., Young, V., and Grunewald, G.C., "Low-Temperature Decomposition of Some Halogenated Hydrocarbons Using Metal Oxide/Porous Carbon Catalysts," *Journal of the American Chemical Society*, 115, pp 6131-6137, 1993.

Petkovska, M., Tondeur, D., Grevillot, G., Granger, J., Mitrović, M., "Temperature-Swing Gas Separation with Electrothermal Desorption Step," *Separation Science and Technology*, 26(2), pp. 425-444, 1991.

Petkovska, M. and Mitrović, M., "Dynamics of Electrothermal Desorption Process: A Heterogeneous One-Dimensional Macroscopic Model," *J. Serb. Chem. Soc.*, 57(5-6), pp. 319-332, 1992.

Rick, B.G., Crittenden, J.C., Cortright, R.D., Tang, S-R., Perram, D.L., and Rigg, T.J., "An Evaluation of the Technical Feasibility of the Air Stripping Solvent Recovery Process: Volume 3: The Regeneration of Granular Activated Carbon with Steam and Liquid CO₂," American Water Works Research Foundation Research Report - Subject Area: Water Treatment and Operations, 1P-5C-90525-8/87-TC, June 1987.

Robinson, R.N., "Chemical Engineering Reference Manual," 4th Edition, Professional Publications, Belmont, CA, 1987.

Rohm and Haas, "Technical Notes: Ambersorb[®] Carbonaceous Adsorbents, Specialty Purifications," August 1992.

Stankiewicz, Zdzislaw, Schreiner, H., "Direct Electrical Heating of Activated Carbon," *Chem.-Ztg.*, 114(12), pp. 379-81, 1990.

Vol'kenshtein, F.F., "The Electronic Theory of Catalysis on Semiconductors," translated by Anderson, N.G., translation edited by Birch, E.J. H., A Pergamon Press Book, The Macmillan Company, New York, 1963.

Woodard, F.E., McMackins, D.E., and Jansson, R.E.W., "Electrosorption of Organics on Three Dimensional Carbon Fiber Electrodes," *Journal of Electroanalytical Chemistry*, **214**, pp 303-330, 1986.

Yeh, G.C., "Ammonia Synthesis with Electrostatically Charged Catalyst," U. S. Patent 3,368,956, Feb. 13 1968.

Ambersorb® is a trademark of the Rohm and Haas Company.

Chapter 4

Electronic Factors of Adsorption on Carbon Fibers

4.1 INTRODUCTION

Gas phase adsorption occurs on the surface and in the pores of the adsorbent. In physisorption the adsorbate (the substance being adsorbed) is held by a combination of van der Waals and electrostatic forces. In contrast, chemisorption occurs with the actual transfer of electron(s) between the adsorbent and the adsorbate. The adsorption phenomenon is usually categorized as physisorption and chemisorption (Sontheimer et al 1988) and it is difficult to distinguish them at times. In micropores the forces from the adjacent walls overlap creating high energy adsorption sites. Chemisorption at these sites may occur while physisorption is simultaneously occurring at lower energy sites, including surface sites not associated with pores. In addition, different molecules with different dipole moments and sizes will have different affinities for various adsorbents.

Two forms of activated carbon cloths (ACC) made from fibers were used as adsorbents in this study. The first form, predominantly used in this study, is a non-woven material with the consistency, texture, and appearance of felt. The second form is a cloth weave where the fibers are spun into long strands which are then woven into a cross pattern to yield a cloth-like appearance. Hayes (1994), in company literature from American Kynol, gives an excellent treatise on how the fibers are made from phenolic precursors (Novoloid fibers). He describes the pyrolyzation process and ways to modify the surface of the materials for a variety of applications. Some characteristics of the fibers are listed in Table 4-1. The impact of an applied potential on the adsorption of organic compounds was evaluated. The organic compounds are of industrial importance and span a wide range of adsorption strengths.

TABLE 4-1. CHARACTERISTICS OF ACTIVATED CARBON MATERIALS

	Cloth Weave	Needled Felt
Diameter, μm	10	10
Density, g/cc	1.4-1.6	0.1
Surface Area, m^2/g	1500	1500
Thermal Conductivity, $\text{W}/\text{m}^\circ\text{K}$	--	0.72

From Hayes (1993, and 1994) and Kuraray Company, Inc.

The carbon fibers are pyrolyzed and activated in one step (Hayes, 1994). The resulting fiber is approximately 95 percent carbon and contains crystallites that are sets of graphitic, or basal, planes stacked one upon another as shown in Figure 4-1. The area between the crystallites is amorphous carbon, probably tetrahedrally bonded, and other impurities (e.g. oxygen, water, etc.) may also be in these interstitial areas. These zones between the crystallites are prone to oxidation during the activation process as the graphitic planes are quite stable. Thus major portions of the areas between the crystallites are etched away during the activation process as shown by the shaded area in Figure 4-1. If the activation process continues then the edges of the crystallites are also etched away. These opened areas become the micropores for adsorption. The crystallites are in random order, giving the fiber an overall amorphous appearance when examined spectroscopically, such as X-ray diffraction reported by Hayes (1994).

Intra particle electron conduction in the crystallites is favored along paths that are parallel to the basal planes as shown by path "A" in Figure 4-1. Conduction perpendicular to the basal planes as shown by path "B" in Figure 4-1 is possible, but it is not the preferential path. Inter particle, or transitions between particles, may occur by hopping as indicated by path "C" in Figure 4-1. The conductive polymer literature describes electrical conduction in polymers in similar terms with the charge carrier hopping from one crystallite to another with distances up to 7 Å (Thakur and Elman, 1989).

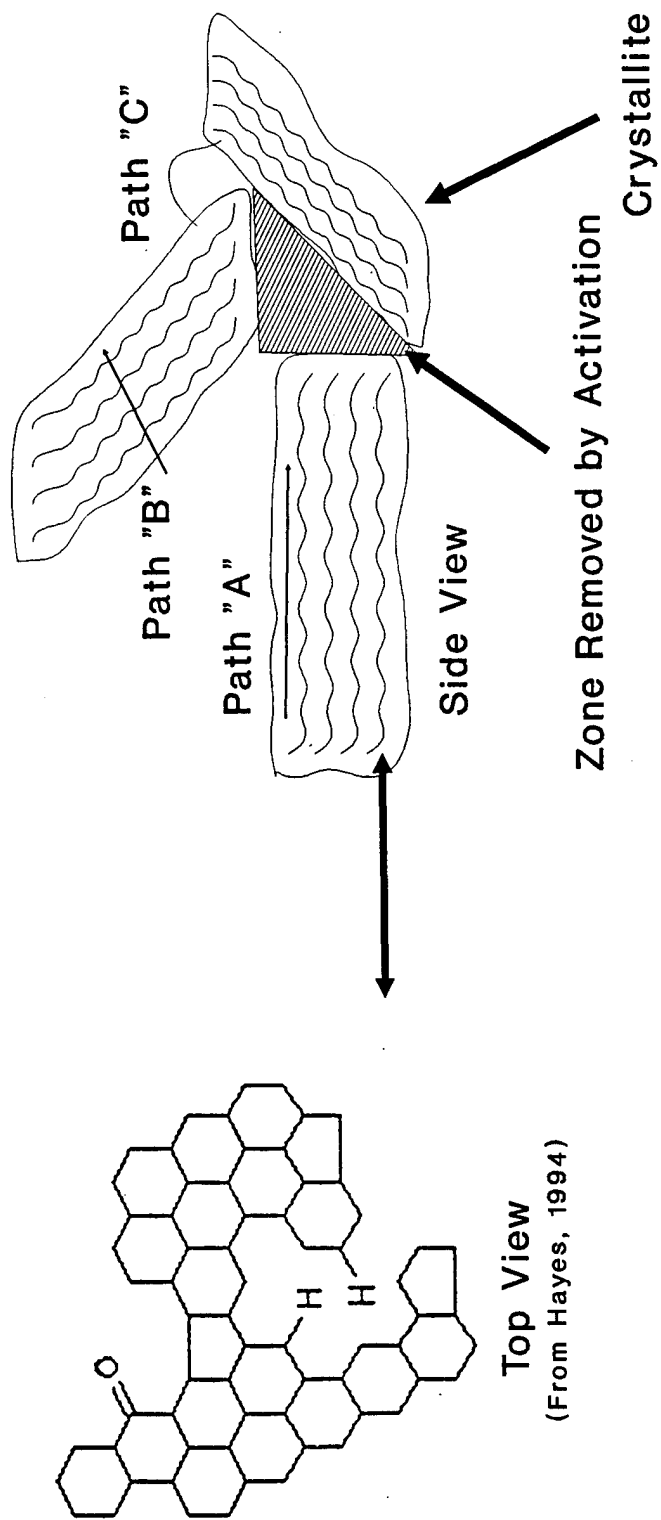


Figure 4-1. Electron Paths in Graphitic Planes and Crystallites in Cloth Fibers

The micropores in the ACC used in this study account for its large surface area. Using nitrogen adsorption data, Cal (1995) reported that all of the pores for the ACC-15 sample (another Novoloid-based activated carbon cloth made by Kynol Inc., similar to the woven structure in this study) were in the micropore region ($d < 2$ nm). This concurs with the report from Hayes (1994) which showed essentially no mesopores in the materials. Hayes also mentions the electrical conductivity of the cloth, and even suggests using it in capacitors because of its high surface area.

Granular activated carbon (GAC) has a different structure, containing micropores, mesopores, and macropores, however the two adsorbents, ACC and GAC, are similar in their adsorption trends. Recent work (Cal, 1995) and related on-going work (Lordgooei, 1995) at the University of Illinois at Urbana-Champaign utilizes the activated carbon cloth made from Novoloid fibers. Cal found that the carbon fibers have the same general adsorption trends as GAC. That is, compounds adsorbed strongly to GAC were found to be strongly adsorbing to the carbon fiber and visa versa. In addition, he found that water competes for the available adsorption sites.

While no references can be found relating the adsorption of organics to resistance change on carbon fibers, others have explored physical changes that can occur when using the cloth material. A group of French researchers (Baudu et al, 1992) found an empirical relationship for the resistance change the carbon cloth undergoes when heated. They modeled both carbon fibers and GAC, resulting in an equation that describes an exponential decay in the resistance with increasing temperature.

In this study seven compounds with varying adsorption potentials were tested to determine the impact of adsorption on activated carbon cloth and the resulting changes in resistance. Static (no flow) and dynamic (with flow) isotherms were conducted to determine the effect of concentration, single solute effects, and water-component interactions on the resistance change in the adsorbent.

4.2 MATERIALS AND METHODS

Tanks of prepared gases were used for the flow through (dynamic) isotherms. Trichloroethylene (TCE) in dry nitrogen (500 parts per million by volume [ppmv]) was purchased from Scott Specialty Gas Company (Riverside, CA). TCE in dry air (15 & 1500 ppmv) was purchased from Matheson Gas Products (Joliet, IL). The gases were used without drying.

The carbon cloth came in two forms and both were provided by the Kuraray Chemical company (Bizen, Okayama, Japan). The non-woven, felt-like material called "Kuractive," (FT 200-15, Lot # FK 622096-1B) is used the most in this study and referred to as "activated carbon cloth". While the woven material is also called "Kuractive" (CH700-15, Lot # CKA 630042-2), it is referred to as "woven" material in this study. The carbon cloths were used "as-received" and not pre-treated prior to use.

All chemicals used in the experiments and analyses were reagent grade or better. Reagent grade dichloromethane (99.9+%), methanol, carbon tetrachloride, tetrachloroethylene, trichloroethylene, and toluene were purchased from Aldrich Chemical Company (Milwaukee, WI). The water came from a laboratory Milli-Q station (Molsheim, France).

For the dynamic isotherms on-line gas-phase samples were analyzed according to the Environmental Protection Agency's Reference Method 23 (Scott Environmental, 1983) using a Hewlett Packard Model 5880A gas chromatograph equipped with a flame ionization detector (FID). Compound separation was performed using a packed column (3 percent DBP 1500, 80/120 Carbowax® B) (Supelco, PA). The gas samples passed through stainless steel lines into a six-port valve (Model RD6P, Valco) that was heated to 160 °C (Valco Instrumentation Temperature Controller). A 50 μ L sample loop attached to the six-port valve provided a gas sample size that yielded a TCE detection limit of about 1 part per million by volume (ppmv).

The experimental set-up used for the static single solute resistance measurements is shown in Figure 4-2a. Pure phase solutions of the chemicals were injected with a disposable syringe (Syringe & PrecisionGlide Needle, 322IM1½ 23GTW, Becton Dickinson & Co., Franklin Lakes, NJ) below the cloth samples, resulting in air concentrations in the isotherm bottle equal to the vapor pressure of the organic at room temperature. Excess was used to ensure complete saturation of the cloth. Nichrome wires held the cloth in place and acted as the electrodes.

The dynamic isotherms were taken in a flow through glass cell (1/4 inch OD, 1/8 inch ID) with stainless steel screens to hold the cloth sections in place as shown in Figure 4-2b. Only trichloroethylene dynamic isotherms were conducted on stacks of circular cloth sections. All dynamic adsorption experiments used 12 cloth sections, except for the work shown in Figure 4-5 which used 48 sections. Nichrome wire was used to connect to the stainless steel screens, with the other end contacting the interior of the stainless steel lines before and after the glass tubing. Exterior connections were then made to the volt-ohm meter using hose clamps and copper wiring (12 gauge).

All experiments were conducted at room temperature and 1 atm unless otherwise noted. The pressure drop across the bed at the different flowrates used in this study changed by less than 0.5 psi and did not significantly alter vapor phase concentrations.

4.3 RESULTS AND DISCUSSION

4.3.1 Adsorbent Characteristics

The fibers in the adsorbent are approximately 10 microns in diameter and have various lengths. The carbon cloth, or needled felt, is a jumble of the fibers entangled together into a cloth. The cloth weave is a series of fibers (40-50) entwined to form a strand. Three strands are woven together to form one cross-hatch material in the final fabric. The adsorbents were activated and carbonized in a single step, with a reported surface area of 1500 m²/g (Hayes, 1993). At pyrolyzation temperatures above 700 °C the

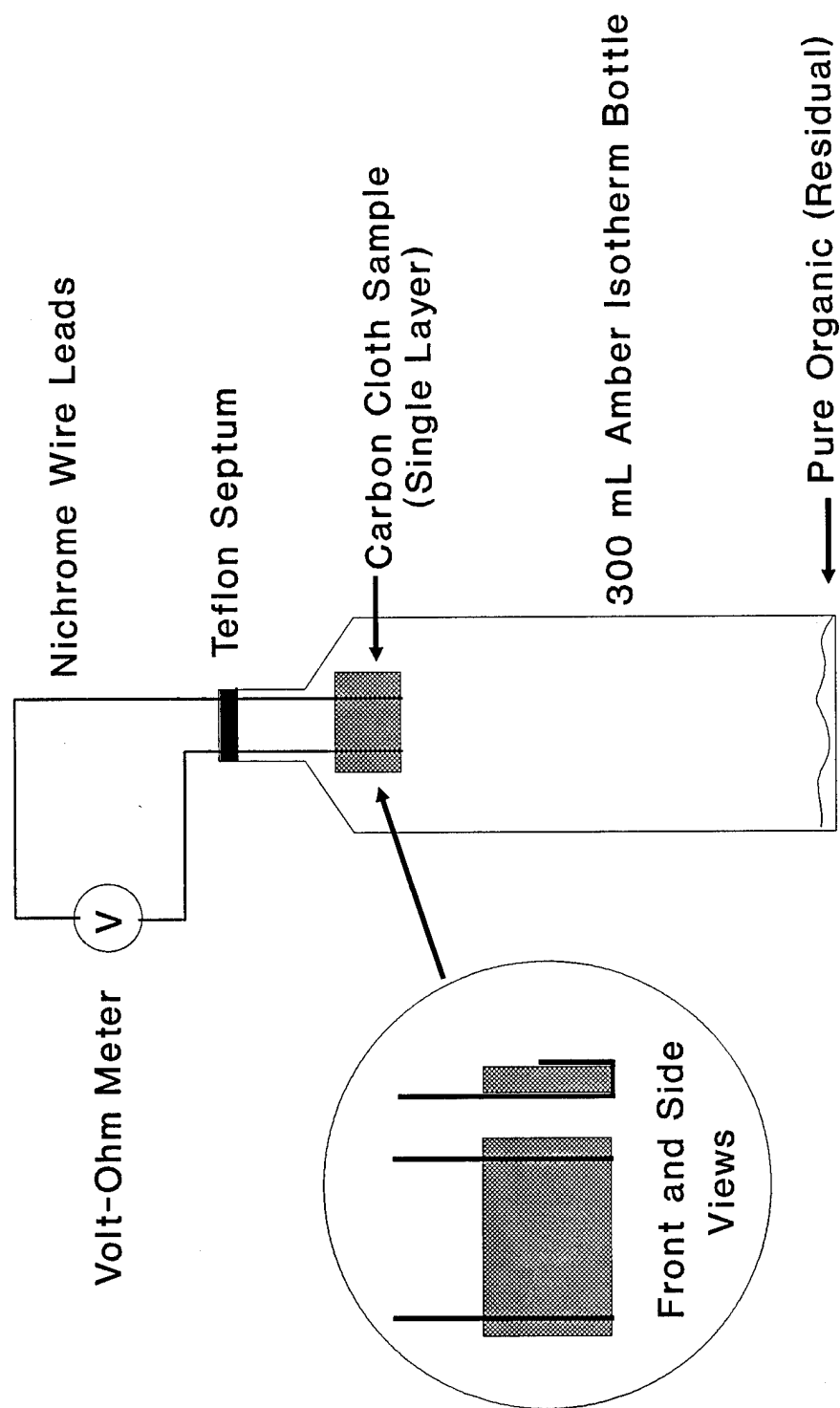


Figure 4-2a. Resistance Isotherm Setup for Cloth

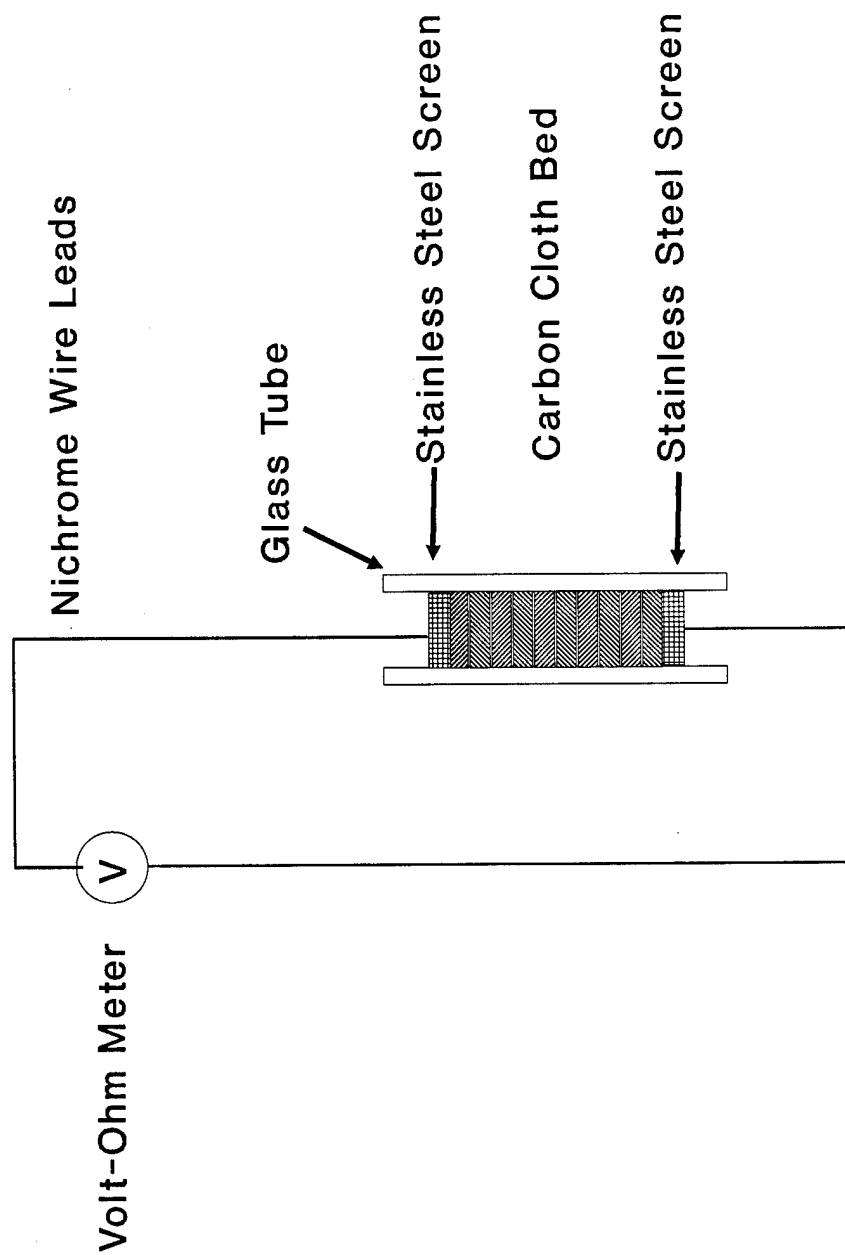


Figure 4-2b. Dynamic Resistance Isotherm Setup for Cloth

Novoloid fibers form graphitic-like structured domains with limited areas of extent that form islands in the amorphous fibers (Hayes, 1994). Fung et al (1994) report that these planes in the fibers are ~2.5 nm in diameter and occur in layers of 1-3 planes to form crystallites. Similar structures were found in carbon films where the graphitic islands are separated by regions of tetrahedrally bonded carbon (McLintock and Orr, 1968).

The carbon cloth adsorbent used in this study has the characteristic of increasing in conductivity with increasing temperature as shown in Figure 4-3. French researchers (Baudu et al, 1992) reported the following exponential relationship for the resistance changes with temperature for carbon fibers and GAC:

$$R_T = R_0 \exp[-b(1/T - 1/T_0)^2]$$

where R_T is the resistance at the temperature "T", R_0 is the resistance at the initial temperature " T_0 ", b is 98 for GAC and 83 for the fiber, and the temperatures are in degrees Celsius. Baudu et al, attribute the difference between the values of " b " to the structural differences between the different materials.

In this study these findings were not collaborated as shown in Figure 4-3. The carbon cloth was found to be linear in the temperature/resistance relationship over the temperature range used in this study. Two configurations of the cloth were used as discussed below, and also another polymer-based adsorbent, Ambersorb® 572 (Rohm and Haas, Philadelphia PA). Figure 4-3 also contains data from early work by McIntosh et al. (1947) showing a linear response with carbon rods made from carbonized zinc chloride/cellulose starting materials. It is not clear which fiber form was used in the work by Baudu et al, but the trend should remain the same for the different cloth materials.

A possible explanation for the difference was thought to be in how the measurements were taken. The cloth sections studied here were allowed to hang free in the temperature controlled oven and were not influenced by pressure due to thermal expansion differences. If the material was contained, heating could cause an increase in

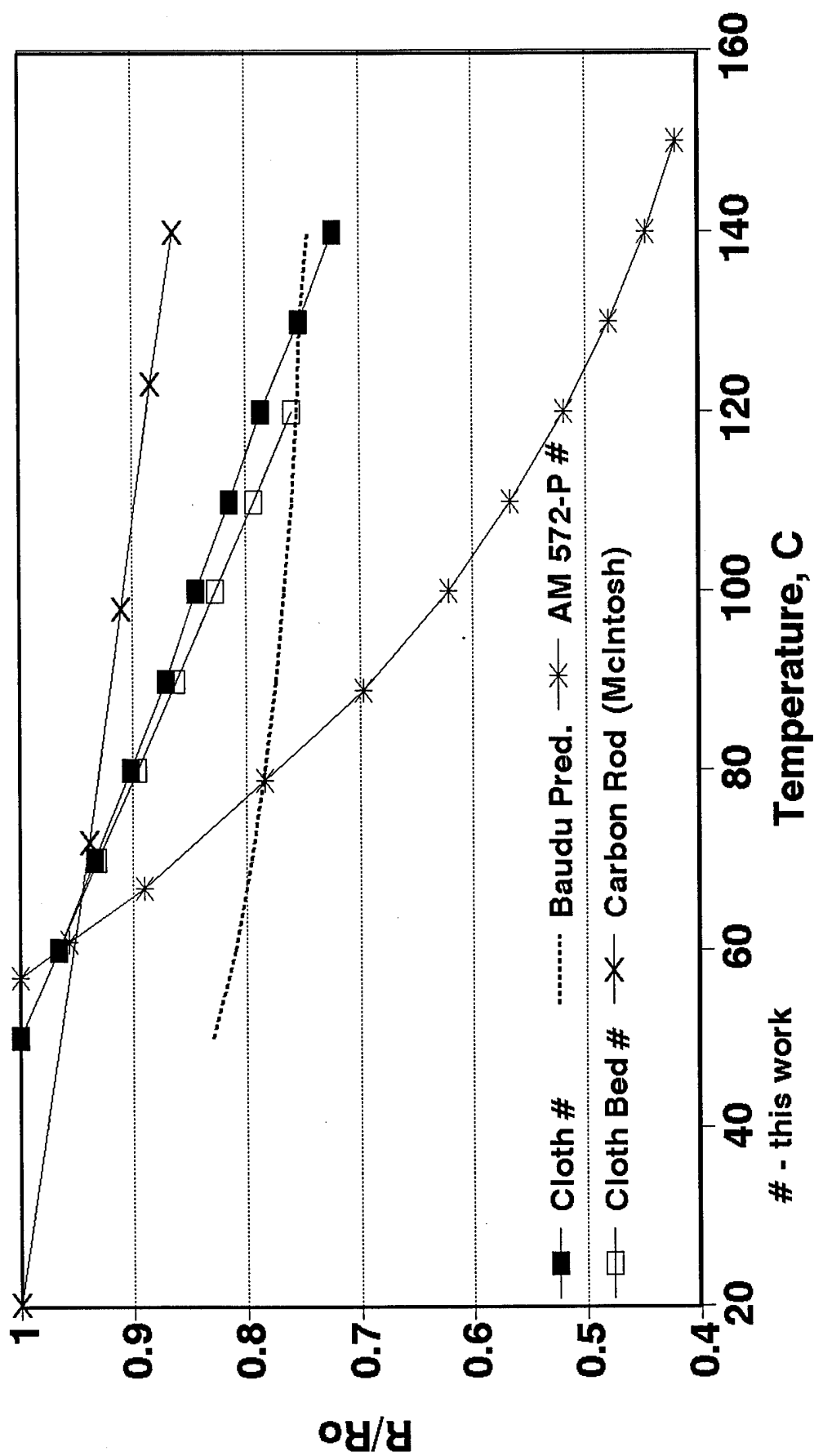


Figure 4-3. Resistance vs Temperature for Carbon Materials

internal pressure, decreasing the electrode/bed contact resistance, artificially lowering the resistance for a given increase in temperature. Using cloth sections stacked up in glass tube between stainless steel screens (the flow through cell for the dynamic isotherms) there was a slight trend in this direction at higher temperatures as shown in Figure 4-3, however, this is not enough to account for the trend predicted.

Fung et al (1991) report the resistance change with temperature over phenolic-based carbon fibers. Over a temperature range of 30 to 300 °K they found the conductivity varied according to Mott's law (Mott, 1987):

$$\sigma(T) = \sigma_0 \exp[-(T_0/T)^{1/p}]$$

where σ is the conductivity, T_0 is a fitting parameter, and $p=2$ in their work. At temperatures above ~100 °K, there appears to be a direct linear relationship between the conductivity and the temperature, evidently in the flat tailing portion of the exponential equation. They were unable to definitively say which conduction mechanism governs the electrical transport at room temperature. Later on the same group (Fung et al, 1994) report that the fibers behave like granular metals and a hopping conduction mechanism is dominant in these porous materials.

The overall resistance of the adsorbent bed is very sensitive to pressure and electronic actions. Firm compression of the cloth against the electrode or an electrical burst across the bed (approximately 0.1 s at 42 VDC) dramatically reduces the resistance of the system. All cloth samples were treated with electrical bursts to reduce the overall resistance of the materials prior to use.

The pressure on the carbon cloth cell could be causing three things: 1) improving the fiber:fiber contact, 2) improving the electrode:bed contact, and/or 3) causing the graphitic planes to be making better contact within the cloth. Karanja et al (1994) investigated the pressure dependence of conductivity on pure and doped samples of a polypropylene polymer film. The material possessed amorphous and crystallite

regions like the carbon fibers. They found that above 2 MPa (20 atm) the conductivities of the materials changed. The pressures here are 2-3 atm (in the compression tests), so the contacts internal to the fiber were neglected.

To investigate the importance of the fiber: fiber contact two experiments were performed. The first one utilized a woven strand (approximately 7 cm long) that was removed from the woven cloth and placed between two glass plates with the strand extending out for direct contact with alligator leads to the volt-ohm meter. Only a slight (0.5 - 1 percent) drop in resistance was noted during compression (ca, 15 psi), however, upon release the conductivity was drastically reduced and in some cases the strand was powderized.

The second experiment to discern the importance of the fiber contacts utilized three strips of the carbon cloth (2 cm by 7 cm). They were stacked up in a star pattern and the central overlapping area of approximately 4 cm² was placed between two glass sheets. Electrical leads were connected to one end of the strip on the bottom and to one end of the strip on the top layer. Upon compression (ca, 30 psi) the resistance dropped by approximately 10 percent and returned to normal when the pressure was released. The experiment was repeated with the leads on opposite ends of the same strip and saw the same result. Thus the fiber: fiber contact is important, and it may not be possible to determine if the electrode: bed or the fiber: fiber contact plays the dominant role. An operating reactor design may utilize large stacks of cloth sections if the majority of the resistance is in the electrode: bed contacts.

The single woven strand, out of its weave, has a resistance on the order of 1000 ohm/cm. A single woven strand, still in its weave (except for the small amount for electrical contact), is approximately 100 ohm/cm. Apparently the direction for the electron flow is not necessarily along the fiber length, but proceeds rather erratically across the material. That is, the preferred electron path, based on the reduced resistance noted, is from one woven fiber to another and not along a single fiber strand. This is

reinforced by the observation in the lab that the resistance from a single point on a carbon woven section is essentially the same ($\pm 2\%$) at points in radial directions, but equal in distances, from the starting point. Thus there are no favored paths (such as along the fibers) in the material.

Electrical bursts along these paths improve the conductivity of the carbon cloth samples. At the points of electrical junction from one fiber direction to another, there may be small resistances that are removed by the sudden current flow from the short electrical bursts. Thus, the bursts would improve the conductivity not only between the electrode and the bed, but also within the bed as well.

4.3.2 Resistance Change upon Adsorption

As the organics fill in the zones between the crystallites, it is thought they interfere with the electron flow. Experiments confirmed this and showed a concentration dependence as well as a compound dependence in the response of the resistance change. Flow through cells allowed for concentrations to be shifted from low to high, while static isotherms allowed for direct comparison of the different compounds and their effects on the resistance change.

Figure 4-4 shows the results of the dynamic adsorption isotherms using dry streams of trichloroethylene (TCE) performed in the flow through cell. The cloth bed was sequentially loaded with 15, 500, and 1500 ppmv TCE in dry air. The bed was allowed to come to equilibrium before switching to the next higher feed concentration.

There appears to be a small increase in resistance when the cloth is exposed to the 15 ppmv concentration. However, at 500 ppmv the resistance decreases as the surface concentration of TCE increases. Since the 500 ppmv feed is in nitrogen and not air as the other two TCE concentrations, the drop in resistance may be due to the loss of oxygen from the surface. However, in separate experiments with nitrogen and oxygen, the cloth showed no difference in conductivity when switching back and forth between nitrogen and

air carrier gases. Thus the loss of resistance is not due to the change in the carrier gas (oxygen or nitrogen).

At 1500 ppmv there is a marked increase in resistance of the bed. Due to the low adsorbent mass in the bed the breakthrough curve and the resistance-change curve appear to overlap one another. However, in a separate experiment, shown in Figure 4-5, it is shown that the resistance change is at the beginning of the loading and not during breakthrough. Figure 4-5 also demonstrates that the resistance change is not due to the electrode:bed interface since there is not a second sharp increase in resistance at the time of breakthrough.

The downward trend at the early times in Figure 4-5 may be the result of the same phenomenon causing the other downward trends noted above. These trends may be from two sources. The first is from the temperature increase due to the heat of adsorption released when the TCE adsorbs to the surface. At low loadings there is not enough adsorbed to alter the temperature and thus the resistance. At 500 ppmv there may be a sufficient amount adsorbed to increase the temperature (which in turn decreases the resistance). While this may occur initially, the continuing reduced resistance over 20 hours as shown in Figure 4-4 at 500 ppmv indicates that it is not a temperature affect. If it were, then the resistance would gradually return as the bed resumed its normal operating temperature once adsorption ceased.

The second source for the downward trend is thought to be the additive effects to the adsorbent from the pi electrons in the double bond of TCE. If TCE is chemisorbed to the adsorbent then an exchange of electrons occurs and the shift in those extra electrons would alter the charge carrier concentration of the adsorbent material. However, as more and more TCE is adsorbed, a barrier to electron flow may have been set up in the adsorbent, causing the resistance to rise. In Figure 4-5, as the concentration front moves through the bed the leading edge initially lowers the resistance of that section. As the front continues the low resistance zone moves down (and eventually out of) the bed. Behind the bed the highly resistive zone develops. At early times in the loading cycle the

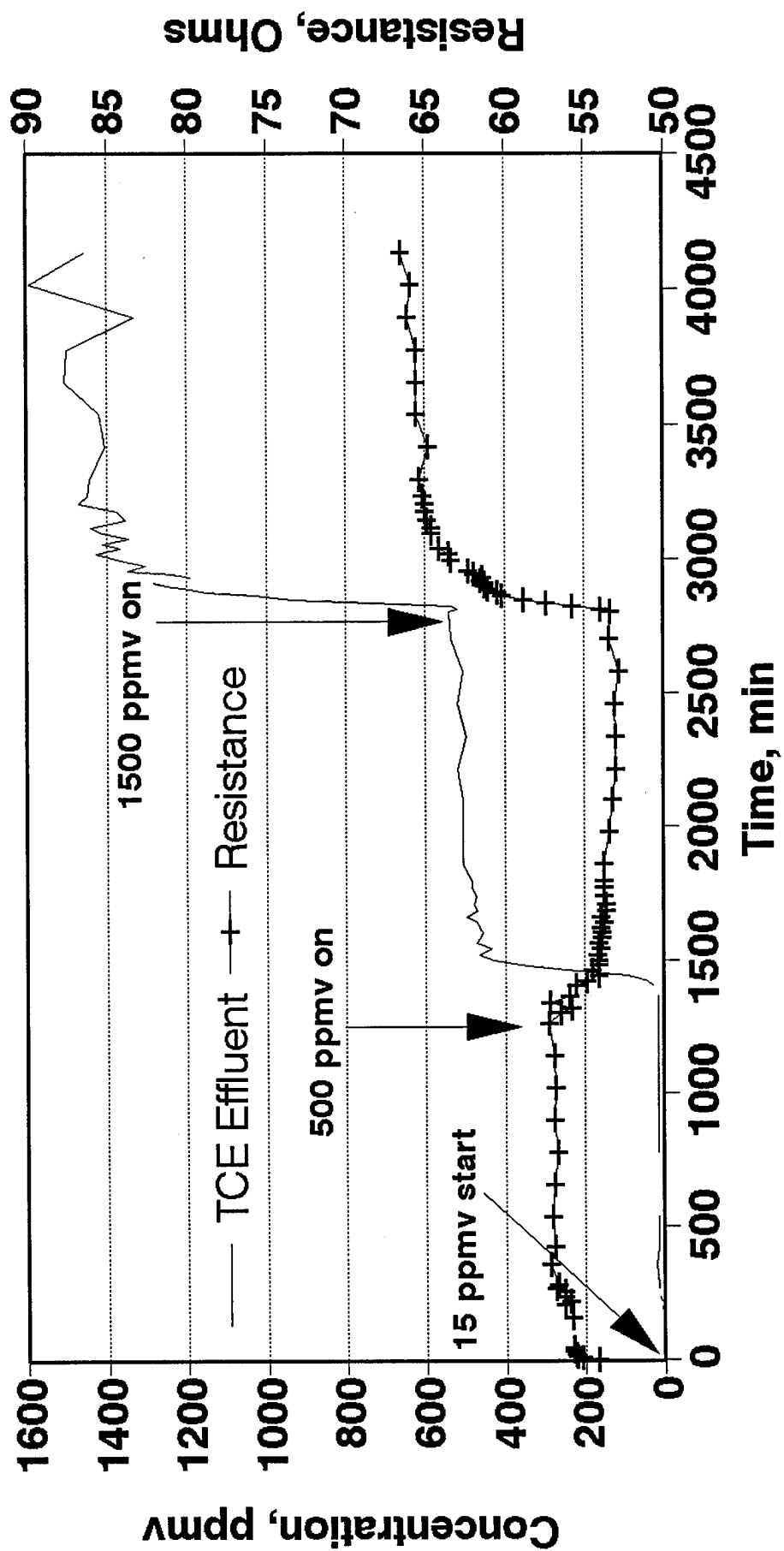


Figure 4-4. Dynamic Isotherm of TCE with Dry Feed (15, 500, and 1500 ppmv) and Resistance Changes on Activated Carbon Cloth (Kuractive)

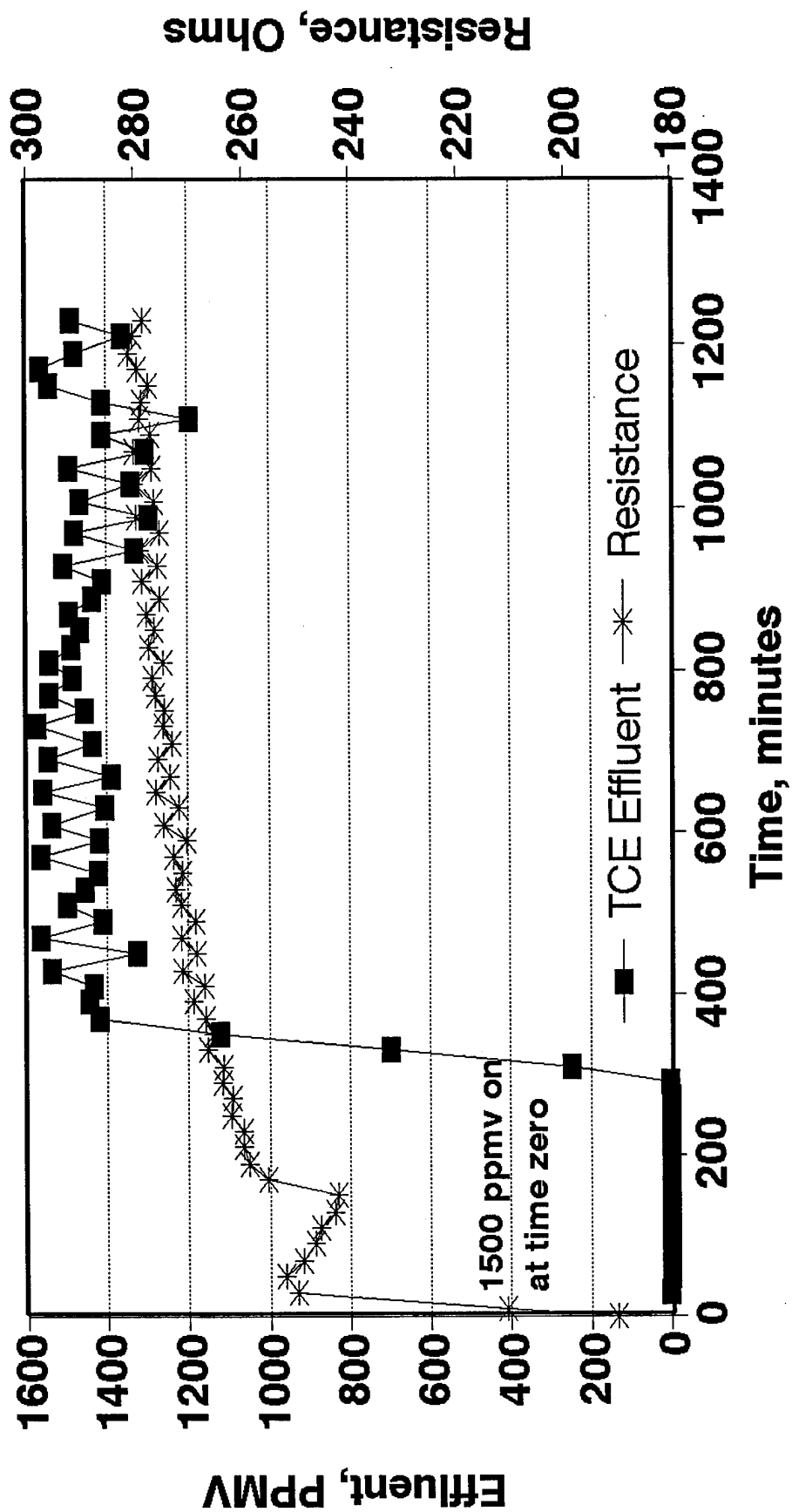


Figure 4-5. 1500 ppmv TCE Humid Feed Loading in Flow Cell over Carbon Cloth

low resistance zone more than balances out the high resistance zone and the overall resistance decreases. As the front moves through the bed the low resistance portion becomes smaller and the high resistance zone dominates for the remainder of the cycle. Further experiments with other double bonded species were conducted to verify the pi-bond-additive effect in static (no-flow) experiments.

A series of static isothermal experiments were conducted using seven chemicals found in industrial operations or remediation efforts that spanned the range of adsorption strengths, from weak to strong. The compounds are: methanol (MeOH), dichloromethane (DCM), carbon tetrachloride (CCl₄), tetrachloroethylene (PCE), TCE, water, and toluene. Each experiment used a fresh section of carbon cloth and thus each had a slightly different initial resistance. The changes in resistance were normalized to the initial resistance of cloth sample to allow a comparison between the different compounds. Figures 4-6 and 4-7 show the compounds and their impact on the resistance of the carbon cloth. Since these compounds were exposed to the chemicals at their vapor pressure it is assumed that pore filling, and not just monolayer adsorption, is occurring.

The polarizability of a compound is an indication of how strongly an organic compound will be held to the adsorbent. In addition, the polarizability of the compounds used in this study (listed in Table 4-2) also impacts the timing as to when the resistance change occurs in the adsorbent. Figure 4-6 shows that the weakly adsorbing compounds with the lowest polarizabilities (methanol and dichloromethane) affect the resistance the fastest. Next comes TCE and carbon tetrachloride, which are intermediately adsorbing compounds. The last to show the upward trend in resistance change are the strongly adsorbing PCE and toluene with the largest polarizabilities. The PCE and toluene lines cross making it difficult to determine which comes out later, but both are later than the other compounds.

TCE, PCE and toluene all have double bonds with pi electrons and should behave the same in the adsorbent. However, the initial dramatic downward shift in resistance by TCE is not as strongly demonstrated in the other two compounds. It is

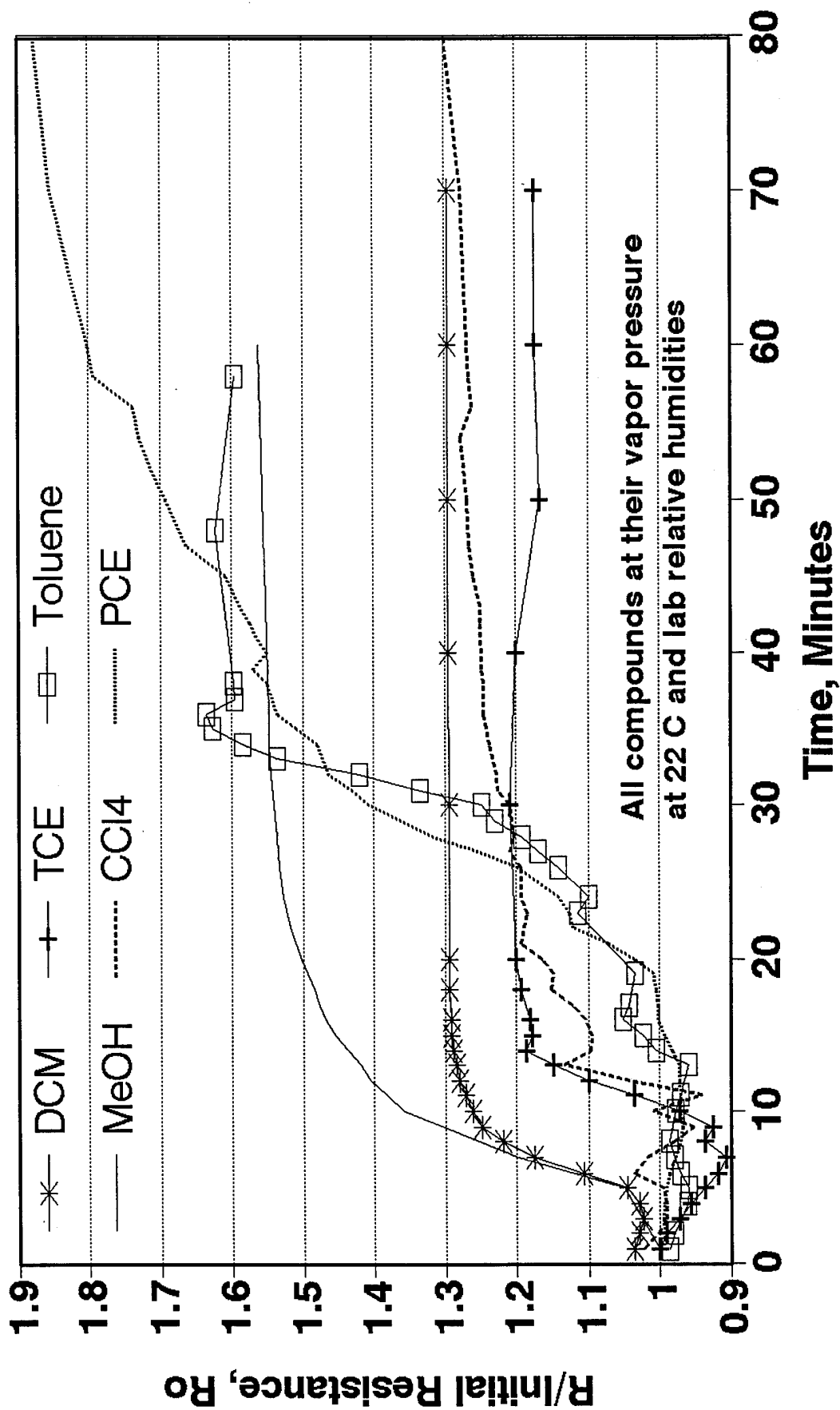


Figure 4-6. Resistance Change Upon Adsorption of Six Compounds on Activated Carbon Cloth (Kuractive)

TABLE 4-2. CHEMICAL CHARACTERISTICS OF SIX COMPOUNDS

COMPOUND	POLARIZ- ABILITY ^a cc-1	MOLAR VOLUME ^b L/mol	VAPOR PRESSURE ^c kPa	ρ^c g/cc	ϵ^d
METHANOL	13.3	.042	14.4	1.54	33.6
DICHLORO- METHANE	17.8	.07	51.8	1.70	9.08
TRICHLORO- ETHYLENE	28.7	.102	8.53	1.53	3.4
CARBON TETRACHLORIDE	31.4	.105	13.3	1.58	2.24
TETRACHLORO- ETHYLENE	35.3	.119	2.10	2.01	--
TOLUENE	34.6	.119	3.23	.756	2.38

a- calculated from molar refraction equation, $(n^2 - 1)/(n^2 + 2) \times \text{Molar volume}$, "n" is refractive index.

b- molar volume from StEPP (Software Estimation of Physical Properties) @ normal boiling point

c- density from StEPP @ 22 °C

d- dielectric constants from CRC Handbook of Chemistry and Physics, 1980

thought that because PCE and toluene are so strongly held by the adsorbent on the way to the micropores, they would take longer to reach the sites altering the resistance of the adsorbent and the influence of their pi electrons may be masked by the blocking mechanism at high concentrations.

In adsorption the adsorbates move by pore and surface diffusion. The driving force for the movement is the concentration of the adsorbate, while the restricting factor is usually the strength of adsorption. If the compound is strongly held then the concentration front moves slowly towards the inner reaches of the adsorbent. However if the compound is weakly held then the concentration front moves as fast as the driving force allows.

Thus, the concentration "front" that moves along the surface toward the high energy sites would be sharper when very strongly or very weakly adsorbing molecules are

used. This indicates that the PCE and toluene reach the micropores later and in much greater initial concentration than the TCE. With these compounds there is no time for the pi electrons to add to the adsorbate carrier concentration as with TCE. Thus, the downward trend in the resistance is not seen since the pi electron contribution to the matrix during the loading cycle is masked with strongly adsorbing compounds.

The height of the plateaus in Figure 4-6 are perplexing. Since the pores contain condensed organics, one would expect the resistance change would be due to the dielectric constant of the organic. However, the dielectric constants listed in Table 4-2 do not correlate with the height of the curves. Neither does the height relate to the concentrations (vapor pressures), also listed in Table 4-2.

Figure 4-7 shows the resistance change upon adsorption for water, TCE and a water/TCE mixture under static conditions. The mixture contained sufficient contaminant to saturate the cloth and keep both compounds at their vapor pressures, yet the water was not covering the TCE in the bottom of the isotherm bottle. The initial response of the mixture follows the TCE line, however the water does impact the system causing a delay in the upward swing of the resistance curve. The water may have condensed in a sufficient number of pores to delay the transfer of TCE to the high energy sites. However, the resistance change appears to be additive. That is, the initial decrease by the TCE appears to have been enhanced by the initial decrease of the water creating a steeper initial slope in the mixture.

4.3.3 Applications

Some useful applications of this finding would be in automatic controls for gas phase regeneration and in capacity predictions. For example, if a large adsorbent bed contained a small cloth resistor near the effluent, one could simply monitor the resistance to determine when the bed was exhausted and required regeneration. While it may be possible to also monitor the extent of the regeneration as well, care must be taken that the

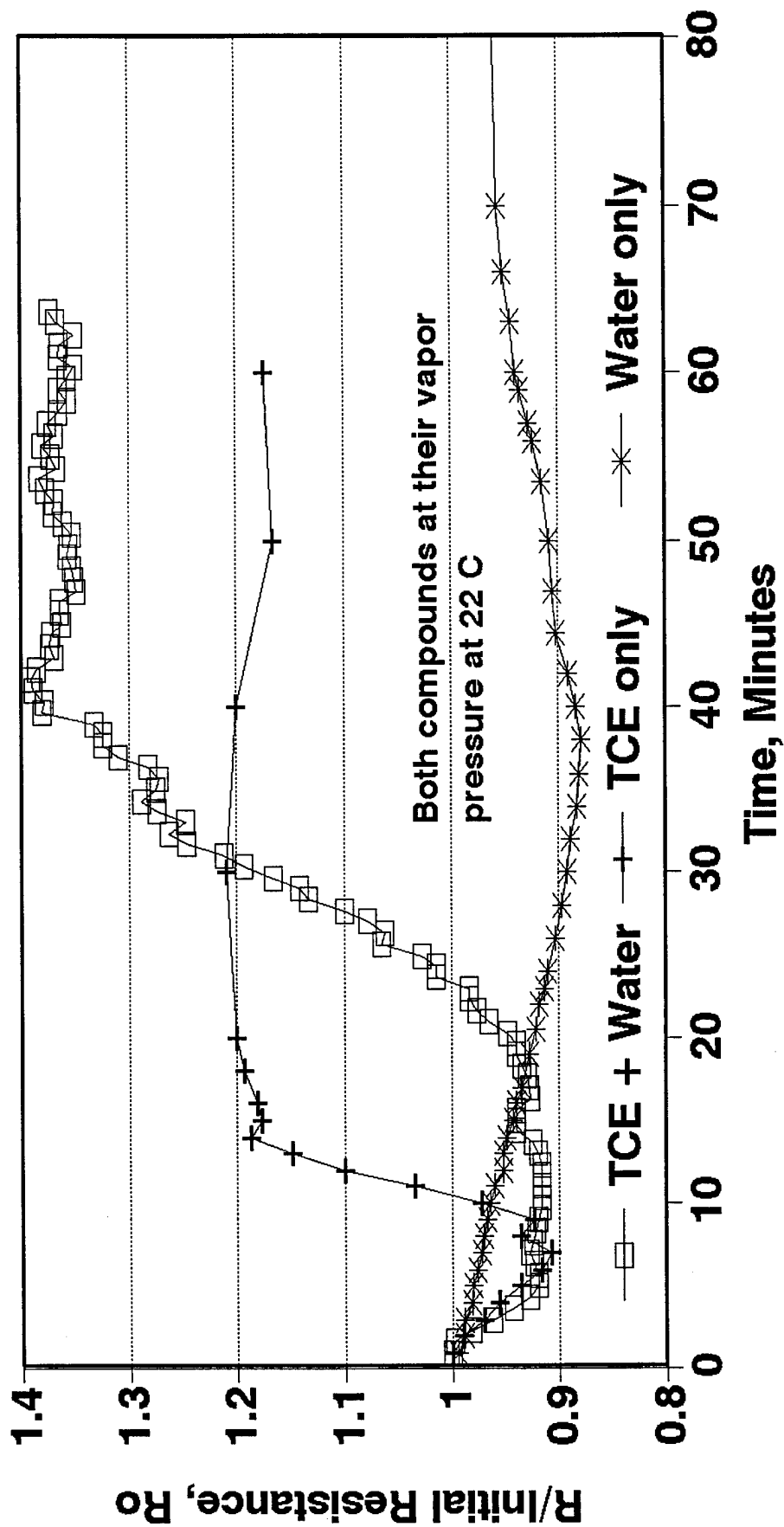


Figure 4-7. Resistance Changes in Mixtures of Trichloroethylene and Water over Carbon Cloth (Kuractive)

resistance change due to the high thermal inputs needed to desorb the organics do not overshadow the resistance change due to desorption.

The other possible application is in determining how a new compound would behave in an existing stream. A static isotherm could be done for the compounds of interest in the existing stream. An additional isotherm could be done with the new compound. If the compound altered the resistance at a later time than the existing stream, then the compound would be held stronger than those compounds. That is, one could predict how strongly or weakly the material would be adsorbed to the adsorbent in relation to the other compounds by knowing the timing of the resistance change in the static isotherms.

4.4 CONCLUSIONS

Neutral organic compounds, in sufficient concentration, can alter the resistance of an activated carbon cloth upon adsorption. The resistance change profile is different for different compounds and for different concentrations of the same compound. At low TCE concentrations (low surface coverage) there is little, if any, resistance change in the design used in this study. Increasing the TCE concentration causes the resistance to drop slightly, while high TCE concentrations increase the resistance significantly. Compounds with large polarizabilities take the longest to cause the upward swing of the resistance curve. These strongly adsorbing compounds are delayed in reaching the areas affecting the resistance change resulting in the delay in the curve. In addition, the conductivity of the adsorbent has a direct linear relationship to temperature. These facts support the concept of the carbon fiber containing crystallites of graphitic-like domains. Electrical conductivity is accomplished by electron hopping from one crystallite to another. Zones between crystallites are the micropores and the adsorption sites are probably at the edge of the basal planes of the crystallites. Thus, adsorption increases the barrier to electron flow and the resistance increases.

Simple tools based on this phenomenon can be employed easily and can reduce monitoring costs, achieve optimum utilization of air phase systems by only regenerating the adsorbent bed when exhausted, and aid engineers in estimating the effects of compounds on the capacity of systems already in use. To expand the usefulness of this work, other compounds and adsorbents should be investigated to further delineate the interactions of the adsorbates and the adsorbent upon adsorption, including multicomponent efforts. In addition other designs need to be evaluated to improve the measurements, especially to define the minimum concentration detection limit for this new process.

4.5 ACKNOWLEDGEMENTS

This work was funded by Environics Directorate of the U.S. Air Force's Armstrong Laboratory, Tyndall AFB FL 32403, Maj Mark Smith, Project Officer. Support from Michigan Technological University is greatly appreciated. Mention of trademarks and trade names of material and equipment does not constitute endorsement or recommendation for use by the U.S. Air Force, nor can this article be used for advertising the product(s).

4.6 REFERENCES

Baudu, M., Le Cloirec, P., and Martin, G., "Thermal Regeneration by Joule Effect of Activated Carbon used for Air Treatment," *Environmental Technology*, Vol 13, pp 423-435, 1992.

Economy, J., and Lin, R.Y., "Adsorption Characteristics of Activated Carbon Fibers," *Applied Polymer Symposium*, No. 29, pp. 199-211, 1976.

Fung, A.W.P., Rao, A.M., Kuriyama, K., Dresselhaus, M.S., Dresselhaus, G., and Endo, M., "Characterization of Activated Carbon Fibers," *Materials Research Society Symposium Proceedings*, Vol 209, pp 335-340, 1991.

Fung, A.W.P., Wang, Z. H., Dresselhaus, M.S., Dresselhaus, G., Pekala, R.W., and Endo, M., "Coulomb-gap Magnetotransport in Granular and Porous Carbon Structures," *Physical Review B*, Vol 49, No 24, pp 173325-17335, 15 June 1994.

Hagen, W., Lambrich, R.E., Lagois, J., "Semiconducting Gas Sensors," *Advances in Solid State Physics*, Vol. 23, p. 259-74, 1983.

Hayes, J. S., "Activated Carbon Fibers and Textiles: Properties and Applications," American Kynol, Inc., Pleasantville, NY, June 1994.

Hayes, J.S., "Novoloid and Related Fibers in Nonwoven Structures," INDEX 93 CONGRESS, Session 2C - Fibres, Geneva, 20 April 1993.

Karanja P., and Nath, R., "Charge Trapping and Conduction in Pure and Iodine-doped Biaxially-oriented Polypropylene," *IEEE Transactions on Dielectrics and Electrical Insulation*, Vol. 1, No. 2, pp 213-223, April 1994.

Law, J.T., "The Adsorption of Gases on a Germanium Surface," *Journal Physical Chemistry*, 59, pg 543, 1955.

Lordgooei, M., Kelly, T., Covington, B., Carmichael, K., Rood, M., and Larson, S., "Development of an Activated Carbon Cloth (ACC) Cryogenic system to Recover and Reuse Toxic Organic Vapors," presented in Section: Carbon-Based Materials for Gas Separations, Purification & Cleanup, American Institute of Chemical Engineers Spring National Meeting, Houston, TX, March 20, 1995.

McIntosh, R., Haines, R.S., and Benson, G.C., "The Effect of Physical Adsorption on the Electrical Resistance of Activated Carbon," *The Journal of Chemical Physics*, Vol 15, No. 1, pp 17-27, Jan. 1947.

McLintock, I.S., and Orr, J.C., "The Effect of Oxygen Adsorption on the Electrical Resistance of Evaporated Carbon Films," *Carbon*, Vol 6, pp 309-323, 1968.

Mott, N.F., Conduction in Non-Crystalline Materials, Oxford University Press, New York, 1987.

Sontheimer, H., Crittenden, J.C., and Summers, S., "Activated Carbon for Water Treatment," 2nd Edition, DVGW-Forschungsstelle, Engler-Bunte-Institut, Karlsruhe University, 1988.

Thakur, M., and Elman, B.S., "Optical and Magnetic Properties of a Nonconjugated Conducting Polymer," *Journal of Chemical Physics*, **90** (3), pp 2042-2044, 1 Feb 1989.

Wedler, G., and Wissmann, P., "Study by Means of the Adsorption of Gases on Thin Metal Films of the Electrical Resistance Changes," *Surface Science*, Vol 26, No. 2, p 389-96, 1971.

Chapter 5

Overall Conclusions and Recommendations

5.1 OVERALL CONCLUSIONS

Catalytic oxidation over a thermally modified Ambersorb 572 can be accomplished at temperatures as low as 110 °C, although many by-products are formed at that temperature. These by-products include chloroform, carbon tetrachloride, tetrachloroethylene, hexachloroethylene, and, under extremely dry conditions, phosgene. If the temperature is maintained at or above 180 °C then complete mineralization of a 1500 ppmv trichloroethylene (TCE) air stream is possible using plain Ambersorb 572. The addition of transition metal oxides do not enhance the catalytic activity of the TCE oxidation reaction under the conditions used in this research (temperatures below 250 °C). Humidity added to the feed stream deactivates all the catalysts except for the plain Ambersorb 572.

Dynamic electric fields applied to the adsorbents used in this work cause the material to be rapidly heated. Depending on the magnitude of the potential, the heat can 1) alter the local humidity of an adsorbent allowing for increased adsorption capacity of organics; 2) thermally drive off the organics from the surface of the adsorbents during regeneration; and 3) provide the activation energy to catalytically oxidize TCE over an Ambersorb-572 based catalyst.

The electron flow path in the carbon cloth fibers is proposed to travel parallel to the basal planes inside crystallites in the material. Electron hopping, from one crystallite to another provides the overall conductivity. The fringe area of the crystallites are suspected to be the micropores where adsorption occurs. Thus, adsorption at those sites alters the overall resistance of the adsorbent. All the adsorbates used in this work (carbon tetrachloride (CCl₄), tetrachloroethylene (PCE), TCE, methanol, water, dichloromethane,

and toluene) eventually increased the resistance of the adsorbent. The time for the rapid upswing in resistance change is directly related to the polarizability of the compound. In addition, the concentration of the adsorbate also plays a key role. At low concentrations there may be no effect. Increasing the concentration of TCE caused the resistance to drop, until a higher concentration was used, causing a rapid rise in the resistance of the carbon cloth. Interference, positively and negatively, in the conductivity of the material occurred.

5.2 OVERALL RECOMMENDATIONS

The catalytic oxidation work with TCE should be expanded to other compounds. Since the chloride radical ($\text{Cl}\cdot$) may play a role in the oxidation, non-chlorinated organics should be investigated. In addition, mixture effects should also be evaluated. Long-term tests should be done immediately to determine how long the catalyst material would function on a TCE stream to allow for a life-time cost analysis to be performed.

Initial cost estimates for the using electrical energy to alter the local relative humidity are not favorable and heating of the air should be used. Evaluations should be made to determine if on-site regeneration could be done by exposing the adsorbent to a clean humidified stream at ambient temperatures. Upon restart there would be a small residual until the bed reached the optimum temperature. This time could be reduced by using the Joule heating to quickly heat the bed, then switching it off for the remainder of the cycle. Evaluations with Joule heating should be done to optimize the adsorption capacity for organics by looking at the competing terms: reduced organic capacity at elevated temperatures and reduced relative humidity at increased temperatures.

The resistance change upon adsorption phenomenon should be evaluated for other adsorbents. Once an optimum one is found, then it should be applied in the field monitoring air. For example a unit could monitor the effluent from an air stripping operation to determine when the gas phase adsorption unit needed regeneration. Another possible application is between the walls of double-walled gas tanks to monitor for leaks.

In addition, single solute and mixtures should be used on different adsorbents and compared to observed time to breakthrough from long-term isotherm studies. These simple tests could then be used to strengthen the database of chemical adsorptabilities onto different adsorbents. These experiments could be done economically and without lengthy isotherm tests.

APPENDIX A

**Raw Data from Adsorption/Desorption Data
from PMI Inc., (Ithaca, NY) for
Ambersorb 572 & MTU-CAT**

BET SURFACE AREA ANALYSIS

12-16-1994

POROUS MATERIALS, INC. ANALYTICAL SERVICES DIVISION
 CORNELL INDUSTRY RESEARCH PARK, BLDG. 4
 ITHACA, NY 14850 USA
 PHONE (607) 257-4267 OR 257-5544

NOTE: RESULTS CALCULATED USING WEIGHT AFTER OUTGASSING.
 TO GET RESULTS USING ORIGINAL WEIGHT, MULTIPLY THESE VALUES BY
 WT AFTER OUTGAS/WT BEFORE OUTGAS

MTU
 Ed. Marchand

SAMPLE ID: Ambersor 572

SPECIFIC SURFACE AREA= 830.9971 M2/GM

SAMPLE WEIGHT= .7196 GM BEFORE OUTGASSING .703 GM AFTER OUTGASSING

Sample Density= 1.5

BET C VALUE= -40.612

SLOPE= 6.107 GM-1

Y INTERCEPT= -.147 GM-1

CORRELATION COEFFICIENT= .995

ADSORBATE= NITROGEN

VA VOLUME= 44.80148 CC

Vit VOLUME= 11.7589 CC

Vln VOLUME= 13.782 CC

INSTRUMENT TEMPERATURE= 305.36 K

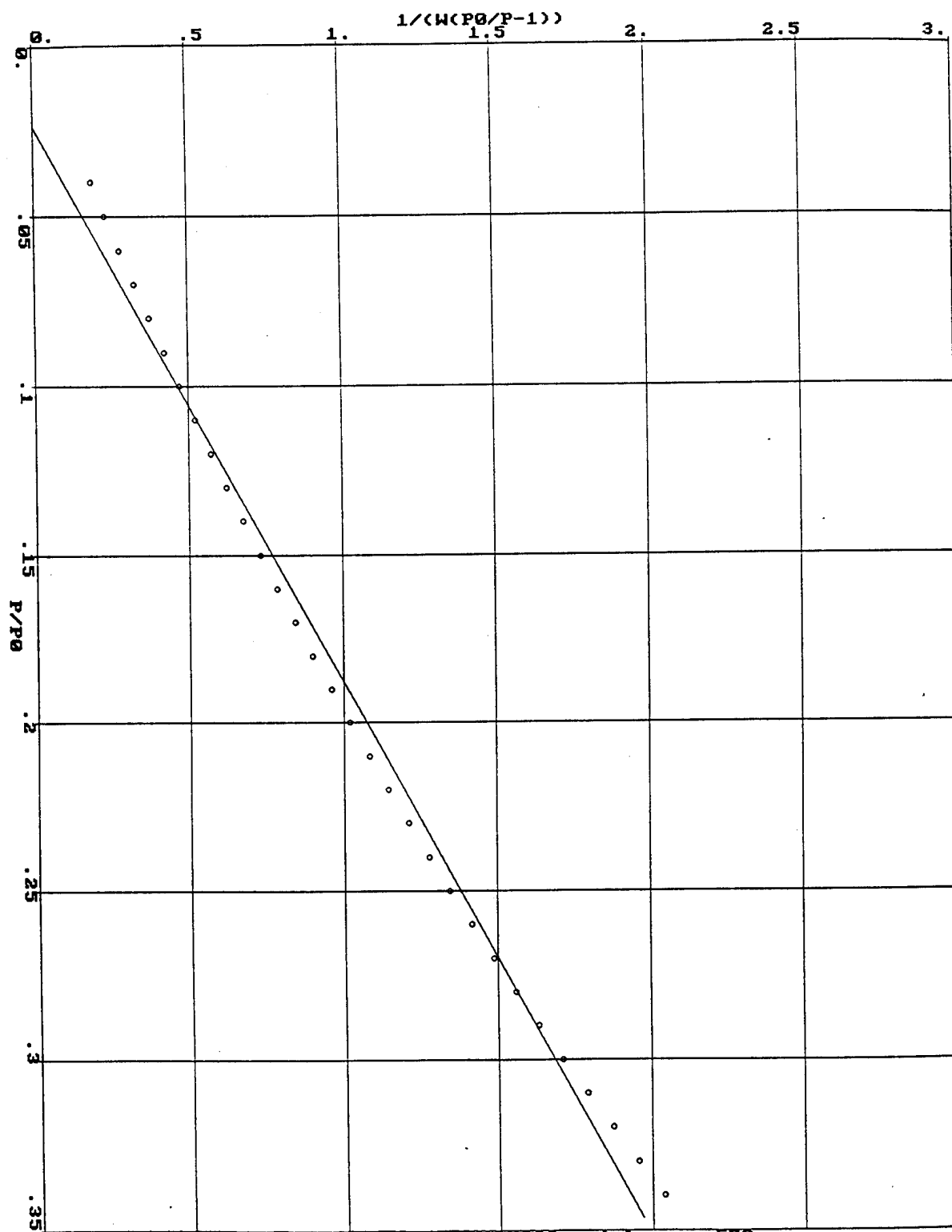
ROOM TEMPERATURE= 296.7 K

W = Wt. of adsorbed gas per gram of sample

SAMPLE OUTGASSED AT 20 DEGREES CELSIUS

DATA POINT	P P0	P0 P	-1 (W(- -1))
9	0.04000000	0.18600000	
10	0.05000000	0.23100000	
11	0.06000000	0.27700000	
12	0.07000000	0.32500000	
13	0.08000000	0.37300000	
14	0.09000001	0.42100000	
15	0.10000000	0.46900000	
16	0.11000000	0.51900000	
17	0.12000000	0.56900000	
18	0.13000000	0.62200000	
19	0.14000000	0.67500000	
20	0.15000000	0.72900000	
21	0.16000000	0.78400000	
22	0.17000000	0.84100000	
23	0.18000000	0.89900000	
24	0.19000000	0.95800000	

25	0.20000000	1.019
26	0.21000000	1.081
27	0.22000000	1.144
28	0.23000000	1.209
29	0.24000000	1.275
30	0.25000000	1.343
31	0.26000000	1.413
32	0.27000000	1.485
33	0.28000000	1.558
34	0.29000000	1.634
35	0.30000000	1.711
36	0.31000000	1.79
37	0.32000000	1.871
38	0.33000000	1.955
39	0.34000000	2.041

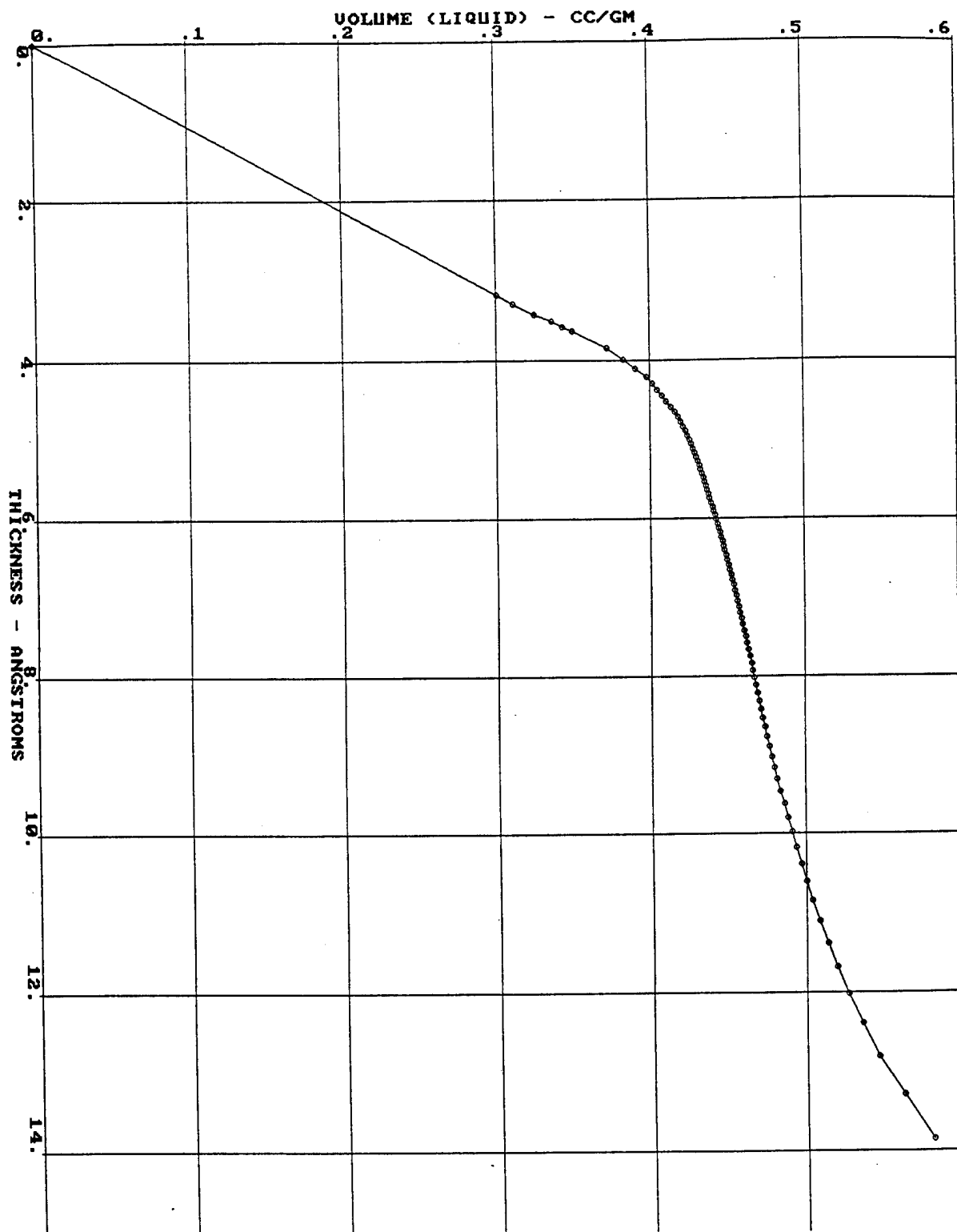


BET SURFACE AREA ANALYSIS - Amberson 572

MICRO PORE CALCULATIONS

Thickness Range Angstroms	Volume (Liquid) cc/g	Hydraulic Radius Angstroms
3.180 - 3.292	0.301	3.236
3.292 - 3.425	0.311	3.359
3.425 - 3.513	0.325	3.469
3.513 - 3.581	0.336	3.547
3.581 - 3.638	0.343	3.610
3.638 - 3.842	0.350	3.740
3.842 - 3.984	0.372	3.913
3.984 - 4.100	0.382	4.042
4.100 - 4.199	0.390	4.149
4.199 - 4.288	0.398	4.244
4.288 - 4.369	0.402	4.329
4.369 - 4.445	0.405	4.407
4.445 - 4.516	0.408	4.481
4.516 - 4.584	0.411	4.550
4.584 - 4.649	0.414	4.617
4.649 - 4.712	0.417	4.681
4.712 - 4.773	0.419	4.742
4.773 - 4.832	0.420	4.802
4.832 - 4.890	0.422	4.861
4.890 - 4.947	0.423	4.918
4.947 - 5.002	0.425	4.974
5.002 - 5.057	0.426	5.030
5.057 - 5.112	0.427	5.084
5.112 - 5.165	0.428	5.139
5.165 - 5.219	0.429	5.192
5.219 - 5.272	0.430	5.245
5.272 - 5.324	0.431	5.298
5.324 - 5.377	0.432	5.350
5.377 - 5.429	0.433	5.403
5.429 - 5.481	0.434	5.455
5.481 - 5.533	0.435	5.507
5.533 - 5.585	0.436	5.559
5.585 - 5.638	0.437	5.612
5.638 - 5.690	0.438	5.664
5.690 - 5.743	0.438	5.716
5.743 - 5.796	0.439	5.769
5.796 - 5.849	0.440	5.822
5.849 - 5.902	0.441	5.875
5.902 - 5.956	0.442	5.929
5.956 - 6.010	0.443	5.983
6.010 - 6.065	0.443	6.038
6.065 - 6.120	0.444	6.093
6.120 - 6.176	0.445	6.148
6.176 - 6.232	0.446	6.204
6.232 - 6.289	0.446	6.261
6.289 - 6.347	0.447	6.318
6.347 - 6.405	0.448	6.376
6.405 - 6.465	0.449	6.435
6.465 - 6.525	0.449	6.495
6.525 - 6.586	0.450	6.555
6.586 - 6.648	0.451	6.617
6.648 - 6.711	0.452	6.679
6.711 - 6.775	0.453	6.743
6.775 - 6.840	0.453	6.807

6.840 -	6.906	0.454	6.873
6.906 -	6.974	0.455	6.940
6.974 -	7.043	0.456	7.009
7.043 -	7.114	0.457	7.078
7.114 -	7.186	0.457	7.150
7.186 -	7.259	0.458	7.222
7.259 -	7.335	0.459	7.297
7.335 -	7.412	0.460	7.373
7.412 -	7.491	0.461	7.452
7.491 -	7.572	0.462	7.532
7.572 -	7.656	0.462	7.614
7.656 -	7.742	0.463	7.699
7.742 -	7.830	0.464	7.786
7.830 -	7.921	0.465	7.876
7.921 -	8.015	0.466	7.968
8.015 -	8.112	0.467	8.064
8.112 -	8.212	0.468	8.162
8.212 -	8.316	0.469	8.264
8.316 -	8.424	0.471	8.370
8.424 -	8.536	0.472	8.480
8.536 -	8.652	0.473	8.594
8.652 -	8.773	0.474	8.712
8.773 -	8.899	0.475	8.836
8.899 -	9.031	0.477	8.965
9.031 -	9.170	0.478	9.101
9.170 -	9.315	0.480	9.242
9.315 -	9.468	0.482	9.391
9.468 -	9.629	0.484	9.548
9.629 -	9.799	0.486	9.714
9.799 -	9.980	0.488	9.890
9.980 -	10.172	0.491	10.076
10.172 -	10.378	0.494	10.275
10.378 -	10.598	0.497	10.488
10.598 -	10.836	0.500	10.717
10.836 -	11.092	0.504	10.964
11.092 -	11.372	0.508	11.232
11.372 -	11.678	0.514	11.525
11.678 -	12.017	0.520	11.847
12.017 -	12.393	0.527	12.205
12.393 -	12.816	0.537	12.605
12.816 -	13.299	0.547	13.058
13.299 -	13.856	0.563	13.577



MICROPORE U-T PLOT - Amberson 572

T-PLOT ANALYSIS:

T-PLOT INTERCEPT: 0.35334
T-PLOT SLOPE: 0.013941
MICROPORE VOLUME: 0.35334 CC/GM

FILM THICKNESS USED BETWEEN 8.000 and 12.000 ANGSTROMS

SURFACE AREA = 139.4092 SQ. M/GM
(MESO AND MACROPORES ONLY)

MICROPORE SURFACE AREA = 691.5879 SQ. M/GM

GAS ADSORPTION/DESORPTION RESULTS

ADSORBATE: NITROGEN

ISOTHERM AND PORE VOLUME DISTRIBUTION

ADSORPTION

P/P0	PORE DIAMETER Å	VOLUME ADSORBED CC/GM STP	LIQ. VOL ADSORBED CC/GM	AVE. POR. DIAM Å	CUMUL. POR. VOL CC/GM	ΔV ----	ΔS ----	SURFACE AREA M2/GM	CUMUL. S. AREA M2/GM
						ΔD	ΔD		
0.994	3246.4	586.3235	0.90294	3246.43	-0-	1.79E-06	2.75E-05	-0-	-0-
0.990	1957.7	584.8974	0.90074	2602.07	0.00230	2.90E-06	6.55E-05	0.03541	0.03541
0.985	1313.5	583.5333	0.89864	1635.60	0.00453	1.56E-05	5.30E-04	0.05451	0.08992
0.980	990.44	579.3146	0.89214	1151.97	0.01157	7.70E-05	0.00338	0.24430	0.33422
0.975	796.1	566.6119	0.87258	893.270	0.03309	2.08E-04	0.01095	0.96380	1.29802
0.970	666.21	545.8799	0.84066	731.155	0.06864	3.78E-04	0.02325	1.94490	3.24292
0.965	573.22	521.5602	0.80320	619.717	0.11075	5.40E-04	0.03820	2.71803	5.96095
0.960	503.33	497.3028	0.76585	538.275	0.15309	6.85E-04	0.05500	3.14639	9.1073
0.955	448.85	473.9495	0.72988	476.088	0.19416	7.90E-04	0.07050	3.45025	12.5576
0.950	405.18	453.6172	0.69857	427.013	0.23009	8.00E-04	0.07900	3.36560	15.9232
0.945	369.37	437.7131	0.67408	387.274	0.25821	7.95E-04	0.08650	2.90468	18.8279
0.940	339.48	424.0804	0.65308	354.426	0.28238	8.80E-04	0.10450	2.72815	21.5560
0.930	292.37	397.8874	0.61275	315.927	0.32948	0.00100	0.13700	5.96352	27.5195
0.920	256.92	378.2267	0.58247	274.646	0.36489	8.75E-04	0.13600	5.15686	32.6764
0.910	229.24	365.8985	0.56348	243.079	0.38664	8.15E-04	0.14350	3.57956	36.2559
0.900	207.02	355.3108	0.54718	218.133	0.40543	7.30E-04	0.14100	3.44483	39.7008
0.890	188.79	348.4164	0.53656	197.905	0.41717	6.65E-04	0.14150	2.37196	42.0727
0.880	173.54	342.307	0.52715	181.161	0.42762	6.35E-04	0.14600	2.30761	44.3804
0.870	160.59	337.6506	0.51998	167.063	0.43532	5.65E-04	0.14100	1.84345	46.2238
0.860	149.46	333.8754	0.51417	155.025	0.44138	5.90E-04	0.15850	1.56571	47.7895
0.850	139.78	330.177	0.50847	144.619	0.44749	5.85E-04	0.16750	1.68994	49.4795
0.840	131.28	327.2249	0.50393	135.532	0.45216	5.05E-04	0.15400	1.37580	50.8553
0.830	123.76	324.8524	0.50027	127.524	0.45569	4.93E-04	0.15950	1.10893	51.9642
0.820	117.06	322.58	0.49677	120.412	0.45914	4.87E-04	0.16600	1.14699	53.1112
0.810	111.04	320.6564	0.49381	114.050	0.46193	4.74E-04	0.17050	0.97637	54.0875
0.800	105.61	318.8483	0.49103	108.323	0.46456	4.87E-04	0.18400	0.97198	55.0595
0.790	100.67	317.1794	0.48846	103.141	0.46697	4.77E-04	0.18950	0.93491	55.9944
0.780	96.177	315.6809	0.48615	98.4258	0.46907	4.96E-04	0.20650	0.85384	56.8483
0.770	92.057	314.1973	0.48386	94.1170	0.47123	5.15E-04	0.22450	0.91555	57.7638
0.760	88.269	312.8355	0.48177	90.1629	0.47316	4.89E-04	0.22150	0.85978	58.6236
0.750	84.77201	311.625	0.47990	86.5203	0.47480	4.64E-04	0.21850	0.75732	59.3809

0.740	81.534	310.5025	0.47817	83.1529	0.47629	4.43E-04	0.21700	0.71524	60.0962
0.730	78.526	309.4843	0.47661	80.0297	0.47758	4.20E-04	0.21350	0.64277	60.7389
0.720	75.723	308.54	0.47515	77.1244	0.47873	3.60E-04	0.18900	0.59949	61.3384
0.710	73.10501	307.7486	0.47393	74.4142	0.47954	3.19E-04	0.17450	0.43631	61.7748
0.700	70.654	306.981	0.47275	71.8794	0.48034	3.31E-04	0.18750	0.44601	62.2208
0.690	68.352	306.2431	0.47161	69.5029	0.48112	3.46E-04	0.20250	0.44389	62.6646
0.680	66.187	305.5225	0.47050	67.2697	0.48189	3.78E-04	0.22850	0.45852	63.1232
0.670	64.14601	304.8023	0.46940	65.1668	0.48270	4.15E-04	0.25850	0.49982	63.6230
0.660	62.219	304.0925	0.46830	63.1825	0.48353	4.06E-04	0.26050	0.52375	64.1467
0.650	60.395	303.4414	0.46730	61.3067	0.48423	3.86E-04	0.25550	0.45717	64.6039
0.640	58.666	302.8139	0.46633	59.5301	0.48490	4.10E-04	0.27950	0.45063	65.0545
0.630	57.024	302.1863	0.46537	57.8447	0.48561	4.53E-04	0.31750	0.48871	65.5432
0.620	55.463	301.5591	0.46440	56.2433	0.48635	4.97E-04	0.35900	0.52605	66.0693
0.610	53.976	300.9316	0.46343	54.7192	0.48712	5.35E-04	0.39700	0.56513	66.6344
0.600	52.558	300.3117	0.46248	53.2668	0.48790	5.10E-04	0.39000	0.58661	67.2210
0.590	51.203	299.7455	0.46161	51.8806	0.48855	4.68E-04	0.36550	0.49850	67.7195
0.580	49.908	299.2052	0.46078	50.5559	0.48914	4.80E-04	0.38450	0.47054	68.1901
0.570	48.668	298.6655	0.45994	49.2884	0.48976	5.20E-04	0.42950	0.50301	68.6931
0.560	47.48	298.1256	0.45911	48.0741	0.49041	5.60E-04	0.47550	0.53773	69.2308
0.550	46.339	297.587	0.45828	46.9094	0.49107	5.85E-04	0.50500	0.56863	69.7994
0.540	45.243	297.0625	0.45748	45.7909	0.49172	5.90E-04	0.52500	0.56304	70.3625
0.530	44.189	296.5487	0.45669	44.7158	0.49235	6.20E-04	0.56000	0.56525	70.9277
0.520	43.174	296.0352	0.45589	43.6812	0.49300	6.70E-04	0.62000	0.59765	71.5254
0.510	42.196	295.5175	0.45510	42.6846	0.49369	7.35E-04	0.70000	0.64425	72.1696
0.500	41.252	294.9929	0.45429	41.7237	0.49442	8.00E-04	0.77500	0.70071	72.8703
0.490	40.341	294.4673	0.45348	40.7962	0.49518	8.50E-04	0.84000	0.73856	73.6089
0.480	39.46	293.9416	0.45267	39.9003	0.49595	9.00E-04	0.91000	0.77348	74.3824
0.470	38.608	293.416	0.45186	39.0339	0.49673	0.00095	0.98500	0.80785	75.1902
0.460	37.783	292.8905	0.45105	38.1954	0.49754	0.00098	1.04000	0.84219	76.0324
0.450	36.984	292.3725	0.45025	37.3833	0.49833	0.00095	1.03000	0.84778	76.8802
0.440	36.208	291.8801	0.44950	36.5959	0.49904	0.00093	1.02000	0.77847	77.6587
0.430	35.456	291.3939	0.44875	35.8319	0.49975	0.00096	1.08000	0.78484	78.4435
0.420	34.725	290.9078	0.44800	35.0901	0.50046	0.00101	1.15500	0.81604	79.2595
0.410	34.014	290.4206	0.44725	34.3691	0.50120	0.00109	1.28000	0.85267	80.1122
0.400	33.322	289.9205	0.44648	33.6679	0.50199	0.00120	1.43500	0.94391	81.0561
0.390	32.648	289.4116	0.44569	32.9853	0.50283	0.00127	1.55500	1.01847	82.0746
0.380	31.992	288.902	0.44491	32.3203	0.50368	0.00132	1.65000	1.05447	83.1291
0.370	31.352	288.3925	0.44412	31.6720	0.50454	0.00137	1.74000	1.08645	84.2155
0.360	30.727	287.8829	0.44334	31.0394	0.50541	0.00145	1.88000	1.11863	85.3341
0.350	30.116	287.3629	0.44254	30.4217	0.50633	0.00159	2.11000	1.20706	86.5412
0.340	29.52	286.8247	0.44171	29.8181	0.50733	0.00171	2.31000	1.34219	87.8834
0.330	28.936	286.2839	0.44088	29.2277	0.50834	0.00176	2.43000	1.38952	89.2729
0.320	28.364	285.743	0.44004	28.6498	0.50936	0.00181	2.55000	1.42128	90.6942
0.310	27.804	285.2	0.43921	28.0837	0.51039	0.00185	2.66500	1.46456	92.1587
0.300	27.254	284.6566	0.43837	27.5287	0.51142	0.00189	2.77000	1.49606	93.6548
0.290	26.714	284.1132	0.43753	26.9841	0.51245	0.00192	2.87000	1.52284	95.1776
0.280	26.184	283.5696	0.43670	26.4492	0.51347	0.00194	2.96500	1.54909	96.7267
0.270	25.663	283.0263	0.43586	25.9234	0.51449	0.00197	3.06500	1.56966	98.2964
0.260	25.149	282.481	0.43502	25.4061	0.51551	0.00208	3.30500	1.60455	99.901
0.250	24.644	281.9178	0.43415	24.8966	0.51660	0.00224	3.63000	1.76136	101.662
0.240	24.145	281.3411	0.43327	24.3943	0.51775	0.00230	3.81500	1.88525	103.548
0.230	23.652	280.7639	0.43238	23.8985	0.51889	0.00243	4.10000	1.90018	105.448
0.220	23.165	280.1624	0.43145	23.4087	0.52013	0.00301	5.20000	2.11817	107.566
0.210	22.683	279.4735	0.43039	22.9242	0.52180	0.00358	6.30000	2.91695	110.483
0.200	22.205	278.7612	0.42929	22.4443	0.52356	0.00365	6.55000	3.13770	113.621
0.190	21.731	278.049	0.42820	21.9683	0.52528	0.00358	6.55000	3.12582	116.746
0.180	21.26	277.3366	0.42710	21.4954	0.52695	0.00349	6.55000	3.10445	119.851
0.170	20.79	276.6234	0.42600	21.0250	0.52856	0.00375	7.20000	3.07375	122.925
0.160	20.322	275.8499	0.42481	20.5561	0.53046	0.00505	10.0000	3.69420	126.619
0.150	19.854	274.9012	0.42335	20.0878	0.53331	0.00605	12.1000	5.67748	132.296

0.140	273.9191
0.130	272.937
0.120	271.9488
0.110	270.6335
0.100	268.7639
0.0900	266.8271
0.0800	264.8903
0.0700	262.9529
0.0600	261.0071
0.0500	258.3368
0.0400	253.5057
0.0300	248.2402
0.0200	241.3405
0.0100	227.008
0.00800	222.928
0.00600	218.1931
0.00400	211.1391
0.00200	202.0771
0.00101	195.2435

SUMMARY SHEET

MTU

Ed. Marchand

SAMPLE ID: Ambersor 572

Total Surface Area = 830.9971 sq. m/gm

Average Pore Diameter (4V/S) = 43.6559 Angstroms

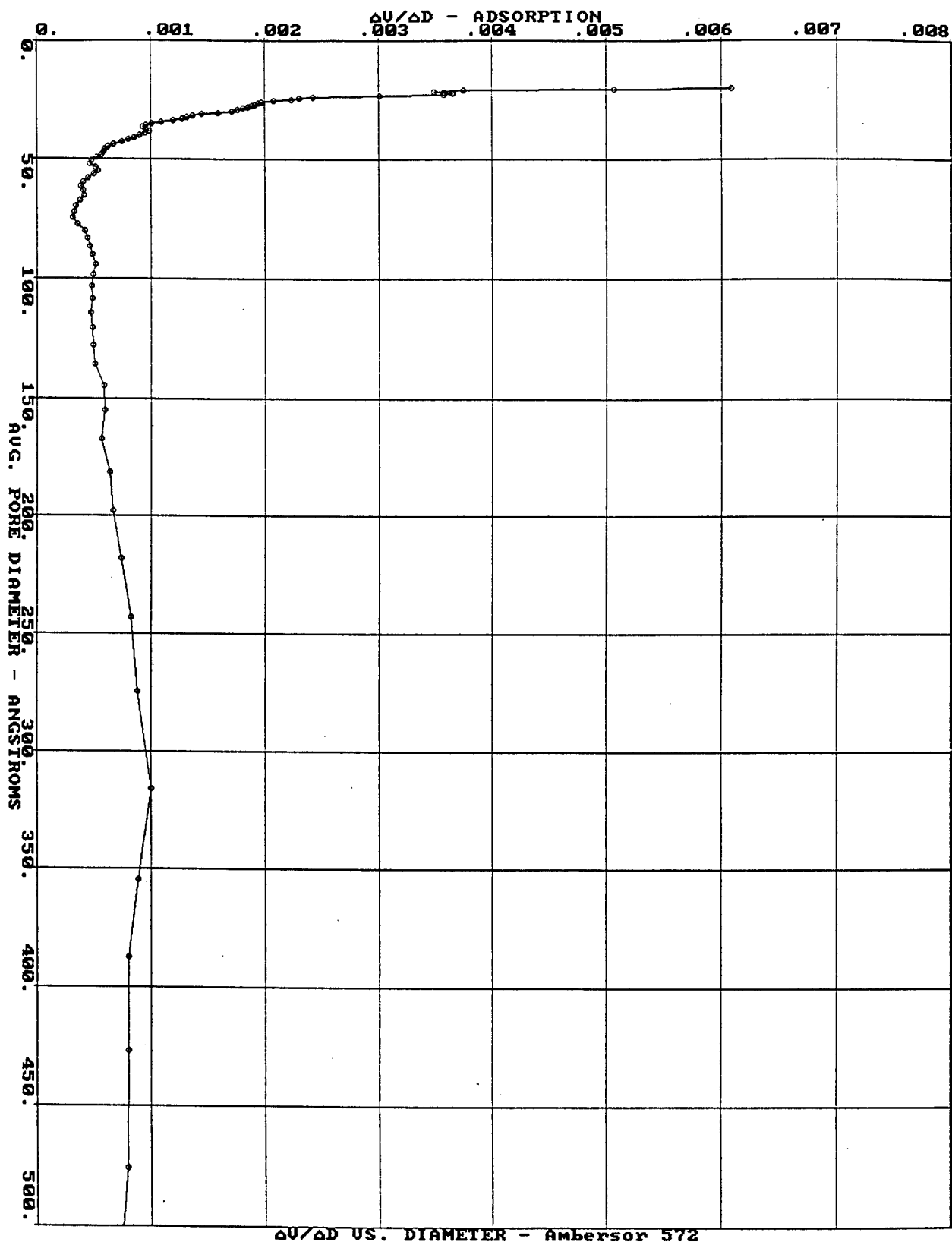
Total Pore Volume = 0.9069 cc/g

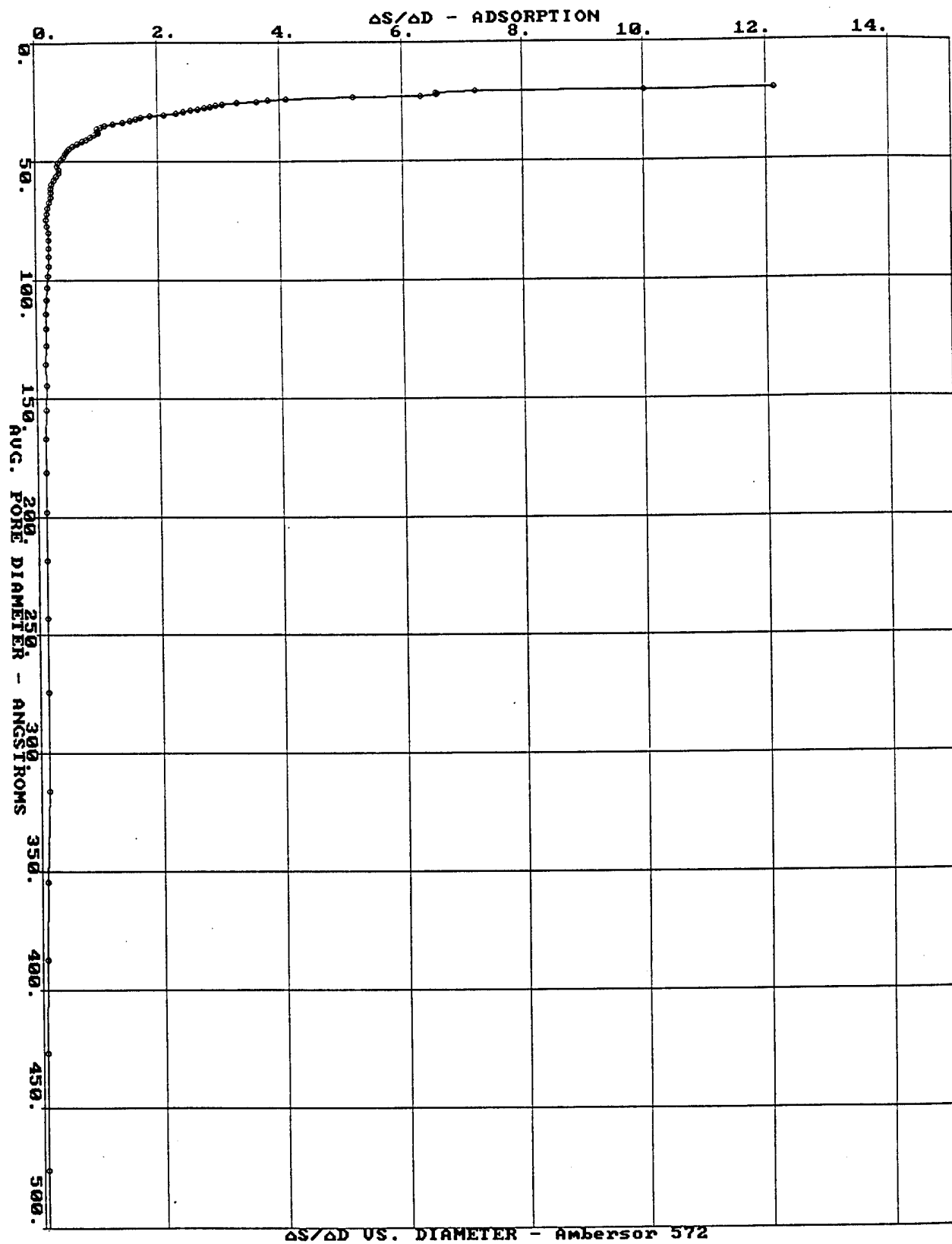
Median Pore Diameter (based on pore volume)= 132.547 Angstroms

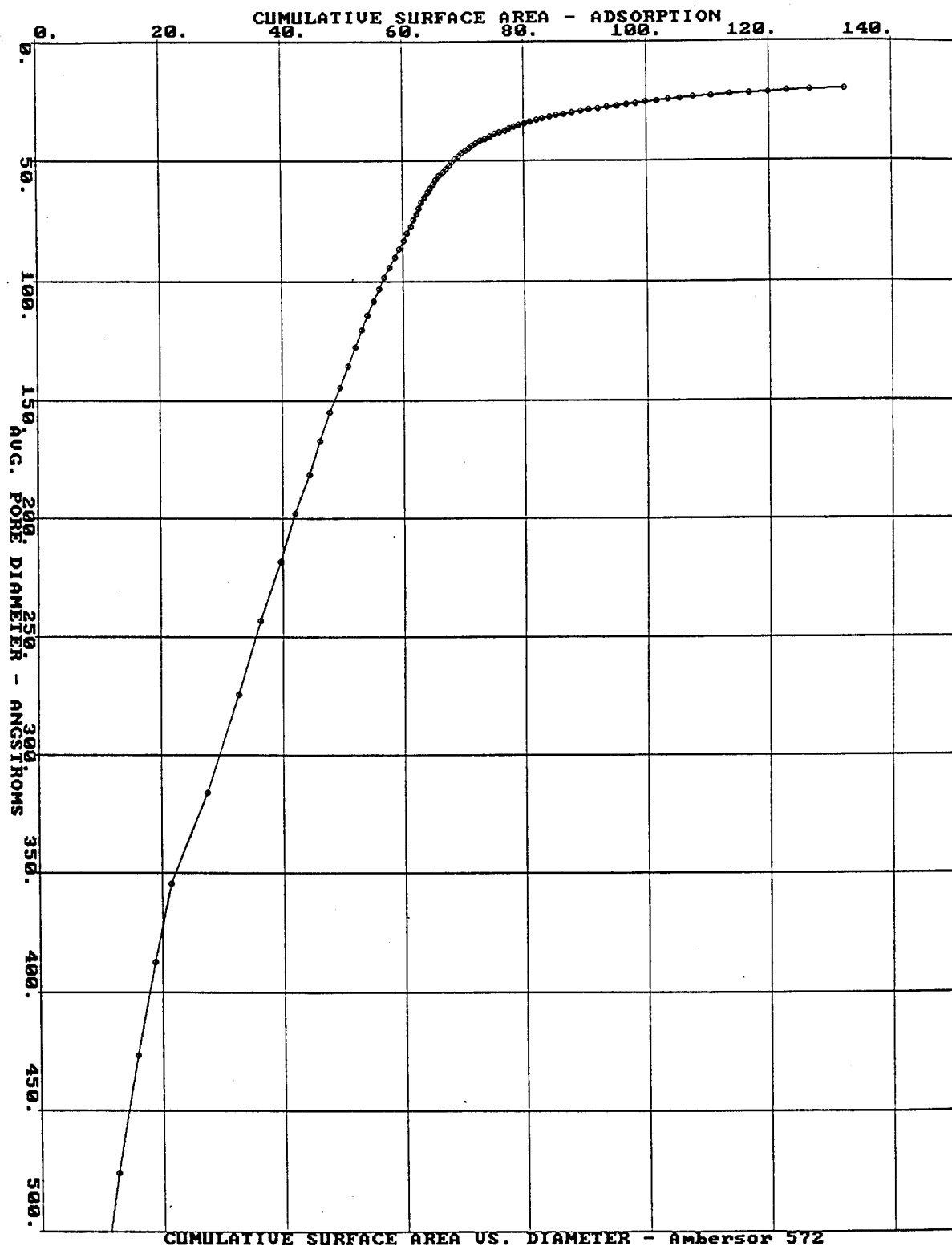
Standard Deviation= 72.8709 Angstroms

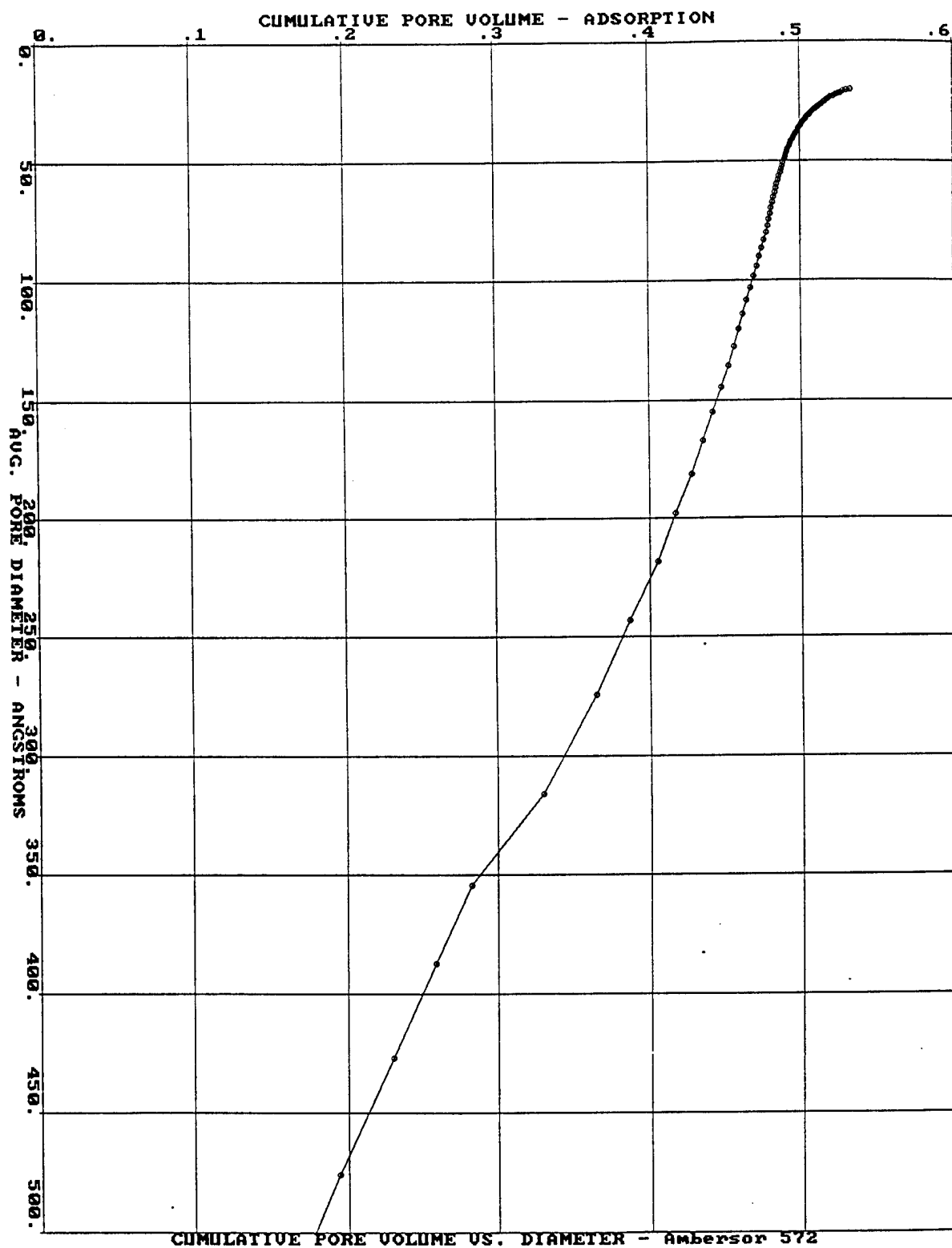
Median Pore Diameter (based on surface area)= 56.03 Angstroms

Standard Deviation= 22.5873 Angstroms









CUMULATIVE PORE VOLUME US. DIAMETER - Amberson 572

GAS ADSORPTION/DESORPTION RESULTS

ADSORBATE: NITROGEN

ISOTHERM AND PORE VOLUME DISTRIBUTION

DESORPTION

P/P0	PORE DIAMETER Å	VOLUME ADSORBED CC/GM STP	LIQ. VOL ADSORBED CC/GM	AVE. POR. DIAM Å	CUMUL. POR. VOL CC/GM	ΔV ----- ΔD	ΔS ----- ΔD	SURFACE AREA M2/GM	CUMUL. S. AREA M2/GM
0.990	1957.7	585.5026	0.90167	1957.70	-0-	2.12E-06	5.15E-05	-0-	-0-
0.985	1313.5	584.6721	0.90040	1635.60	0.00137	2.38E-06	7.50E-05	0.03339	0.03339
0.980	990.44	584.1822	0.89964	1151.97	0.00218	2.54E-06	1.04E-04	0.02818	0.06156
0.975	796.1	583.8838	0.89918	893.270	0.00267	3.02E-06	1.55E-04	0.02222	0.08378
0.970	666.21	583.626	0.89878	731.155	0.00311	4.14E-06	2.54E-04	0.02368	0.10746
0.965	573.22	583.3671	0.89839	619.717	0.00355	6.00E-06	4.26E-04	0.02840	0.13585
0.960	503.33	583.0847	0.89795	538.275	0.00403	9.15E-06	7.40E-04	0.03617	0.17202
0.955	448.85	582.745	0.89743	476.088	0.00463	2.84E-05	0.00261	0.04992	0.22195
0.950	405.18	581.7145	0.89584	427.013	0.00648	2.16E-04	0.02210	0.17331	0.39525
0.945	369.37	574.6946	0.88503	387.274	0.01930	8.70E-04	0.09700	1.32471	1.71996
0.940	339.48	553.5632	0.85249	354.426	0.05830	0.00177	0.21300	4.40164	6.12160
0.930	292.37	490.2859	0.75504	315.927	0.17653	0.00300	0.41650	14.9687	21.0903
0.920	256.92	426.907	0.65744	274.646	0.29619	0.00281	0.43450	17.4279	38.5182
0.910	229.24	391.8633	0.60347	243.079	0.36186	0.00164	0.28000	10.8070	49.3252
0.900	207.02	378.6347	0.58310	218.133	0.38509	0.00113	0.22000	4.25814	53.5833
0.890	188.79	366.2789	0.56407	197.905	0.40709	0.00134	0.28500	4.44838	58.0317
0.880	173.54	354.1259	0.54535	181.161	0.42917	0.00136	0.31250	4.87527	62.9070
0.870	160.59	344.7998	0.53099	167.063	0.44579	0.00100	0.24700	3.97776	66.8847
0.860	149.46	339.5018	0.52283	155.025	0.45422	6.85E-04	0.18300	2.17529	69.0600
0.850	139.78	335.4441	0.51658	144.619	0.46027	6.50E-04	0.18650	1.67387	70.7339
0.840	131.28	331.6517	0.51074	135.532	0.46600	6.15E-04	0.18700	1.69005	72.4239
0.830	123.76	328.6333	0.50610	127.524	0.47023	5.80E-04	0.18800	1.32774	73.7517
0.820	117.06	325.8041	0.50174	120.412	0.47424	6.40E-04	0.22000	1.33084	75.0825
0.810	111.04	323.0048	0.49743	114.050	0.47836	6.35E-04	0.23000	1.44456	76.5271
0.800	105.61	320.6497	0.49380	108.323	0.48161	5.35E-04	0.20350	1.20088	77.7280
0.790	100.67	318.7209	0.49083	103.141	0.48400	4.66E-04	0.18500	0.92927	78.6572
0.780	96.177	317.007	0.48819	98.4258	0.48602	4.09E-04	0.17000	0.81944	79.4767
0.770	92.057	315.5401	0.48593	94.1170	0.48756	3.92E-04	0.17050	0.65442	80.1311
0.760	88.269	314.1149	0.48374	90.1629	0.48911	3.98E-04	0.18000	0.68703	80.8181
0.750	84.77201	312.8078	0.48172	86.5203	0.49047	4.01E-04	0.18950	0.62757	81.4457
0.740	81.534	311.546	0.47978	83.1529	0.49180	3.83E-04	0.18750	0.64374	82.0894

0.730	78.526	310.4243	0.47805	80.0297	0.49287	3.43E-04	0.17450	0.53398	82.6234
0.720	75.723	309.3876	0.47646	77.1244	0.49380	3.34E-04	0.17600	0.48235	83.1058
0.710	73.10501	308.3997	0.47494	74.4142	0.49468	2.56E-04	0.13900	0.47209	83.5778
0.700	70.654	307.6019	0.47371	71.8794	0.49512	1.72E-04	0.09700	0.24706	83.8249
0.690	68.352	306.8543	0.47256	69.5029	0.49550	1.82E-04	0.10650	0.21574	84.0406
0.680	66.187	306.1076	0.47141	67.2697	0.49593	2.22E-04	0.13400	0.25833	84.2990
0.670	64.14601	305.3604	0.47026	65.1668	0.49643	2.64E-04	0.16450	0.30336	84.6023
0.660	62.219	304.6137	0.46911	63.1825	0.49698	3.06E-04	0.19700	0.34697	84.9493
0.650	60.395	303.8682	0.46796	61.3067	0.49757	3.11E-04	0.20550	0.38947	85.3388
0.640	58.666	303.1697	0.46688	59.5301	0.49808	2.60E-04	0.17650	0.34361	85.6824
0.630	57.024	302.5356	0.46590	57.8447	0.49846	2.41E-04	0.16950	0.25655	85.9389
0.620	55.463	301.9068	0.46494	56.2433	0.49886	2.73E-04	0.19700	0.28435	86.2233
0.610	53.976	301.2821	0.46397	54.7192	0.49928	2.68E-04	0.19850	0.31411	86.5374
0.600	52.558	300.6964	0.46307	53.2668	0.49964	2.43E-04	0.18500	0.26436	86.8017
0.590	51.203	300.1326	0.46220	51.8806	0.49996	2.58E-04	0.20100	0.24925	87.0510
0.580	49.908	299.5696	0.46134	50.5559	0.50032	2.96E-04	0.23750	0.28253	87.3335
0.570	48.668	299.0066	0.46047	49.2884	0.50071	3.37E-04	0.27700	0.31800	87.6515
0.560	47.48	298.4435	0.45960	48.0741	0.50113	3.76E-04	0.31700	0.35375	88.0053
0.550	46.339	297.8825	0.45874	46.9094	0.50158	3.73E-04	0.32200	0.38377	88.3891
0.540	45.243	297.3502	0.45792	45.7909	0.50197	3.35E-04	0.29600	0.33791	88.7270
0.530	44.189	296.8421	0.45714	44.7158	0.50231	3.37E-04	0.30450	0.30041	89.0274
0.520	43.174	296.3353	0.45636	43.6812	0.50267	3.75E-04	0.34750	0.32893	89.3563
0.510	42.196	295.8282	0.45558	42.6846	0.50305	4.15E-04	0.39350	0.36229	89.7186
0.500	41.252	295.3216	0.45480	41.7237	0.50346	4.69E-04	0.45500	0.39312	90.1117
0.490	40.341	294.8083	0.45400	40.7962	0.50392	6.40E-04	0.64000	0.44848	90.5602
0.480	39.46	294.2354	0.45312	39.9003	0.50461	8.90E-04	0.90500	0.69135	91.2515
0.470	38.608	293.6225	0.45218	39.0339	0.50546	0.00102	1.06000	0.87475	92.1263
0.460	37.783	293.0128	0.45124	38.1954	0.50633	0.00092	0.97000	0.90300	93.0293
0.450	36.984	292.469	0.45040	37.3833	0.50697	6.95E-04	0.75000	0.68548	93.7148
0.440	36.208	291.9785	0.44965	36.5959	0.50743	6.10E-04	0.67500	0.50510	94.2199
0.430	35.456	291.4899	0.44889	35.8319	0.50790	6.45E-04	0.73000	0.52810	94.7480
0.420	34.725	291.0017	0.44814	35.0901	0.50839	6.90E-04	0.79500	0.55710	95.3050
0.410	34.014	290.5133	0.44739	34.3691	0.50890	7.30E-04	0.86000	0.58850	95.8936
0.400	33.322	290.025	0.44664	33.6679	0.50942	7.80E-04	0.93500	0.61832	96.5119
0.390	32.648	289.5338	0.44588	32.9853	0.50996	8.45E-04	1.04000	0.66191	97.1738
0.380	31.992	289.0366	0.44512	32.3203	0.51055	0.00091	1.13500	0.72161	97.8954
0.370	31.352	288.5387	0.44435	31.6720	0.51114	0.00095	1.21500	0.75470	98.6501
0.360	30.727	288.0405	0.44358	31.0394	0.51175	0.00099	1.29500	0.78548	99.436
0.350	30.116	287.5424	0.44282	30.4217	0.51237	0.00104	1.38500	0.81337	100.249
0.340	29.52	287.0413	0.44204	29.8181	0.51301	0.00115	1.56000	0.85802	101.107
0.330	28.936	286.5232	0.44125	29.2277	0.51373	0.00127	1.76000	0.98510	102.092
0.320	28.364	285.9991	0.44044	28.6498	0.51448	0.00133	1.87500	1.04875	103.141
0.310	27.804	285.4748	0.43963	28.0837	0.51524	0.00136	1.96000	1.07661	104.217
0.300	27.254	284.9507	0.43882	27.5287	0.51599	0.00143	2.10000	1.09975	105.317
0.290	26.714	284.4166	0.43800	26.9841	0.51680	0.00165	2.47500	1.19070	106.508
0.280	26.184	283.8481	0.43713	26.4492	0.51776	0.00187	2.85000	1.45374	107.962
0.270	25.663	283.2701	0.43624	25.9234	0.51876	0.00193	3.00000	1.54501	109.507
0.260	25.149	282.6923	0.43535	25.4061	0.51975	0.00196	3.12000	1.56322	111.070
0.250	24.644	282.1093	0.43445	24.8966	0.52076	0.00210	3.41000	1.61969	112.690
0.240	24.145	281.5049	0.43352	24.3943	0.52186	0.00224	3.70500	1.80621	114.496
0.230	23.652	280.8939	0.43258	23.8985	0.52298	0.00226	3.82000	1.87106	116.367
0.220	23.165	280.2829	0.43164	23.4087	0.52408	0.00224	3.86500	1.87410	118.241
0.210	22.683	279.6718	0.43069	22.9242	0.52515	0.00235	4.14000	1.87118	120.112
0.200	22.205	279.035	0.42971	22.4443	0.52633	0.00295	5.30000	2.10338	122.215
0.190	21.731	278.3096	0.42860	21.9683	0.52796	0.00352	6.45000	2.95973	125.175
0.180	21.26	277.5607	0.42744	21.4954	0.52966	0.00356	6.70000	3.17444	128.350
0.170	20.79	276.8118	0.42629	21.0250	0.53131	0.00344	6.60000	3.13156	131.481
0.160	20.322	276.0622	0.42514	20.5561	0.53289	0.00369	7.25000	3.07645	134.558
0.150	19.854	275.2496	0.42388	20.0878	0.53476	0.00400	7.95000	3.73042	138.288
0.140		274.2463							

0.130	273.199
0.120	272.1515
0.110	271.103
0.100	269.8837
0.0900	268.0038
0.0800	265.9261
0.0700	263.8468
0.0600	261.7609
0.0500	258.9777
0.0400	253.9745
0.0300	248.4888
0.0200	241.6162
0.0100	228.3449
0.00800	224.6267
0.00600	220.2782
0.00400	214.0376
0.00200	206.0367
0.00100	199.9052

SUMMARY SHEET

MTU

Ed. Marchand

SAMPLE ID: Ambersor 572

Total Surface Area = 830.9971 sq. m/gm

Average Pore Diameter (4V/S) = 43.5948 Angstroms

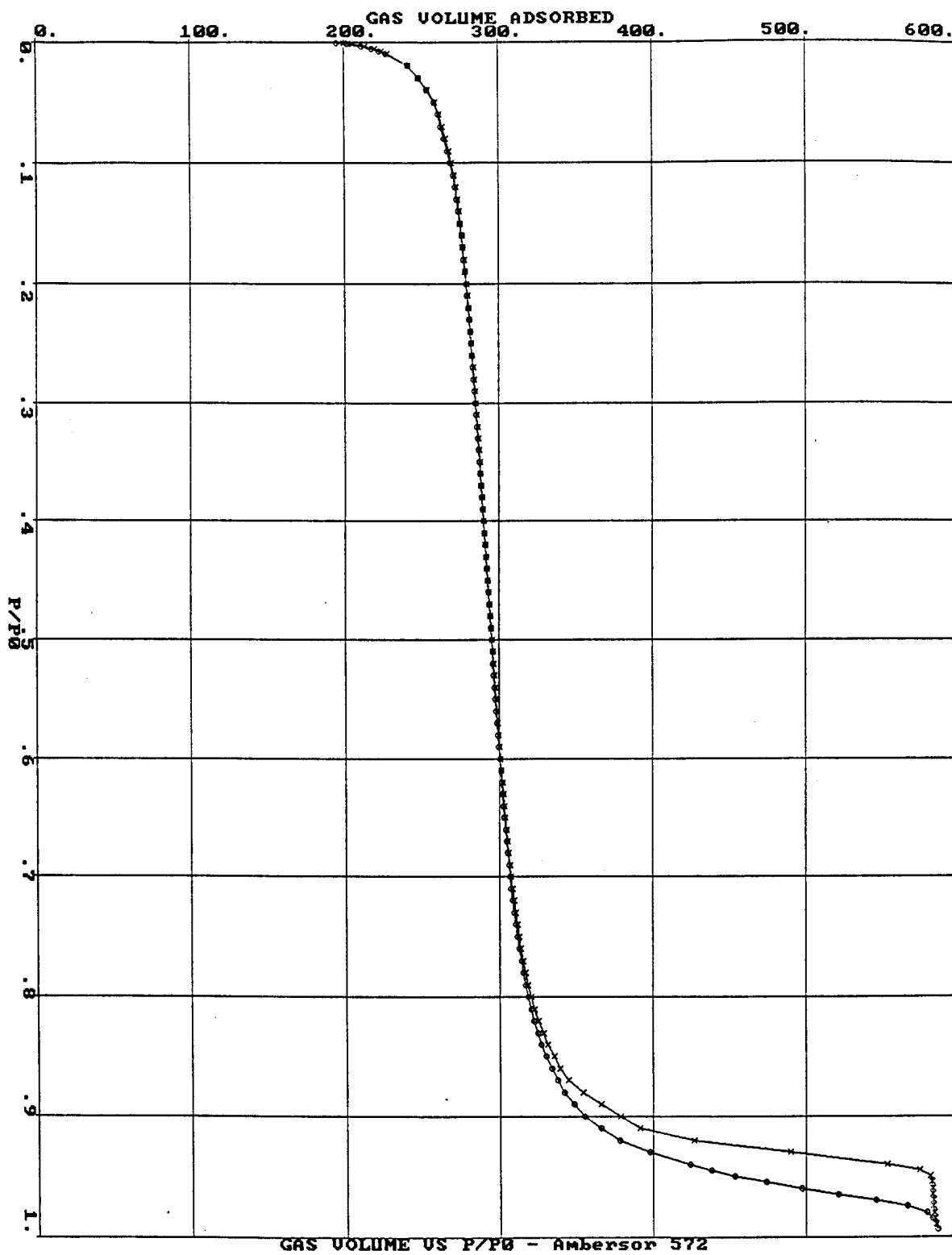
Total Pore Volume = 0.9057 cc/g

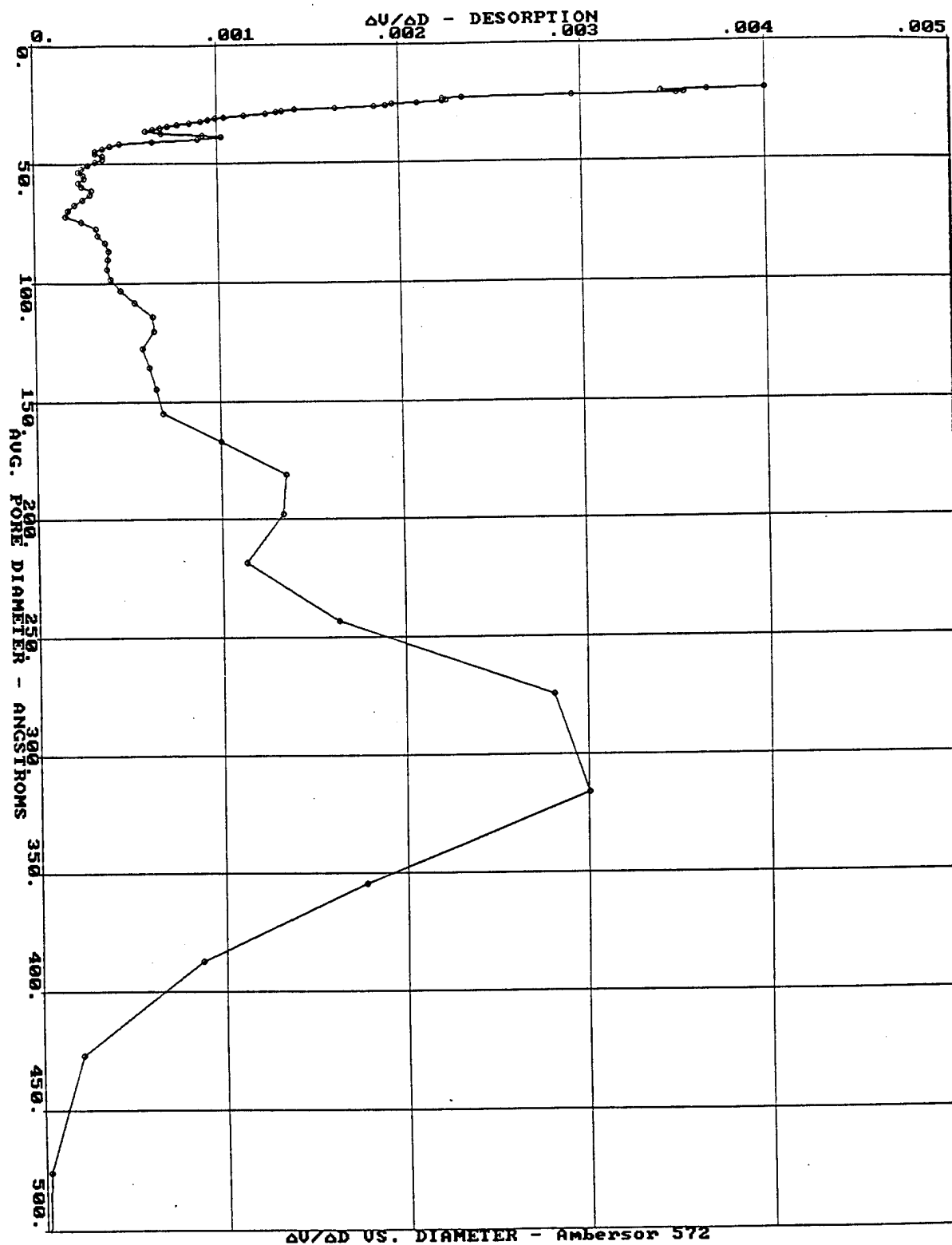
Median Pore Diameter (based on pore volume)= 156.995 Angstroms

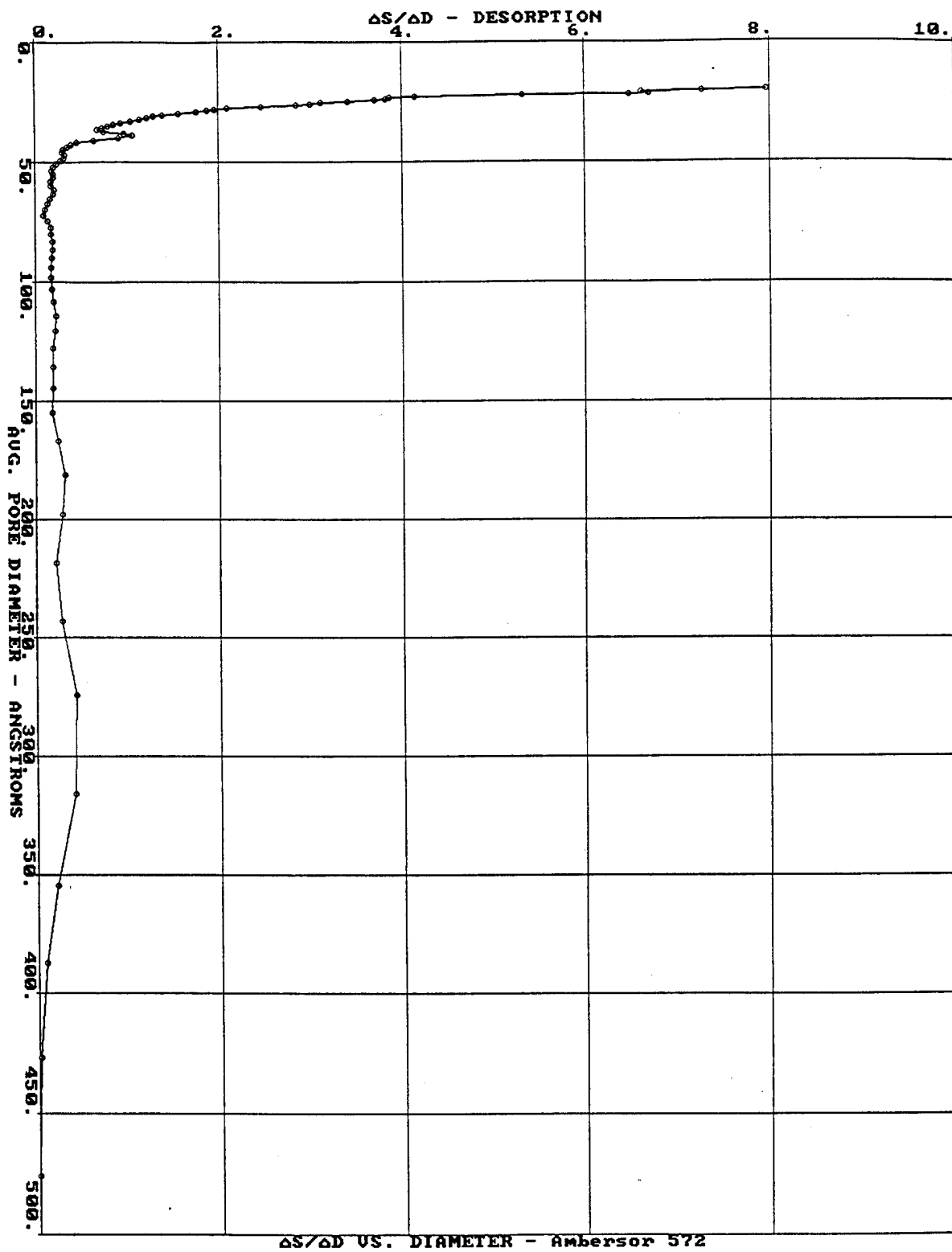
Standard Deviation= 74.3549 Angstroms

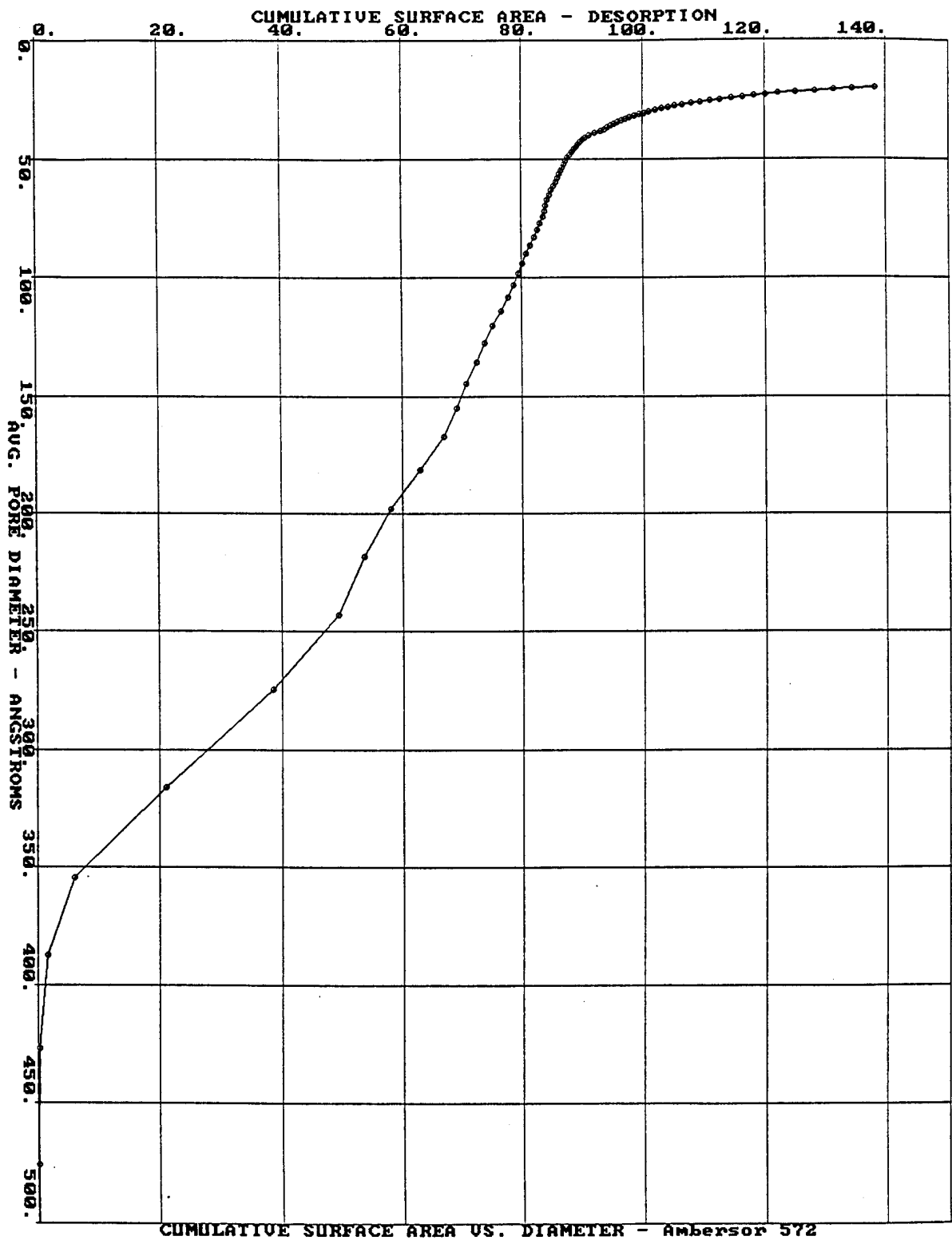
Median Pore Diameter (based on surface area)= 154.502 Angstroms

Standard Deviation= 28.0087 Angstroms

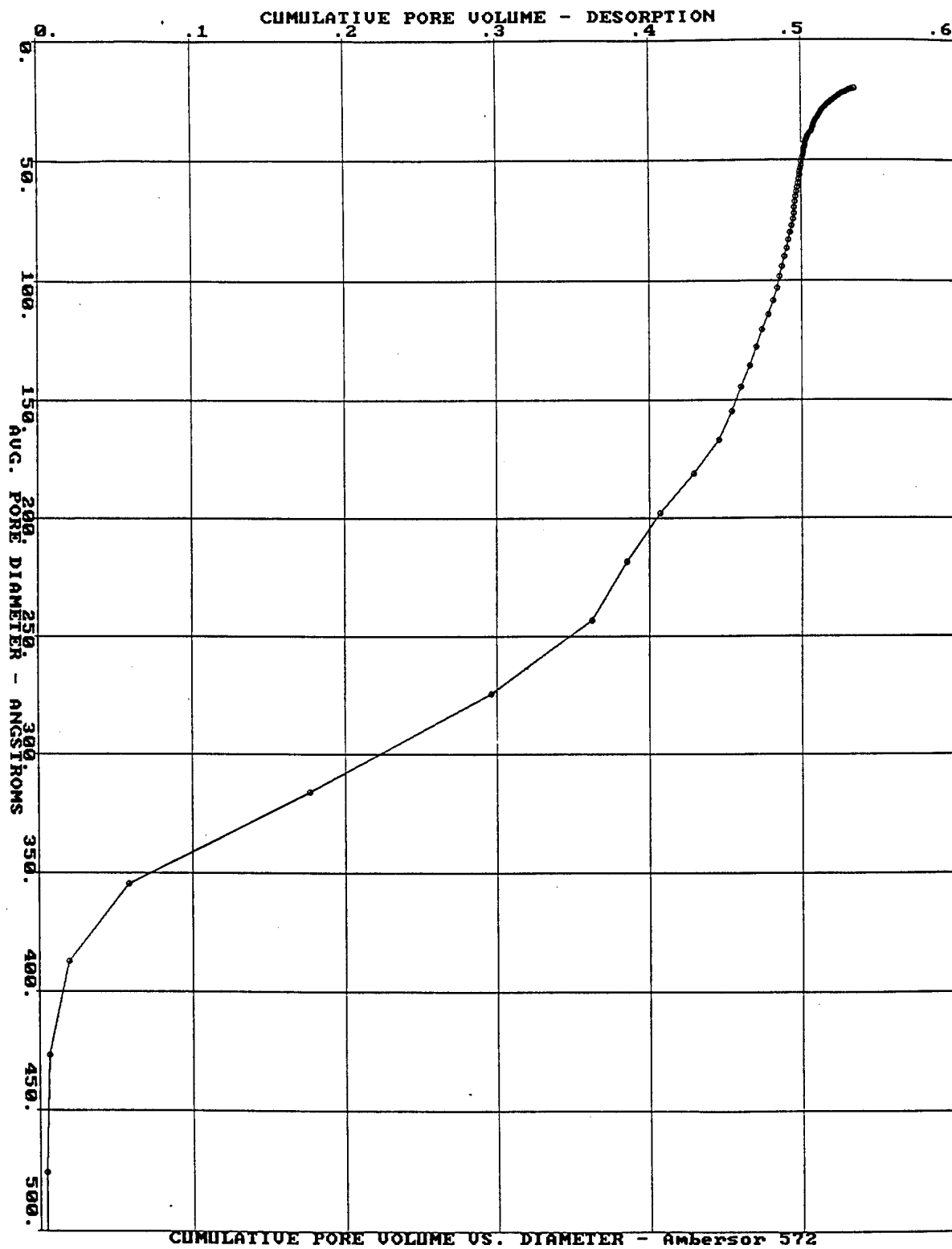








CUMULATIVE SURFACE AREA US. DIAMETER - Ambersor 572



BET SURFACE AREA ANALYSIS

12-16-1994

POROUS MATERIALS, INC. ANALYTICAL SERVICES DIVISION
 CORNELL INDUSTRY RESEARCH PARK, BLDG. 4
 ITHACA, NY 14850 USA
 PHONE (607) 257-4267 OR 257-5544

NOTE: RESULTS CALCULATED USING WEIGHT AFTER OUTGASSING.
 TO GET RESULTS USING ORIGINAL WEIGHT, MULTIPLY THESE VALUES BY
 WT AFTER OUTGAS/WT BEFORE OUTGAS

MTU
 Ed. Marchand

SAMPLE ID: Amsorcat (MTU-CAT)

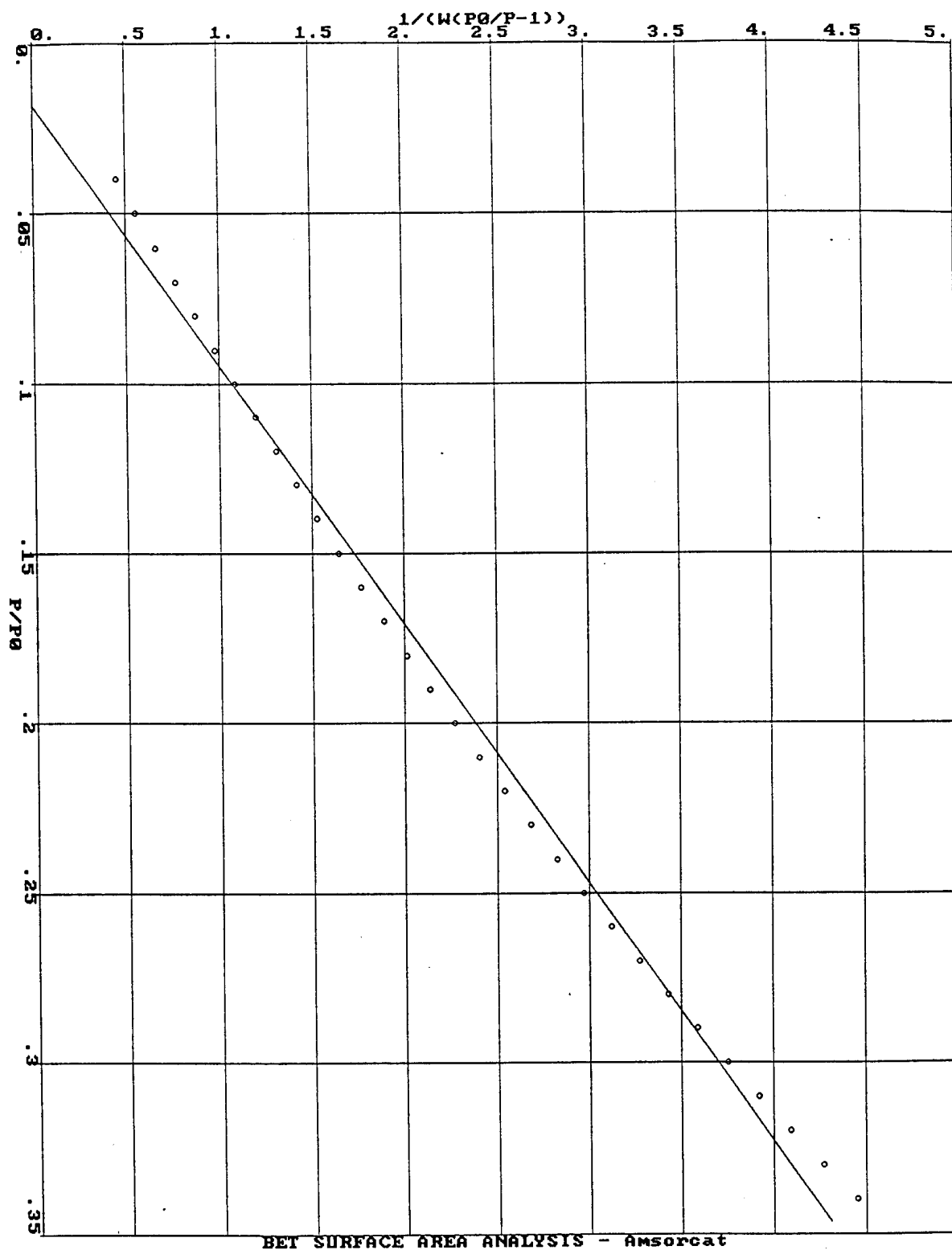
SPECIFIC SURFACE AREA= 324.7001 M2/GM

SAMPLE WEIGHT= .8409 GM BEFORE OUTGASSING .831 GM AFTER OUTGASSING
 Sample Density= 1.5
 BET C VALUE= -52.112
 SLOPE= 13.161 GM-1
 Y INTERCEPT= -.248 GM-1
 CORRELATION COEFFICIENT= .996
 ADSORBATE= NITROGEN
 VA VOLUME= 44.9502 CC
 vit VOLUME= 11.14068 CC
 Vln VOLUME= 14.155 CC
 INSTRUMENT TEMPERATURE= 305.36 K
 ROOM TEMPERATURE= 296.7 K
 W = Wt. of adsorbed gas per gram of sample

SAMPLE OUTGASSED AT 20 DEGREES CELSIUS

DATA POINT	P P0	P0 P (W(- -1))	-1
9	0.04000000	0.44900000	
10	0.05000000	0.55200000	
11	0.06000000	0.65900000	
12	0.07000000	0.76600000	
13	0.08000000	0.87300000	
14	0.09000001	0.97900000	
15	0.10000000	1.085	
16	0.11000000	1.194	
17	0.12000000	1.304	
18	0.13000000	1.415	
19	0.14000000	1.526	
20	0.15000000	1.641	
21	0.16000000	1.762	
22	0.17000000	1.885	
23	0.18000000	2.011	
24	0.19000000	2.138	

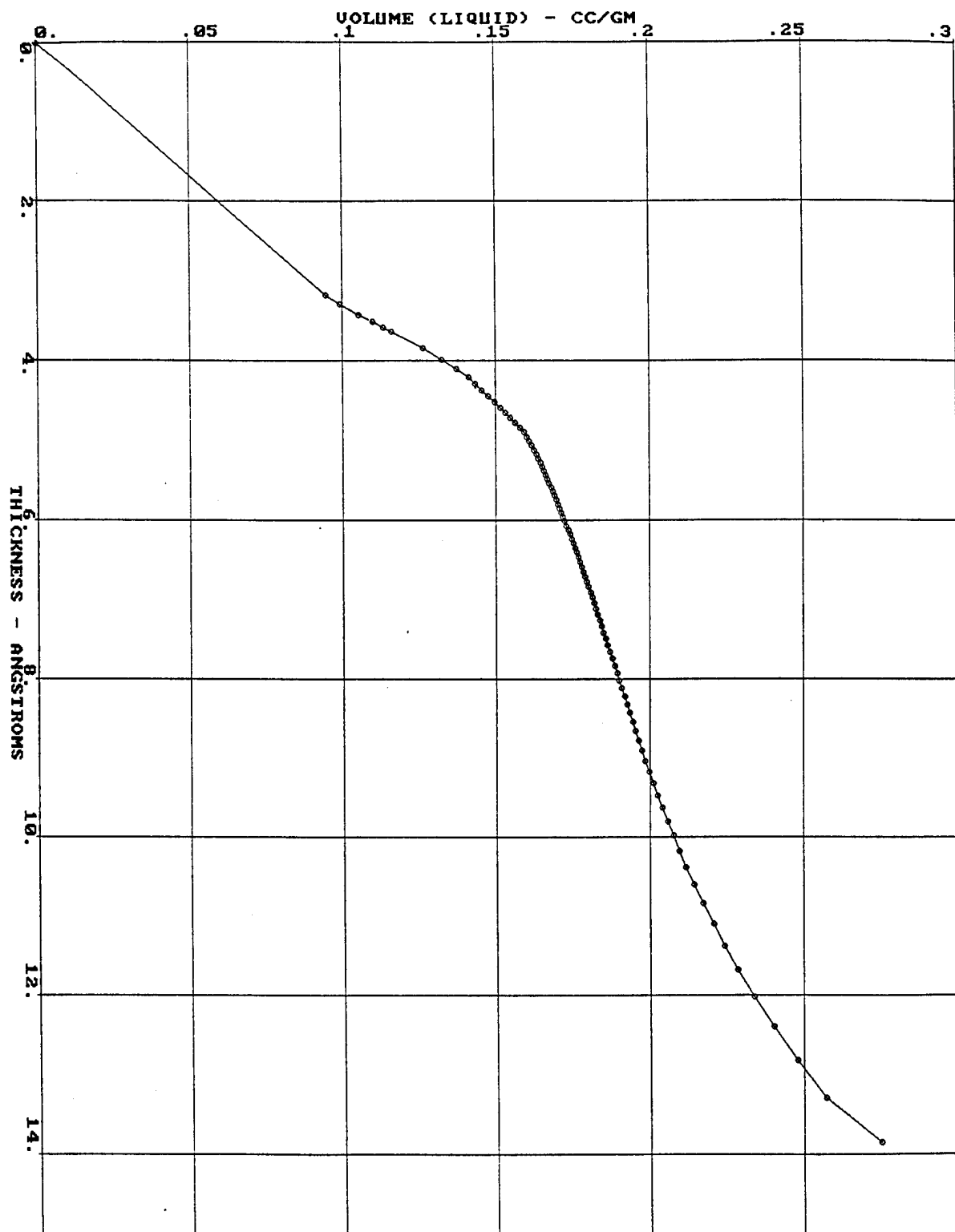
25	0.20000000	2.268
26	0.21000000	2.402
27	0.22000000	2.54
28	0.23000000	2.68
29	0.24000000	2.824
30	0.25000000	2.971
31	0.26000000	3.12
32	0.27000000	3.273
33	0.28000000	3.429
34	0.29000000	3.588
35	0.30000000	3.752
36	0.31000000	3.92
37	0.32000000	4.093
38	0.33000000	4.27
39	0.34000000	4.453



MICRO PORE CALCULATIONS

Thickness Range Angstroms		Volume (Liquid) cc/g	Hydraulic Radius Angstroms
3.180 -	3.292	0.095	3.236
3.292 -	3.425	0.099	3.359
3.425 -	3.513	0.105	3.469
3.513 -	3.581	0.110	3.547
3.581 -	3.638	0.113	3.610
3.638 -	3.842	0.116	3.740
3.842 -	3.984	0.126	3.913
3.984 -	4.100	0.132	4.042
4.100 -	4.199	0.137	4.149
4.199 -	4.288	0.141	4.244
4.288 -	4.369	0.143	4.329
4.369 -	4.445	0.145	4.407
4.445 -	4.516	0.148	4.481
4.516 -	4.584	0.150	4.550
4.584 -	4.649	0.152	4.617
4.649 -	4.712	0.153	4.681
4.712 -	4.773	0.155	4.742
4.773 -	4.832	0.156	4.802
4.832 -	4.890	0.158	4.861
4.890 -	4.947	0.159	4.918
4.947 -	5.002	0.160	4.974
5.002 -	5.057	0.161	5.030
5.057 -	5.112	0.162	5.084
5.112 -	5.165	0.163	5.139
5.165 -	5.219	0.163	5.192
5.219 -	5.272	0.164	5.245
5.272 -	5.324	0.165	5.298
5.324 -	5.377	0.165	5.350
5.377 -	5.429	0.166	5.403
5.429 -	5.481	0.166	5.455
5.481 -	5.533	0.167	5.507
5.533 -	5.585	0.167	5.559
5.585 -	5.638	0.168	5.612
5.638 -	5.690	0.169	5.664
5.690 -	5.743	0.169	5.716
5.743 -	5.796	0.170	5.769
5.796 -	5.849	0.170	5.822
5.849 -	5.902	0.171	5.875
5.902 -	5.956	0.171	5.929
5.956 -	6.010	0.172	5.983
6.010 -	6.065	0.172	6.038
6.065 -	6.120	0.173	6.093
6.120 -	6.176	0.174	6.148
6.176 -	6.232	0.174	6.204
6.232 -	6.289	0.175	6.261
6.289 -	6.347	0.175	6.318
6.347 -	6.405	0.176	6.376
6.405 -	6.465	0.176	6.435
6.465 -	6.525	0.177	6.495
6.525 -	6.586	0.177	6.555
6.586 -	6.648	0.178	6.617
6.648 -	6.711	0.179	6.679
6.711 -	6.775	0.179	6.743
6.775 -	6.840	0.180	6.807

6.840 -	6.906	0.180	6.873
6.906 -	6.974	0.181	6.940
6.974 -	7.043	0.181	7.009
7.043 -	7.114	0.182	7.078
7.114 -	7.186	0.183	7.150
7.186 -	7.259	0.183	7.222
7.259 -	7.335	0.184	7.297
7.335 -	7.412	0.184	7.373
7.412 -	7.491	0.185	7.452
7.491 -	7.572	0.186	7.532
7.572 -	7.656	0.186	7.614
7.656 -	7.742	0.187	7.699
7.742 -	7.830	0.188	7.786
7.830 -	7.921	0.189	7.876
7.921 -	8.015	0.189	7.968
8.015 -	8.112	0.190	8.064
8.112 -	8.212	0.191	8.162
8.212 -	8.316	0.192	8.264
8.316 -	8.424	0.193	8.370
8.424 -	8.536	0.193	8.480
8.536 -	8.652	0.194	8.594
8.652 -	8.773	0.195	8.712
8.773 -	8.899	0.196	8.836
8.899 -	9.031	0.197	8.965
9.031 -	9.170	0.199	9.101
9.170 -	9.315	0.200	9.242
9.315 -	9.468	0.201	9.391
9.468 -	9.629	0.202	9.548
9.629 -	9.799	0.204	9.714
9.799 -	9.980	0.206	9.890
9.980 -	10.172	0.208	10.076
10.172 -	10.378	0.210	10.275
10.378 -	10.598	0.212	10.488
10.598 -	10.836	0.214	10.717
10.836 -	11.092	0.217	10.964
11.092 -	11.372	0.221	11.232
11.372 -	11.678	0.224	11.525
11.678 -	12.017	0.228	11.847
12.017 -	12.393	0.234	12.205
12.393 -	12.816	0.240	12.605
12.816 -	13.299	0.248	13.058
13.299 -	13.856	0.257	13.577



MICROPORE U-T PLOT - Amsorcat

T-PLOT ANALYSIS:

T-PLOT INTERCEPT: 0.10706
T-PLOT SLOPE: 0.010190
MICROPORE VOLUME: 0.10706 CC/GM

FILM THICKNESS USED BETWEEN 8.000 and 12.000 ANGSTROMS

SURFACE AREA = 101.8956 SQ. M/GM
(MESO AND MACROPORES ONLY)

MICROPORE SURFACE AREA = 222.8045 SQ. M/GM

GAS ADSORPTION/DESORPTION RESULTS

ADSORBATE: NITROGEN

ISOTHERM AND PORE VOLUME DISTRIBUTION

ADSORPTION

P/P0	PORE DIAMETER Å	VOLUME ADSORBED CC/GM STP	LIQ. VOL ADSORBED CC/GM	AVE. POR. DIAM Å	CUMUL. POR. VOL CC/GM	ΔV ----	ΔS ----	SURFACE AREA M2/GM	CUMUL. S. AREA M2/GM
						ΔD	ΔD		
1.000	141650	340.1398	0.52382	141655	-0-	8.00E-08	4.37E-08	-0-	-0-
0.997	5711.8	333.0673	0.51292	73683.3	0.01094	3.99E-06	3.32E-05	0.00594	0.00594
0.995	3883.5	328.4128	0.50576	4797.63	0.01833	6.95E-06	8.40E-05	0.06167	0.06761
0.990	1957.7	316.3942	0.48725	2920.59	0.03762	1.92E-05	4.45E-04	0.26416	0.33177
0.985	1313.5	307.5428	0.47362	1635.60	0.05205	4.44E-05	0.00146	0.35277	0.68453
0.980	990.44	296.7394	0.45698	1151.97	0.06995	7.85E-05	0.00331	0.62173	1.30626
0.975	796.1	286.0157	0.44046	893.270	0.08794	1.22E-04	0.00630	0.80550	2.11176
0.970	666.21	275.1239	0.42369	731.155	0.10642	1.77E-04	0.01080	1.01099	3.12275
0.965	573.22	264.2112	0.40689	619.717	0.12513	2.40E-04	0.01695	1.20758	4.33033
0.960	503.33	253.3761	0.39020	538.275	0.14389	3.12E-04	0.02505	1.39380	5.72413
0.955	448.85	242.5921	0.37359	476.088	0.16273	3.99E-04	0.03585	1.58299	7.30712
0.950	405.18	231.6586	0.35675	427.013	0.18201	4.95E-04	0.04920	1.80617	9.1133
0.945	369.37	220.7989	0.34003	387.274	0.20132	5.85E-04	0.06400	1.99469	11.1080
0.940	339.48	210.2879	0.32384	354.426	0.22015	6.40E-04	0.07550	2.12490	13.2329
0.930	292.37	193.0715	0.29733	315.927	0.25120	6.95E-04	0.09600	3.93120	17.1641
0.920	256.92	178.8804	0.27548	274.646	0.27698	7.55E-04	0.11850	3.75433	20.9184
0.910	229.24	167.036	0.25724	243.079	0.29861	6.05E-04	0.10450	3.56084	24.4792
0.900	207.02	161.056	0.24803	218.133	0.30898	4.69E-04	0.09050	1.90000	26.3792
0.890	188.79	156.0846	0.24037	197.905	0.31756	4.78E-04	0.10150	1.73565	28.1149
0.880	173.54	151.8067	0.23378	181.161	0.32495	4.67E-04	0.10750	1.63075	29.7456
0.870	160.59	148.3571	0.22847	167.063	0.33080	4.18E-04	0.10350	1.40012	31.1458
0.860	149.46	145.7035	0.22438	155.025	0.33512	3.88E-04	0.10350	1.11521	32.2610
0.850	139.78	143.3818	0.22081	144.619	0.33887	4.18E-04	0.11950	1.03637	33.2973
0.840	131.28	141.1017	0.21730	135.532	0.34265	4.29E-04	0.13050	1.11570	34.4130
0.830	123.76	139.1696	0.21432	127.524	0.34577	3.92E-04	0.12650	0.97837	35.3914
0.820	117.06	137.5602	0.21184	120.412	0.34826	3.50E-04	0.11950	0.82750	36.2189
0.810	111.04	136.2071	0.20976	114.050	0.35025	3.50E-04	0.12600	0.69903	36.9179
0.800	105.61	134.8885	0.20773	108.323	0.35224	3.76E-04	0.14250	0.73594	37.6539
0.790	100.67	133.6413	0.20581	103.141	0.35414	3.78E-04	0.15000	0.73619	38.3901
0.780	96.177	132.5179	0.20408	98.4258	0.35581	3.68E-04	0.15300	0.67868	39.0687
0.770	92.057	131.4884	0.20249	94.1170	0.35731	3.50E-04	0.15150	0.63940	39.7081

0.760	88.269	130.5769	0.20109	90.1629	0.35859	3.32E-04	0.15000	0.56419	40.2723
0.750	84.77201	129.7358	0.19979	86.5203	0.35974	3.35E-04	0.15800	0.53123	40.8036
0.740	81.534	128.9315	0.19855	83.1529	0.36084	3.34E-04	0.16350	0.53151	41.3351
0.730	78.526	128.1924	0.19742	80.0297	0.36182	3.21E-04	0.16300	0.49168	41.8268
0.720	75.723	127.5086	0.19636	77.1244	0.36271	3.32E-04	0.17550	0.45789	42.2846
0.710	73.10501	126.8288	0.19532	74.4142	0.36362	3.45E-04	0.18900	0.49023	42.7749
0.700	70.654	126.19	0.19433	71.8794	0.36446	3.24E-04	0.18350	0.46762	43.2425
0.690	68.352	125.6138	0.19345	69.5029	0.36517	3.21E-04	0.18750	0.40679	43.6493
0.680	66.187	125.0438	0.19257	67.2697	0.36589	3.52E-04	0.21250	0.42983	44.0791
0.670	64.14601	124.4741	0.19169	65.1668	0.36664	3.82E-04	0.23800	0.46237	44.5415
0.660	62.219	123.9131	0.19083	63.1825	0.36740	3.76E-04	0.24100	0.48024	45.0217
0.650	60.395	123.3988	0.19003	61.3067	0.36806	3.61E-04	0.23900	0.42693	45.4487
0.640	58.666	122.9025	0.18927	59.5301	0.36868	3.82E-04	0.26050	0.42288	45.8715
0.630	57.024	122.4059	0.18851	57.8447	0.36934	4.17E-04	0.29250	0.45333	46.3249
0.620	55.463	121.9098	0.18774	56.2433	0.37002	4.54E-04	0.32750	0.48241	46.8073
0.610	53.976	121.4135	0.18698	54.7192	0.37072	4.67E-04	0.34600	0.51316	47.3204
0.600	52.558	120.9396	0.18625	53.2668	0.37138	4.14E-04	0.31450	0.49295	47.8134
0.590	51.203	120.5247	0.18561	51.8806	0.37187	3.71E-04	0.28950	0.38329	48.1967
0.580	49.908	120.1205	0.18499	50.5559	0.37236	3.90E-04	0.31250	0.38304	48.5797
0.570	48.668	119.7165	0.18436	49.2884	0.37286	4.23E-04	0.34750	0.40799	48.9877
0.560	47.48	119.3122	0.18374	48.0741	0.37338	4.55E-04	0.38350	0.43442	49.4221
0.550	46.339	118.9089	0.18312	46.9094	0.37392	4.69E-04	0.40500	0.45750	49.8796
0.540	45.243	118.518	0.18252	45.7909	0.37443	4.66E-04	0.41200	0.44810	50.3277
0.530	44.189	118.1389	0.18193	44.7158	0.37492	4.80E-04	0.43500	0.43851	50.7662
0.520	43.174	117.7607	0.18135	43.6812	0.37543	5.10E-04	0.47500	0.46035	51.2266
0.510	42.196	117.3824	0.18077	42.6846	0.37594	5.35E-04	0.50500	0.48524	51.7118
0.500	41.252	117.0095	0.18019	41.7237	0.37646	5.25E-04	0.50500	0.49227	52.2041
0.490	40.341	116.6549	0.17965	40.7962	0.37692	5.15E-04	0.51000	0.45447	52.6585
0.480	39.46	116.3049	0.17911	39.9003	0.37738	5.35E-04	0.54500	0.46148	53.1200
0.470	38.608	115.955	0.17857	39.0339	0.37785	5.70E-04	0.59000	0.48407	53.6041
0.460	37.783	115.6052	0.17803	38.1954	0.37834	6.00E-04	0.63500	0.50668	54.1108
0.450	36.984	115.255	0.17749	37.3833	0.37883	6.50E-04	0.70500	0.53123	54.6420
0.440	36.208	114.8978	0.17694	36.5959	0.37937	7.30E-04	0.80500	0.58253	55.2245
0.430	35.456	114.5299	0.17638	35.8319	0.37995	7.95E-04	0.89500	0.65083	55.8754
0.420	34.725	114.1609	0.17581	35.0901	0.38055	8.30E-04	0.95500	0.67989	56.5552
0.410	34.014	113.7931	0.17524	34.3691	0.38115	8.45E-04	0.99500	0.69873	57.2540
0.400	33.322	113.4301	0.17468	33.6679	0.38174	8.65E-04	1.03500	0.70055	57.9545
0.390	32.648	113.0684	0.17413	32.9853	0.38233	8.95E-04	1.09500	0.71781	58.6723
0.380	31.992	112.7068	0.17357	32.3203	0.38293	0.00093	1.16000	0.74046	59.4128
0.370	31.352	112.3453	0.17301	31.6720	0.38353	0.00094	1.19500	0.76286	60.1757
0.360	30.727	111.9904	0.17247	31.0394	0.38411	0.00091	1.18500	0.75028	60.9259
0.350	30.116	111.645	0.17193	30.4217	0.38466	0.00091	1.20500	0.71958	61.6455
0.340	29.52	111.3004	0.17140	29.8181	0.38521	0.00093	1.26000	0.73523	62.3807
0.330	28.936	110.9559	0.17087	29.2277	0.38576	0.00096	1.32000	0.75422	63.1350
0.320	28.364	110.6113	0.17034	28.6498	0.38631	0.00099	1.38500	0.77372	63.9087
0.310	27.804	110.2656	0.16981	28.0837	0.38687	0.00110	1.59000	0.79861	64.7073
0.300	27.254	109.8973	0.16924	27.5287	0.38754	0.00132	1.94000	0.96367	65.6710
0.290	26.714	109.504	0.16864	26.9841	0.38831	0.00145	2.17500	1.15105	66.8220
0.280	26.184	109.1094	0.16803	26.4492	0.38909	0.00148	2.25500	1.17870	68.0007
0.270	25.663	108.7146	0.16742	25.9234	0.38987	0.00149	2.32500	1.19708	69.1978
0.260	25.149	108.32	0.16681	25.4061	0.39064	0.00147	2.34500	1.21050	70.4083
0.250	24.644	107.9309	0.16621	24.8966	0.39137	0.00136	2.20500	1.17995	71.5882
0.240	24.145	107.5605	0.16564	24.3943	0.39200	0.00124	2.05500	1.03709	72.6253
0.230	23.652	107.1944	0.16508	23.8985	0.39260	0.00121	2.05000	1.00535	73.6307
0.220	23.165	106.8283	0.16452	23.4087	0.39319	0.00120	2.07500	1.00571	74.6364
0.210	22.683	106.4615	0.16395	22.9242	0.39377	0.00145	2.56000	1.00821	75.6446
0.200	22.205	106.0476	0.16331	22.4443	0.39458	0.00224	4.03500	1.44682	77.0914
0.190	21.731	105.5372	0.16253	21.9683	0.39590	0.00282	5.15000	2.38996	79.4814
0.180	21.26	105.0132	0.16172	21.4954	0.39725	0.00283	5.30000	2.51601	81.9974
0.170	20.79	104.4892	0.16091	21.0250	0.39856	0.00274	5.25000	2.49138	84.4888

0.160	20.322	103.9651	0.16011	20.5561	0.39982	0.00280	5.50000	2.45414	86.9429
0.150	19.854	103.414	0.15926	20.0878	0.40118	0.00291	5.80000	2.71716	89.6601
0.140		102.5898							
0.130		101.5774							
0.120		100.5577							
0.110		99.53788							
0.100		98.47074							
0.0900		97.18792							
0.0800		95.83294							
0.0700		94.47759							
0.0600		93.12139							
0.0500		91.64537							
0.0400		89.11286							
0.0300		85.92187							
0.0200		82.05936							
0.0100		75.33739							
0.00800		73.49759							
0.00600		71.3625							
0.00400		68.27911							
0.00200		64.38936							
0.00101		61.47793							

SUMMARY SHEET

MTU

Ed. Marchand

SAMPLE ID: Amsorcat

Total Surface Area = 324.7001 sq. m/gm

Average Pore Diameter (4V/S) = 64.8157 Angstroms

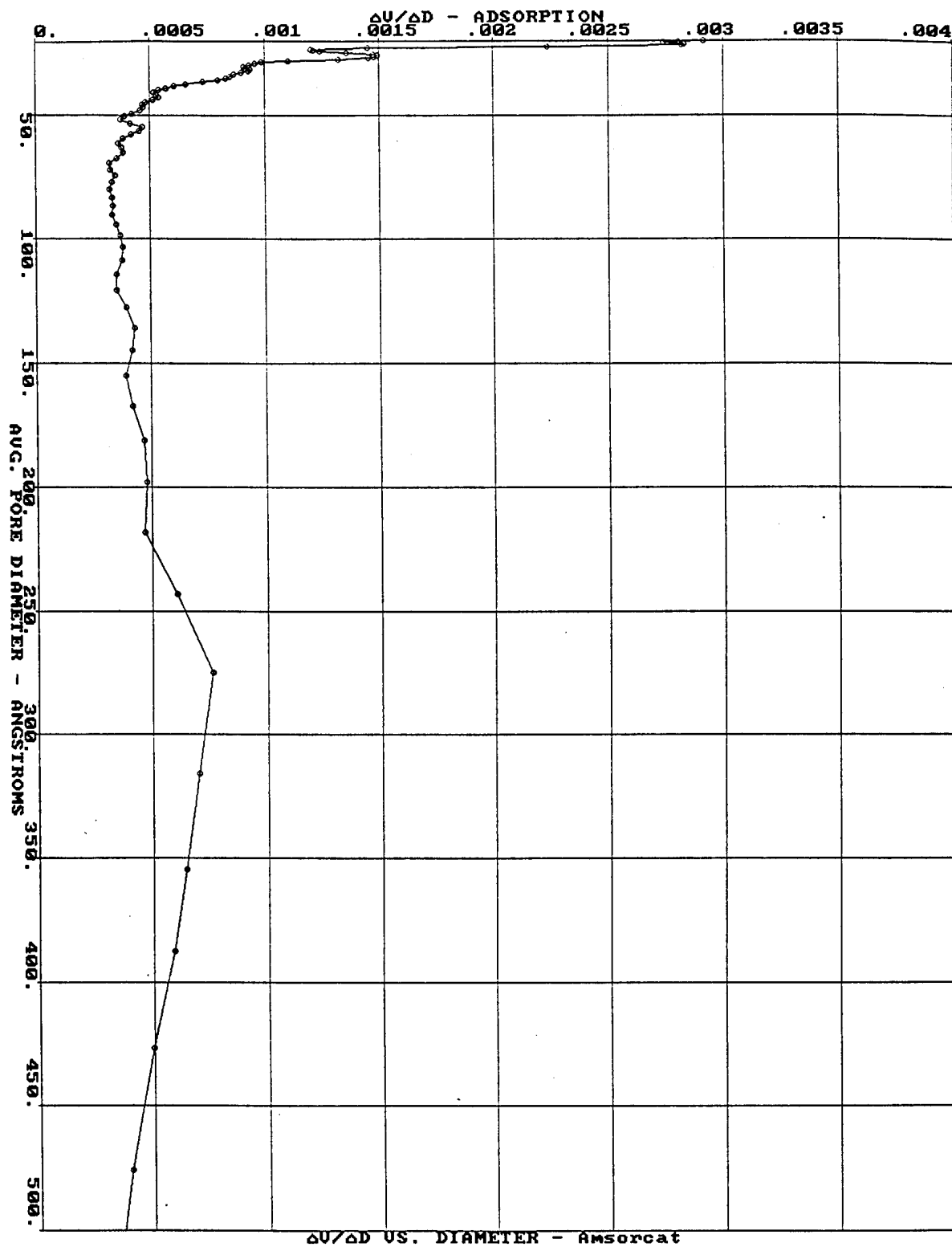
Total Pore Volume = 0.5261 cc/g

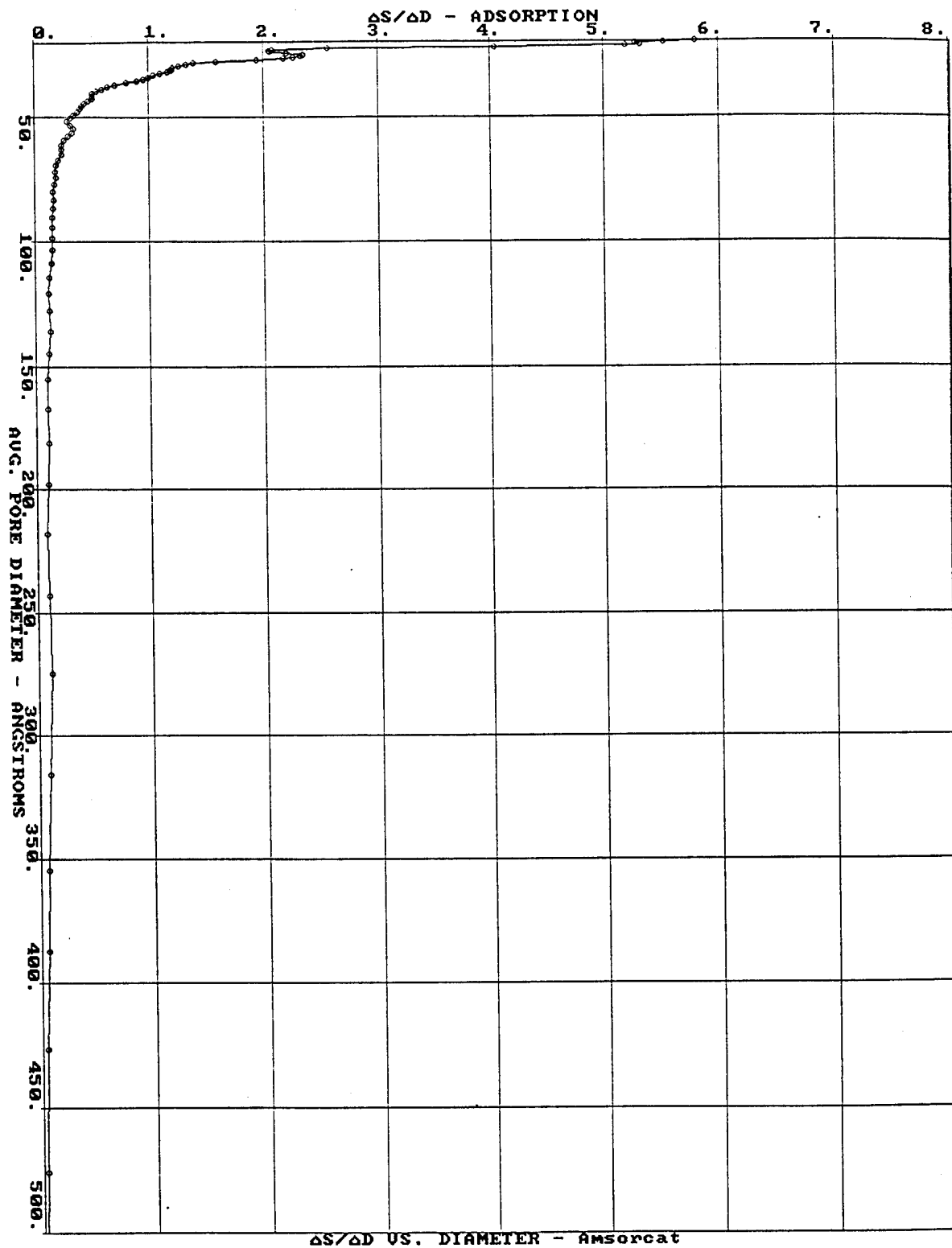
Median Pore Diameter (based on pore volume)= 296.913 Angstroms

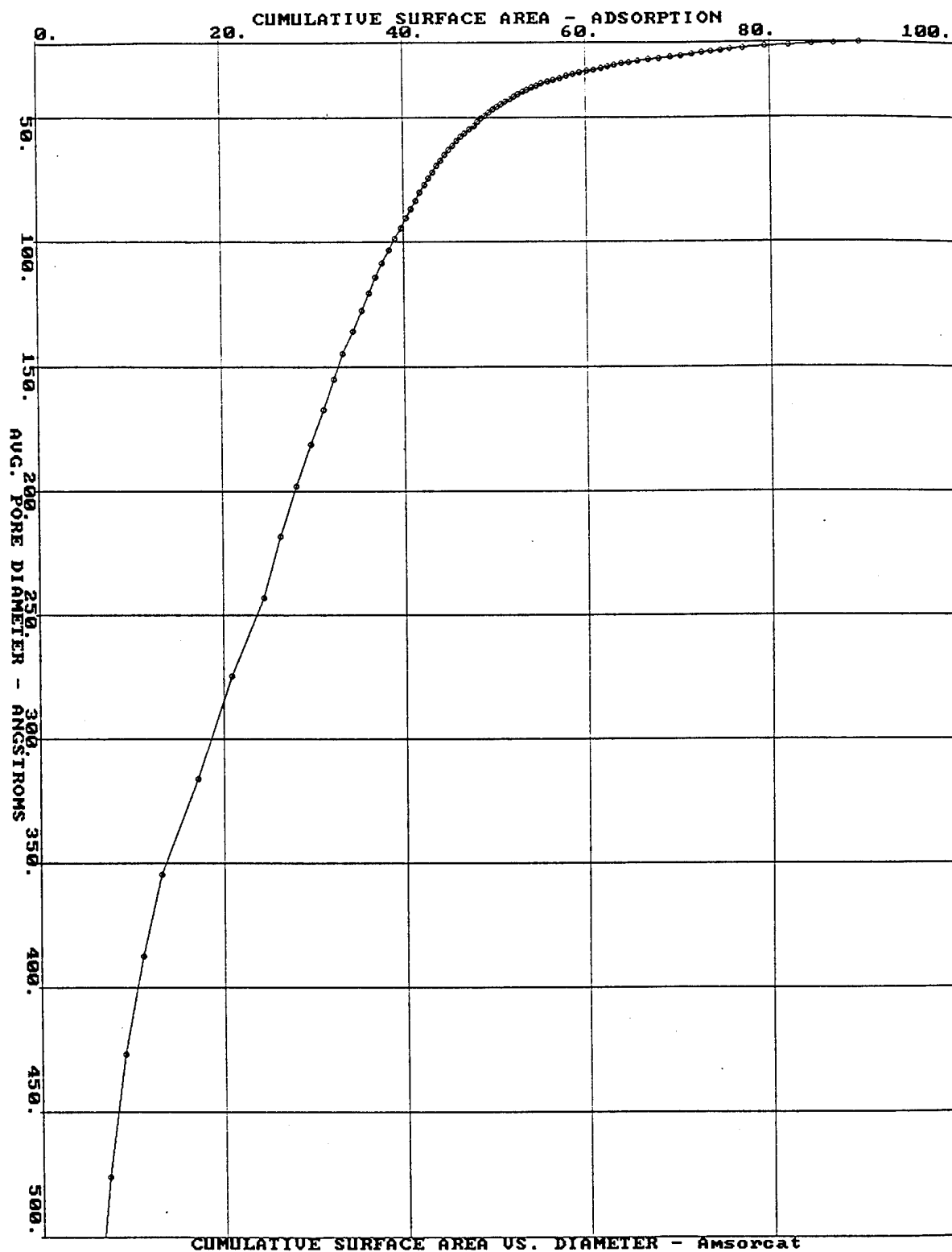
Standard Deviation= 79.3122 Angstroms

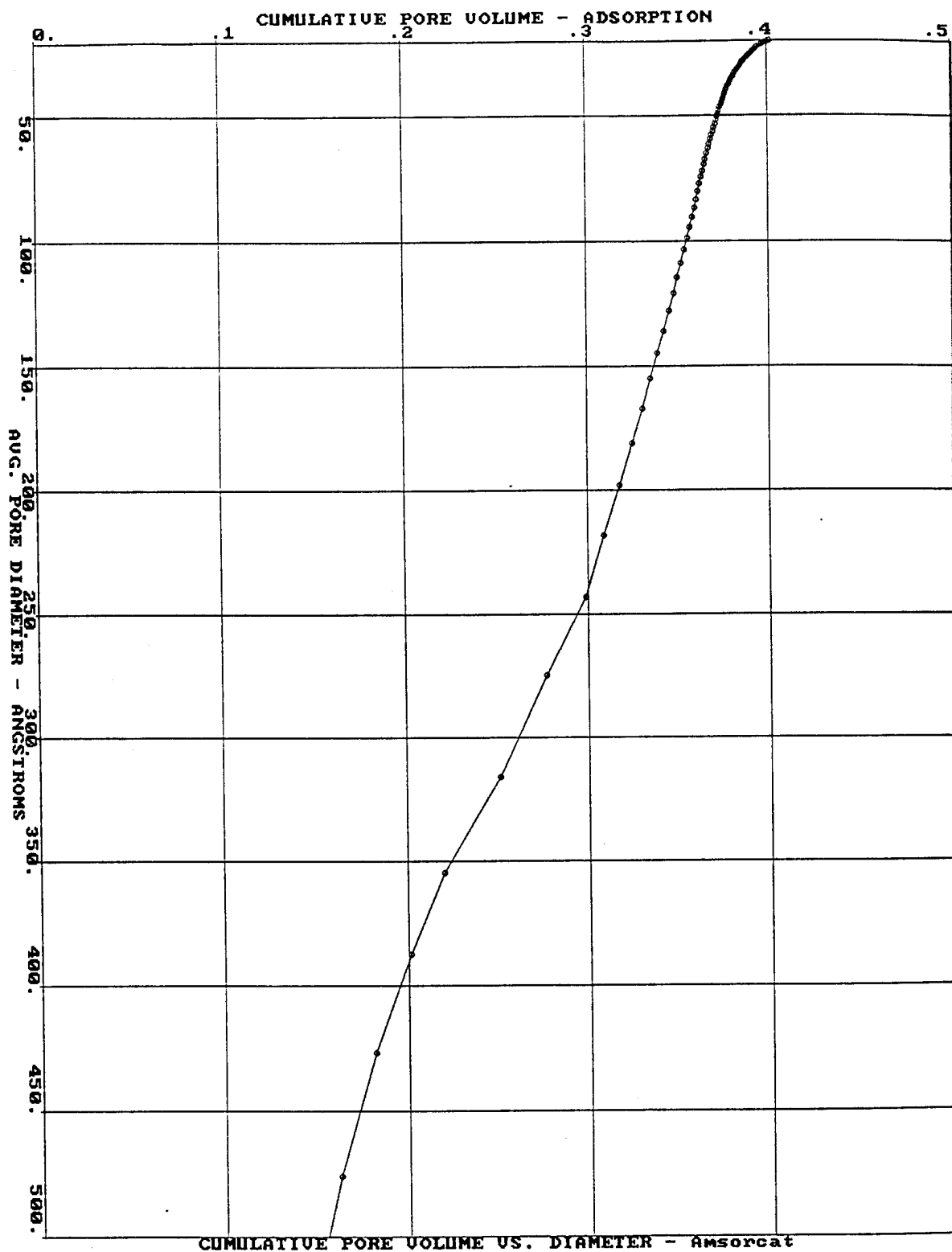
Median Pore Diameter (based on surface area)= 63.974 Angstroms

Standard Deviation= 23.5888 Angstroms









GAS ADSORPTION/DESORPTION RESULTS

ADSORBATE: NITROGEN

ISOTHERM AND PORE VOLUME DISTRIBUTION

DESORPTION

P/P0	PORE DIAMETER Å	VOLUME ADSORBED CC/GM STP	LIQ. VOL ADSORBED CC/GM	AVE. POR. DIAM Å	CUMUL. POR. VOL CC/GM	ΔV ----- ΔD	ΔS ----- ΔD	SURFACE AREA M2/GM	CUMUL. S. AREA M2/GM
0.995	3883.5	339.3051	0.52253	3883.49	-0-	7.05E-07	9.65E-06	-0-	-0-
0.990	1957.7	338.4578	0.52122	2920.59	0.00136	1.35E-06	3.11E-05	0.01867	0.01867
0.985	1313.5	337.841	0.52028	1635.60	0.00237	2.41E-06	7.80E-05	0.02462	0.04330
0.980	990.44	337.2859	0.51942	1151.97	0.00329	2.61E-06	1.06E-04	0.03188	0.07517
0.975	796.1	336.9962	0.51897	893.270	0.00377	2.31E-06	1.17E-04	0.02144	0.09662
0.970	666.21	336.8216	0.51871	731.155	0.00405	2.61E-06	1.59E-04	0.01573	0.11235
0.965	573.22	336.6602	0.51846	619.717	0.00432	4.65E-06	3.34E-04	0.01738	0.12973
0.960	503.33	336.4172	0.51808	538.275	0.00474	1.54E-05	0.00127	0.03103	0.16076
0.955	448.85	335.7192	0.51701	476.088	0.00598	5.55E-05	0.00510	0.10388	0.26464
0.950	405.18	333.7324	0.51395	427.013	0.00956	2.11E-04	0.02140	0.33520	0.59984
0.945	369.37	327.5268	0.50439	387.274	0.02088	6.55E-04	0.07250	1.16943	1.76927
0.940	339.48	312.2777	0.48091	354.426	0.04899	0.00125	0.15050	3.17304	4.94231
0.930	292.37	268.3468	0.41325	315.927	0.13101	0.00160	0.21800	10.3837	15.3260
0.920	256.92	240.1876	0.36989	274.646	0.18369	0.00127	0.19700	7.67239	22.9984
0.910	229.24	223.6478	0.34442	243.079	0.21434	0.00125	0.22050	5.04465	28.0430
0.900	207.02	207.4409	0.31946	218.133	0.24481	0.00165	0.32050	5.58637	33.6294
0.890	188.79	189.6526	0.29207	197.905	0.27891	0.00229	0.48900	6.89328	40.5227
0.880	173.54	169.1	0.26041	181.161	0.31915	0.00221	0.50500	8.88455	49.4072
0.870	160.59	156.6159	0.24119	167.063	0.34299	0.00118	0.28800	5.70731	55.1145
0.860	149.46	152.3343	0.23459	155.025	0.34976	6.10E-04	0.16450	1.74638	56.8609
0.850	139.78	148.5173	0.22872	144.619	0.35577	6.05E-04	0.17450	1.66241	58.5233
0.840	131.28	145.2164	0.22363	135.532	0.36086	4.98E-04	0.15050	1.50386	60.0272
0.830	123.76	142.9145	0.22009	127.524	0.36392	4.18E-04	0.13500	0.96099	60.9882
0.820	117.06	140.7715	0.21679	120.412	0.36679	3.93E-04	0.13350	0.95306	61.9413
0.810	111.04	138.9967	0.21405	114.050	0.36897	3.36E-04	0.12100	0.76212	62.7034
0.800	105.61	137.4786	0.21172	108.323	0.37067	3.39E-04	0.12850	0.63068	63.3341
0.790	100.67	135.9785	0.20941	103.141	0.37246	3.36E-04	0.13350	0.69180	64.0259
0.780	96.177	134.6802	0.20741	98.4258	0.37387	2.72E-04	0.11250	0.57298	64.5988
0.770	92.057	133.6074	0.20576	94.1170	0.37483	2.52E-04	0.10950	0.40883	65.0077
0.760	88.269	132.5473	0.20412	90.1629	0.37585	2.83E-04	0.12800	0.45259	65.4603
0.750	84.77201	131.516	0.20253	86.5203	0.37688	2.45E-04	0.11500	0.47675	65.9370

0.740	81.534	130.6682	0.20123	83.1529	0.37753	1.85E-04	0.09050	0.31023	66.2472
0.730	78.526	129.8975	0.20004	80.0297	0.37804	1.74E-04	0.08850	0.25893	66.5062
0.720	75.723	129.1625	0.19891	77.1244	0.37854	1.78E-04	0.09350	0.25457	66.7607
0.710	73.10501	128.4582	0.19783	74.4142	0.37901	1.40E-04	0.07650	0.25319	67.0139
0.700	70.654	127.8569	0.19690	71.8794	0.37926	9.30E-05	0.05250	0.14129	67.1552
0.690	68.352	127.2978	0.19604	69.5029	0.37945	9.80E-05	0.05750	0.11109	67.2663
0.680	66.187	126.739	0.19518	67.2697	0.37970	1.27E-04	0.07650	0.14369	67.4100
0.670	64.14601	126.1805	0.19432	65.1668	0.37998	1.57E-04	0.09800	0.17642	67.5864
0.660	62.219	125.6217	0.19346	63.1825	0.38031	1.80E-04	0.11600	0.21032	67.7967
0.650	60.395	125.0738	0.19261	61.3067	0.38066	1.44E-04	0.09500	0.22371	68.0204
0.640	58.666	124.597	0.19188	59.5301	0.38084	8.95E-05	0.06100	0.11963	68.1401
0.630	57.024	124.1504	0.19119	57.8447	0.38096	9.10E-05	0.06400	0.08805	68.2281
0.620	55.463	123.7038	0.19050	56.2433	0.38113	9.90E-05	0.07150	0.11553	68.3437
0.610	53.976	123.2755	0.18984	54.7192	0.38127	7.70E-06	0.00487	0.10323	68.4469
0.600	52.558	122.9399	0.18933	53.2668	0.38116	-1.0E-04	-0.078000	-0.080406	68.3665
0.590	51.203	122.6353	0.18886	51.8806	0.38099	-1.2E-04	-0.093000	-0.132500	68.2340
0.580	49.908	122.3309	0.18839	50.5559	0.38084	-1.0E-04	-0.082500	-0.113930	68.1200
0.570	48.668	122.0266	0.18792	49.2884	0.38073	-8.6E-05	-0.070500	-0.095131	68.0249
0.560	47.48	121.7222	0.18745	48.0741	0.38064	-6.3E-05	-0.053000	-0.075752	67.9492
0.550	46.339	121.4145	0.18698	46.9094	0.38058	-6.3E-06	-0.004945	-0.047646	67.9015
0.540	45.243	121.0851	0.18647	45.7909	0.38062	6.05E-05	0.05400	0.03336	67.9349
0.530	44.189	120.7466	0.18595	44.7158	0.38071	9.80E-05	0.08900	0.08099	68.0159
0.520	43.174	120.4081	0.18543	43.6812	0.38082	1.23E-04	0.11400	0.10240	68.1183
0.510	42.196	120.0693	0.18491	42.6846	0.38095	1.49E-04	0.14150	0.12476	68.2430
0.500	41.252	119.7304	0.18438	41.7237	0.38111	1.87E-04	0.18200	0.14655	68.3896
0.490	40.341	119.3852	0.18385	40.7962	0.38130	2.40E-04	0.23800	0.18945	68.5790
0.480	39.46	119.0331	0.18331	39.9003	0.38153	2.82E-04	0.28600	0.23567	68.8147
0.470	38.608	118.6807	0.18277	39.0339	0.38179	3.12E-04	0.32300	0.25912	69.0738
0.460	37.783	118.3283	0.18223	38.1954	0.38206	3.37E-04	0.35650	0.28153	69.3554
0.450	36.984	117.9776	0.18169	37.3833	0.38233	3.15E-04	0.34050	0.29720	69.6526
0.440	36.208	117.6463	0.18118	36.5959	0.38255	2.67E-04	0.29400	0.24083	69.8934
0.430	35.456	117.3274	0.18068	35.8319	0.38274	2.61E-04	0.29400	0.20948	70.1029
0.420	34.725	117.009	0.18019	35.0901	0.38294	2.84E-04	0.32750	0.22675	70.3296
0.410	34.014	116.6908	0.17970	34.3691	0.38315	2.98E-04	0.35000	0.24506	70.5747
0.400	33.322	116.3765	0.17922	33.6679	0.38336	2.88E-04	0.34600	0.24597	70.8206
0.390	32.648	116.07	0.17875	32.9853	0.38355	2.86E-04	0.35000	0.22693	71.0476
0.380	31.992	115.7647	0.17828	32.3203	0.38374	3.05E-04	0.38200	0.23841	71.2860
0.370	31.352	115.4592	0.17781	31.6720	0.38394	3.28E-04	0.41800	0.25642	71.5424
0.360	30.727	115.1538	0.17734	31.0394	0.38415	3.54E-04	0.46050	0.27243	71.8148
0.350	30.116	114.847	0.17686	30.4217	0.38438	4.07E-04	0.54000	0.29613	72.1110
0.340	29.52	114.5325	0.17638	29.8181	0.38464	4.64E-04	0.62500	0.35552	72.4665
0.330	28.936	114.2153	0.17589	29.2277	0.38493	4.95E-04	0.68000	0.38694	72.8534
0.320	28.364	113.8979	0.17540	28.6498	0.38521	5.10E-04	0.72500	0.40306	73.2565
0.310	27.804	113.5804	0.17491	28.0837	0.38551	5.55E-04	0.80500	0.41773	73.6742
0.300	27.254	113.2561	0.17441	27.5287	0.38583	6.80E-04	1.00500	0.47511	74.1493
0.290	26.714	112.9127	0.17389	26.9841	0.38625	7.90E-04	1.18500	0.61696	74.7663
0.280	26.184	112.5661	0.17335	26.4492	0.38668	8.15E-04	1.25000	0.65178	75.4181
0.270	25.663	112.2195	0.17282	25.9234	0.38711	8.25E-04	1.29000	0.66278	76.0809
0.260	25.149	111.8727	0.17228	25.4061	0.38754	8.65E-04	1.37500	0.67311	76.7540
0.250	24.644	111.5196	0.17174	24.8966	0.38799	0.00096	1.55000	0.72919	77.4832
0.240	24.145	111.1547	0.17118	24.3943	0.38850	0.00102	1.68500	0.82953	78.3127
0.230	23.652	110.7882	0.17061	23.8985	0.38900	0.00102	1.72000	0.84512	79.1578
0.220	23.165	110.4216	0.17005	23.4087	0.38950	0.00100	1.73500	0.84425	80.0021
0.210	22.683	110.0551	0.16948	22.9242	0.38998	0.00105	1.84000	0.83712	80.8392
0.200	22.205	109.6774	0.16890	22.4443	0.39050	0.00134	2.41000	0.93188	81.7711
0.190	21.731	109.2547	0.16825	21.9683	0.39125	0.00163	3.00500	1.36002	83.1311
0.180	21.26	108.818	0.16758	21.4954	0.39204	0.00166	3.11500	1.48210	84.6132
0.170	20.79	108.3812	0.16691	21.0250	0.39281	0.00159	3.06000	1.45147	86.0647
0.160	20.322	107.9433	0.16623	20.5561	0.39354	0.00188	3.70500	1.41988	87.4845
0.150	19.854	107.4467	0.16547	20.0878	0.39457	0.00220	4.38000	2.05188	89.5364

0.140	106.8453
0.130	106.2304
0.120	105.6154
0.110	104.9997
0.100	104.2879
0.0900	103.2498
0.0800	102.1306
0.0700	101.0109
0.0600	99.88666
0.0500	98.40459
0.0400	95.953
0.0300	93.34013
0.0200	90.05223
0.0100	83.99156
0.00800	82.30693
0.00600	80.3519
0.00400	77.44178
0.00200	73.68878
0.00100	70.83205

SUMMARY SHEET

MTU

Ed. Marchand

SAMPLE ID: Amsorcat

Total Surface Area = 324.7001 sq. m/gm

Average Pore Diameter (4V/S) = 64.6566 Angstroms

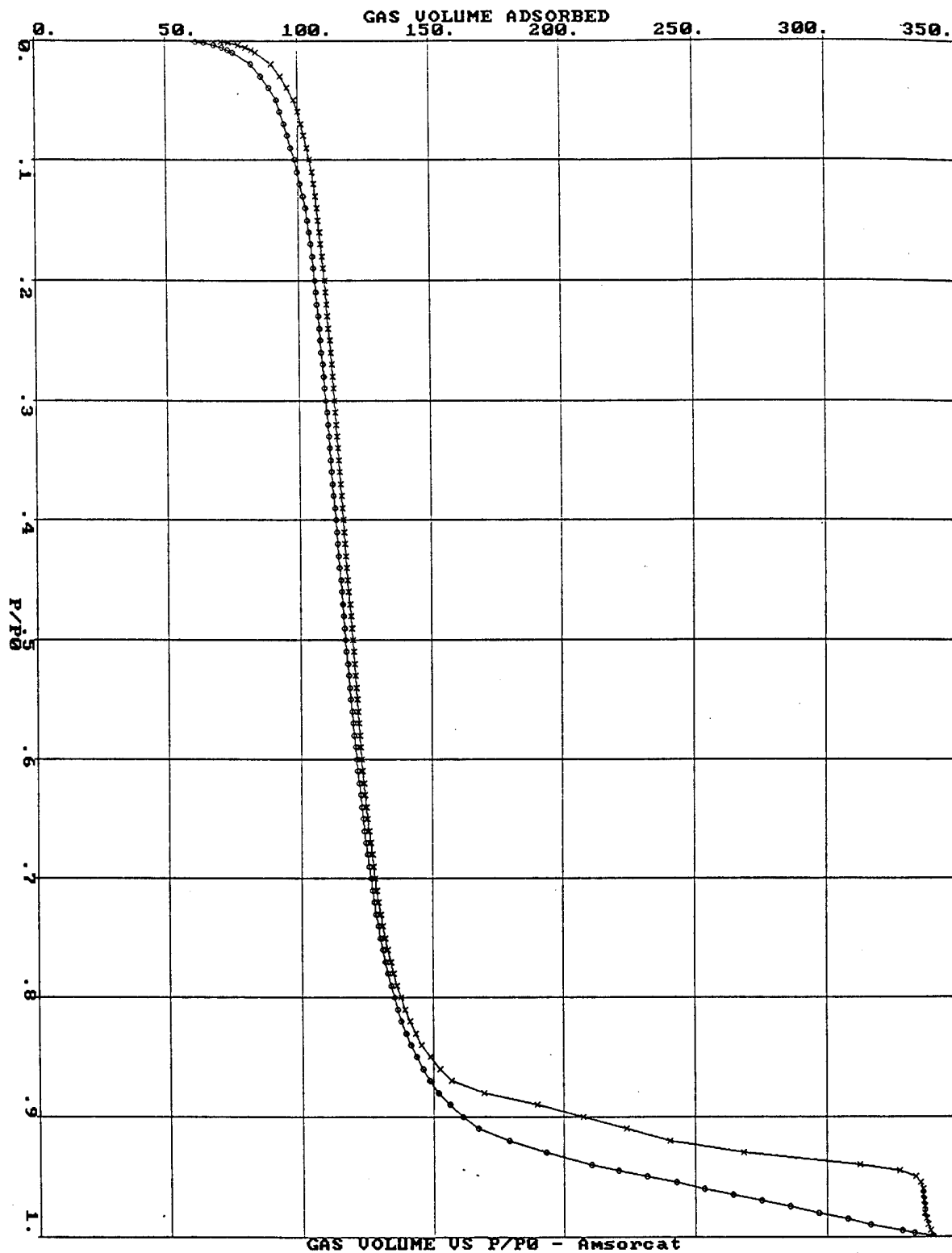
Total Pore Volume = 0.5249 cc/g

Median Pore Diameter (based on pore volume)= 207.682 Angstroms

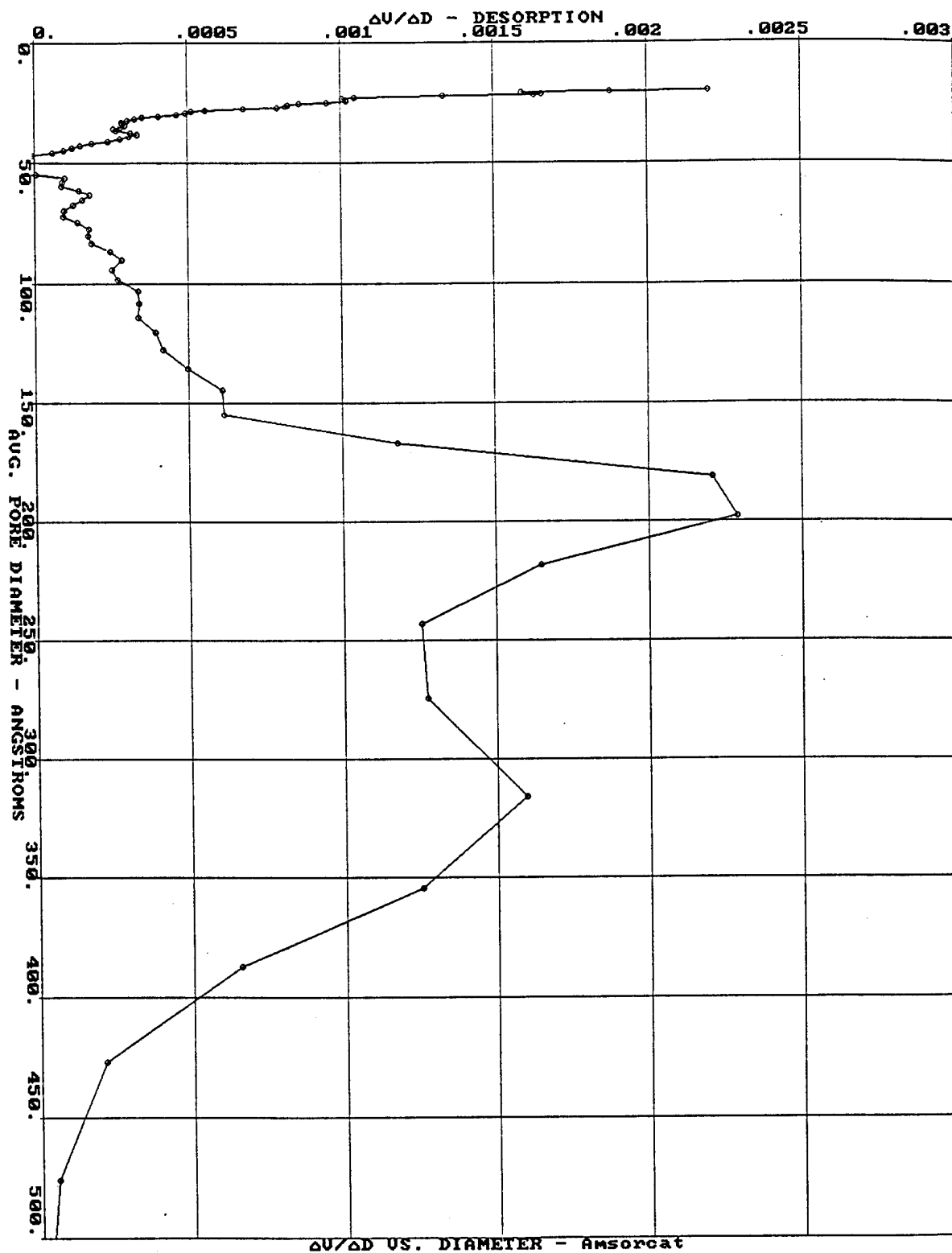
Standard Deviation= 86.4755 Angstroms

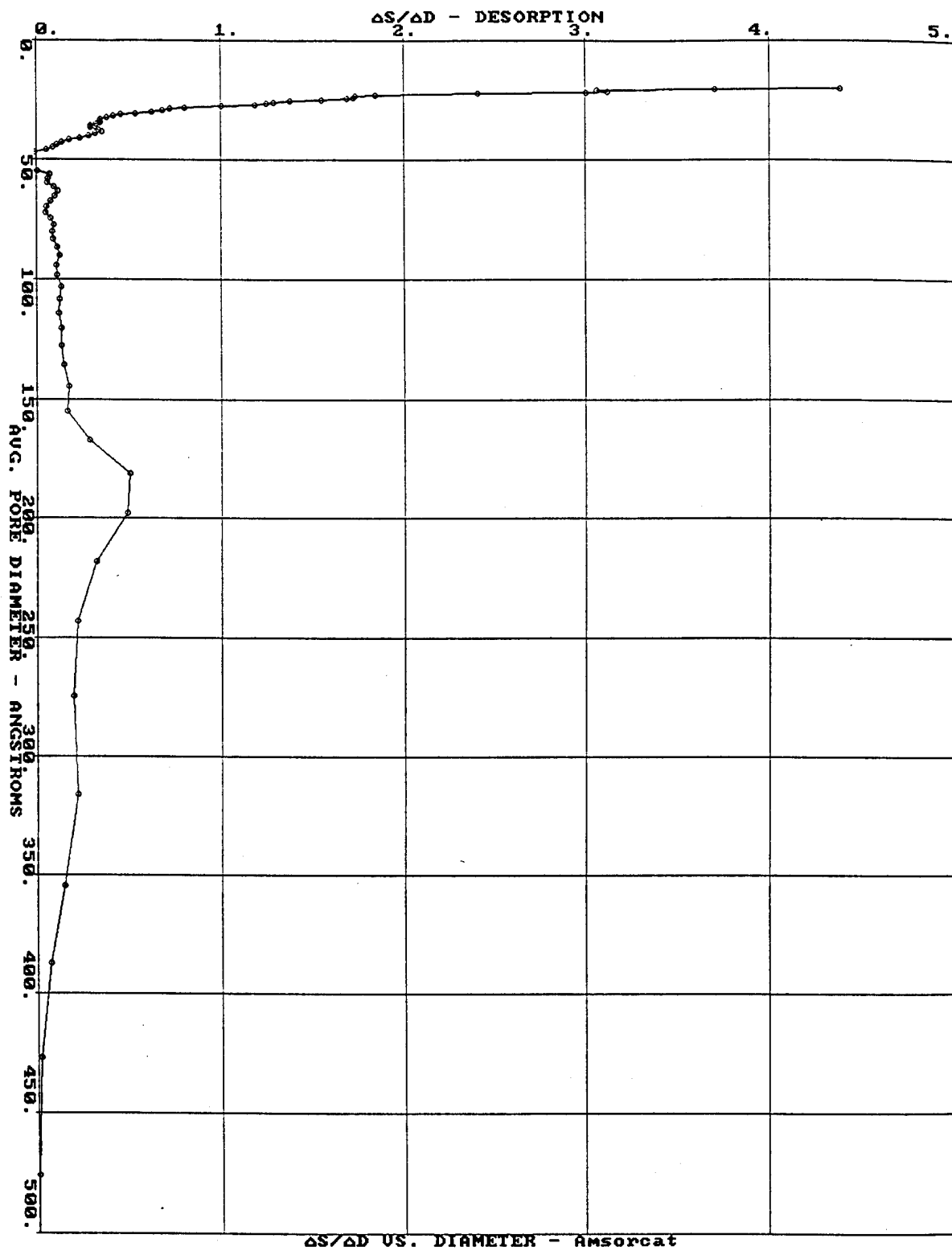
Median Pore Diameter (based on surface area)= 189.903 Angstroms

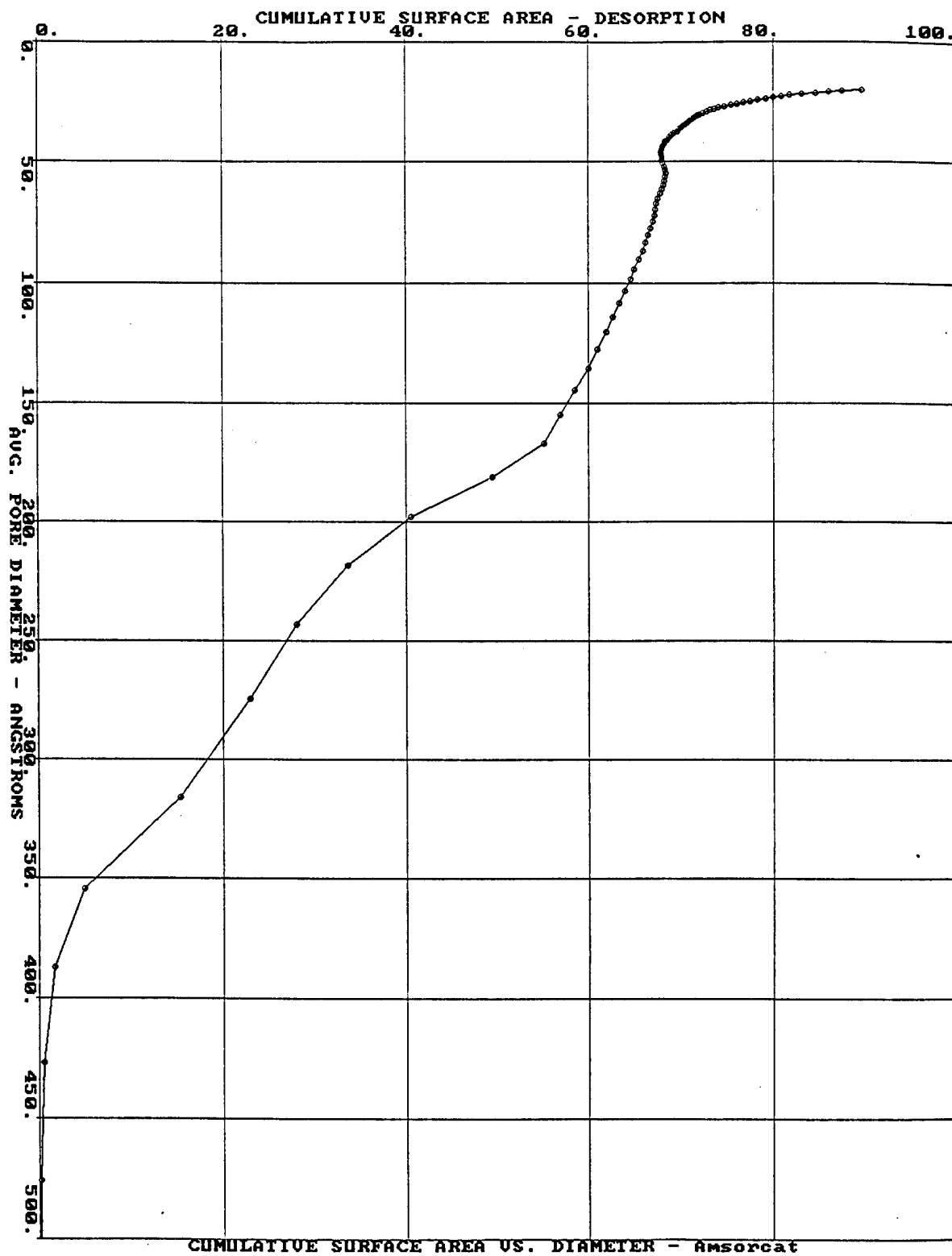
Standard Deviation= 36.1261 Angstroms



GAS VOLUME VS P/P_0 - Amsoecat







APPENDIX B

**Quattro Pro Spreadsheets with Data for
the Figures Used in this Dissertation**

Gas adsorption/desorption results from PMI, Inc.
 (Figure 2-3, PhD Dissertation, 2/96)
 Analysis done 16 Dec 1994

P/Po	ADSORPTION		DESORPTION	
	MTU-CAT	AM 572	MTU-CAT	AM 572
1	340			
0.997	333			
0.995	328	586	339	
0.99	316	585	338.4	585.5
0.985	308	583	337.8	584.7
0.98	297	579	337.3	584.1
0.975	286	567	337	583.9
0.97	275	546	336.8	583.6
0.965	264	521	336.7	583.4
0.96	253	497	336.4	583.1
0.955	242	474	335.7	582.7
0.95	232	454	333.7	581.7
0.945	221	438	327.5	574.7
0.94	210	424	312.3	553.6
0.93	193	398	268.3	490.3
0.92	179	378	240.2	426.9
0.91	167	366	223.6	391.9
0.9	161	355	207.4	378
0.89	156	348	189.6	366
0.88	151.8	342	169.1	354
0.87	148.4	338	156	344.8
0.86	145.7	333.8	152.3	339.5
0.85	143.4	330.2	148.5	335.4
0.84	141.1	327.2	145.2	331.6
0.83	139.2	324.8	142.9	328.6
0.82	137.6	322.6	140.8	325.8
0.81	136.2	320.6	139	323
0.8	134.9	318.8	137.5	320.6
0.79	133.6	317.2	136	318.7
0.78	132.5	315.7	134.7	317
0.77	131.5	314.2	133.6	315.5
0.76	130.6	312.8	132.5	314.1
0.75	129.7	311.6	131.5	312.8
0.74	128.9	310.5	130.7	311.5
0.73	128.2	309.5	129.9	310.4
0.72	127.5	308.5	129.2	309.4
0.71	126.8	307.7	128.4	308.4
0.7	126.2	307	127.8	307.6
0.69	125.6	306.2	127.3	306.8
0.68	125	305.5	126.7	306.1
0.67	124.5	304.8	126.2	305.4
0.66	123.9	304.1	125.6	304.6
0.65	123.4	303.4	125.1	303.9
0.64	122.9	302.8	124.6	303.2
0.63	122.4	302.2	124.2	302.5
0.62	121.9	301.6	123.7	301.9

0.61	121.4	300.9	123.3	301.3
0.6	120.9	300.3	122.9	300.7
0.59	120.5	299.7	122.6	300.1
0.58	120.1	299.2	122.3	299.6
0.57	119.7	298.7	122	299
0.56	119.3	298.1	121.7	298.4
0.55	118.9	297.6	121.4	297.9
0.54	118.5	297.1	121.1	297.4
0.53	118.1	296.5	120.7	296.8
0.52	117.8	296	120.4	296.3
0.51	117.4	295.5	120.1	295.8
0.5	117	295	119.7	295.3
0.49	116.6	294.5	119.4	294.8
0.48	116.3	293.9	119	294.2
0.47	116	293.4	118.7	293.6
0.46	115.6	292.9	118.3	293
0.45	115.2	292.4	118	292.5
0.44	114.9	291.9	117.6	292
0.43	114.5	291.4	117.3	291.5
0.42	114.2	290.9	117	291
0.41	113.8	290.4	116.7	290.5
0.4	113.4	289.9	116.4	290
0.39	113.1	289.4	116.1	289.5
0.38	112.7	288.9	115.8	289
0.37	112.3	288.4	115.4	288.5
0.36	112	287.9	115.2	288
0.35	111.6	287.4	114.8	287.5
0.34	111.3	286.8	114.5	287
0.33	111	286.3	114.2	286.5
0.32	110.6	285.7	113.9	286
0.31	110.3	285.2	113.6	285.5
0.3	109.9	284.6	113.2	285
0.29	109.5	284.1	112.9	284.4
0.28	109.1	283.6	112.6	283.8
0.27	108.7	283	112.2	283.3
0.26	108.3	282.5	111.9	282.7
0.25	107.9	281.9	111.5	282.1
0.24	107.6	281.3	111.2	281.5
0.23	107.2	280.8	110.8	280.9
0.22	106.8	280.2	110.4	280.3
0.21	106.5	279.5	110	279.7
0.2	106	278.8	109.7	279
0.19	105.5	278	109.2	278.3
0.18	105	277.3	108.8	277.6
0.17	104.5	276.6	108.4	276.8
0.16	104	275.8	107.9	276.1
0.15	103.4	274.9	107.4	275.2
0.14	102.6	273.9	106.8	274.2
0.13	101.6	272.9	106.2	273.2
0.12	100.6	271.9	105.6	272.2
0.11	99.5	270.6	105	271.1
0.1	98.5	268.8	104.3	269.9

0.09	97.2	266.8	103.2	268
0.08	95.8	264.9	102.1	265.9
0.07	94.5	263	101	263.8
0.06	93.1	261	99.9	261.8
0.05	91.6	258.3	98.4	259
0.04	89.1	253.5	96	254
0.03	85.9	248	93.3	248.5
0.02	82	241	90	241.6
0.01	75.3	227	84	228
0.008	73.5	223	82.3	224.6
0.006	71.4	218	80.4	220
0.004	68.3	211	77.4	214
0.002	64.4	202	73.7	206
0.00101	61.5	195	70.8	199.9

Figure 2-4, PhD Dissertation, 2/96
 BET Adsorption Isotherm and Pore Volume
 Distribution data from PMI, Inc.

Plain Ambersorb 572			SuperCat	
Pore Dia (A)	$\Delta V/\Delta D$	$\Delta S/\Delta D$	$\Delta V/\Delta D$	$\Delta S/\Delta D$
1958	2E-06	5E-05	1.4E-06	3.1E-05
1313	2E-06	8E-05	2.4E-06	7.8E-05
990	2E-06	0.0001	2.6E-06	0.00011
796	3E-06	0.00016	2.3E-06	0.00012
666	4E-06	0.00025	2.6E-06	0.00016
573	6E-06	0.0004	4.7E-06	0.00033
503	9E-06	0.0007	1.5E-05	0.00127
448	3E-05	0.0026	5.6E-05	0.0051
405	0.0002	0.0221	0.00021	0.0214
369	0.00087	0.097	0.00066	0.0725
339	0.00177	0.213	0.00125	0.1505
292	0.003	0.416	0.0016	0.218
256	0.0028	0.434	0.00127	0.197
229	0.0016	0.28	0.00125	0.22
207	0.0011	0.22	0.00165	0.32
188	0.0013	0.285	0.00229	0.489
173	0.0014	0.312	0.00221	0.505
160	0.001	0.247	0.00118	0.288
149	0.0007	0.183	0.00061	0.1645
139	0.00065	0.186	0.0006	0.1745
131	0.0006	0.187	0.0005	0.1505
123	0.0006	0.188	0.00042	0.135
117	0.0006	0.22	0.00039	0.1335
111	0.0006	0.23	0.00034	0.121
105	0.0005	0.203	0.00034	0.128
100	0.0005	0.185	0.00034	0.133
96	0.0004	0.17	0.00027	0.112
92	0.0004	0.1705	0.00025	0.109
88	0.0004	0.18	0.00028	0.128
85	0.0004	0.189	0.00025	0.115
81	0.0004	0.1875	0.00019	0.09
78	0.00034	0.174	0.00017	0.088

76	0.00033	0.176	0.00018	0.094
73	0.00026	0.139	0.00014	0.076
71	0.00017	0.097	9E-05	0.052
68	0.00018	0.106	9.8E-05	0.058
66	0.00022	0.134	0.00013	0.076
64	0.00026	0.164	0.00016	0.098
62	0.00031	0.197	0.00018	0.116
60	0.00031	0.206	0.00014	0.095
59	0.00026	0.176	9E-05	0.061
57	0.00024	0.169	9E-05	0.064
55	0.00027	0.197	0.0001	0.072
54	0.00027	0.198	7.7E-06	0.0049
52.6	0.00024	0.185	-0.0001	-0.078
51	0.00026	0.201	-0.0001	-0.093
50	0.0003	0.237	-0.0001	-0.0825
49	0.00034	0.277	-8.6E-05	-0.0705
47	0.00038	0.317	-6.3E-05	-0.053
46	0.00037	0.322	-6.3E-06	-0.0049
45	0.00034	0.296	6E-05	0.054
44	0.00034	0.304	9.8E-05	0.089
43	0.00038	0.347	0.00012	0.114
42	0.00041	0.393	0.00015	0.141
41	0.00047	0.455	0.00019	0.182
40	0.00064	0.64	0.00024	0.238
39.5	0.00089	0.905	0.00028	0.286
38.6	0.001	1.06	0.00031	0.323
37.8	0.00092	0.97	0.00034	0.356
37	0.0007	0.75	0.00032	0.34
36	0.00061	0.675	0.00027	0.294
35.4	0.00064	0.73	0.00026	0.294
34.7	0.00069	0.795	0.00028	0.327
34	0.00073	0.86	0.0003	0.35
33.3	0.00078	0.935	0.00029	0.346
32.6	0.00085	1.04	0.00029	0.35
32	0.00091	1.135	0.00031	0.382
31.4	0.00095	1.215	0.00033	0.418
30.7	0.00099	1.295	0.00035	0.46
30.1	0.001	1.385	0.00041	0.54
29.5	0.00115	1.56	0.00046	0.625
29	0.00127	1.76	0.0005	0.68

28.4	0.00133	1.875	0.00051	0.725
27.8	0.00136	1.96	0.00056	0.805
27.2	0.00143	2.1	0.00068	1.005
26.7	0.00165	2.475	0.00079	1.185
26.2	0.00187	2.85	0.00082	1.25
25.7	0.00193	3	0.00083	1.29
25.1	0.00196	3.12	0.00087	1.38
24.6	0.0021	3.41	0.00096	1.55
24.1	0.00224	3.705	0.00102	1.68
23.6	0.00226	3.82	0.00102	1.72
23.1	0.00224	3.86	0.001	1.74
22.7	0.00235	4.14	0.00105	1.84
22.2	0.00295	5.3	0.00134	2.41
21.7	0.00352	6.45	0.00163	3
21.3	0.00356	6.7	0.00166	3.115
20.8	0.00344	6.6	0.00159	3.06
20.3	0.00369	7.25	0.00188	3.705
20	0.004	7.95	0.0022	4.38

Figure 2-5 in PhD Dissertation 2/96

Huffman Lab results on elemental analysis of catalysts/supports

Weight percentages:

	AM-572-P	MTU-CAT	Methanol rinsed MTU-CAT	Accuracy (+/- %)
Carbon	95.51	71.11	76.29	0.3
Hydrogen	0.41	0.36	0.92	0.1
Sulfur	1.45	1.31	1.2	0.1
Chlorine	0	21.87	14.29	0.3

Figure 2-6, PhD Dissertation, 2/96

	1320	240379
	TIME(MIN)	GC AREA
Jan 2-C	240	1941
EBCT=17 s	360	947
T=190 C	480	645
	600	0
	720	0
	840	0
	960	0
	1080	0
	1200	0
	1320	7446
	1440	61406
	1560	127824
	1680	194242
	1800	189043
	1920	166637
	2040	137586
	2160	116557
	2280	88735
	2400	67220
	2520	49764
	2640	35321
	2760	25618
	2880	17368
	3000	11559
	3120	0
	3240	4935
	3360	3593
	3480	2572
	3600	1950
	3720	1471
	3840	1141
	3960	741
	4080	595
	4200	381
	4320	0
	4440	0
		PPM EFFLUENT
		5
		3
		2
		0
		0
		0
		0
		20
		167
		349
		530
		516
		454
		375
		318
		242
		183
		136
		96
		70
		47
		32
		0
		13
		10
		7
		5
		4
		3
		2
		2
		1
		0
		0

	4560	0	0
	4680	0	0
	4800	0	0
	4920	0	0
	5040	0	0
	5160	1073	3
	5280	7090	19
	5400	31892	87
	5520	72924	199
	5640	105200	287
	5760	122000	333
	5880	125000	341
am572-m	60	1200	3
T=175 C	180	827	2
EBCT=17s	300	680	2
	420	0	0
	540	0	0
	660	0	0
	780	0	0
	900	0	0
	1020	0	0
	1140	733	2
	1260	4400	12
	1380	25600	70
	1500	77450	211
	1620	185300	505
	1740	283000	772
	1860	394000	1075
	1980	414000	1129
	2100	401000	1094
	2220	388000	1058
	2340	325000	886
	2580	242000	660
	2820	190000	518
	2940	140000	382
	3060	127000	346
	3660	56000	153
	3780	46000	125
	3900	38600	105

4020	31800	87
4140	27200	74
4260	23500	64
4380	19250	53
4500	15300	42
4620	12100	33
4740	7430	20
4860	5360	15
4980	4124	11
5100	3060	8
5220	2078	6
5340	1684	5
5460	1293	4
5580	1058	3
5700	878	2
5820	690	2
5940	589	2
6060	525	1
6180	0	0
6300	0	0
6420	0	0
6540	0	0
6660	0	0
6780	0	0
6900	0	0
7020	0	0
7140	0	0
7260	0	0
7380	0	0
7500	0	0
7620	0	0
7740	552	2
7860	1888	5
7980	7518	21
8100	22269	61
8220	46202	126

Fig 2-8 PhD Dissertation, 2/96

AM 572 plain, 180 C heat tape, then on Joule heating. See page 26/27 of book 6.

Time	Temp	Volts	Ohms	GC area for CCl4	GC Values/10
0	180	0	30	1240	
2.3	180	5	29		
3.3	177	5	26		
4	175	6	24		
5	174	6	28	1541	
6	172	7.5	23		
8	169	9	21		
10	167	9	21		
11	166	12	20		
12	167	12	24	3954	
15.5	166	12	22		
17	165	12.5	21		
20	165	14	19		
21	166	14	22	7094	
29	167	14	22		
31	167	14	22		
32	166.5	14	24	6291	
41	165	14.5	21		
46	165	15	22		
59	164	15	27		
61	163	17	26		
63	162	17			
69	160			1977	
70	157	8	11		
71		9	9		
73	158	9	9		
76.2	159			1241	
82.5	160	8	8		
88	165			820	
0					124
5					154
12					395
21					709
32					629
69					198
76.2					124
88					82

Figure 3-3, PhD Dissertation, 2/96
Temp 38 C unless otherwise noted
Cloth Isotherms under various conditions

				Condition
TCE,ppm	15	500	1500	Feed Gas
mg/g ==	18	71	164	Dry
	16	74	131	80% RH, no Joule heating
	15.5	64	129	80% RH, 0.7V (6 mA)
	17			80% RH, 1 V (20 mA)
	1.7			80% RH at 25 C
	7.7			Joule heating capacity @42C (still at 80% RH)

Note: RH measured at room temperature (22 C) and not at the temperatures noted above.

Figure 3-4, PhD Dissertation, 2/96

Joulsorption with humidity @ 15 ppmv. Temperature upper, lower, and humidity sens
Book 7, pp 93-96, 21 Dec 1995

Adsorbent: K-Cloth, 12 sections in 1/4" glass tube, (0.0167 g)

Flow is 48 ml/min at start

Time	T upper	T lower	Humidity @	Temp	Real RH	GC area	Conc (pp
0							
5	26.5	28	57	26	53		
10	26.5	28	59	27	56		
15	27	28	62	27	58		
20	26.5	28	61	26	55	0	0
30	26.5	27.5	67	26	60		
40						0	0
60						44	16.10
80						56.6	20.71
85	26.5	27	82	26	78		
100						69.4	25.39
110	26	27	82	26	78		
120	26.5	27.5	84	26	78		
140						58.1	21.26
160	25.5	27	83	25	74	40.7	14.89
180						41.7	15.26
200						41.1	15.04
220						39	14.27
240						40.7	14.89
260						35.9	13.13
280	24	26	82	23	68	38.2	13.98
284	24.5	26	81	24	73		
288	24.5	26	83	24	74		
292	24.5	26	84	24	75		
296	25	26	86	24	76		
300	25	26	87	25	80	7.85	3.925
304	25	26	87	24	79		
310	25	26	88	25	83		
320	25	26	88	24	80	5.73	2.865
330	25	26.5	85	25	78		
340	25	26.5	86	25	79	5.11	2.555
350	25	26.5	85	25	78		
360	25	26	84	25	78	5.85	2.925
370	24.5	27	87	24	72		
380	25	27	89	25	80	4.7	2.35
390	25	27	91	25	81		
400						4.1	2.05

420						3.5	1.75
440						3.6	1.8
460						2.72	1.36
480						2.5	1.25
500						2.79	1.395
520						3.03	1.515
540						3.7	1.85
560						5.6	2.8
580						9.7	4.85
600						14	7
620						18.4	9.2
640						22.4	11.2
660						24.7	12.35
680						22	11
700						27.8	13.9
720						29.7	14.85
780						31.6	15.8
840						30.8	15.4
900						31	15.5
960						30.8	15.4
1020						29.7	14.85
1080						29.4	14.7
1140						29.1	14.55
1154	24.5	26.5	81	24	71		
1157	24.5	26	80	24	70		
1160	25	26	69	25	66	11.4	5.7
1162	25	26	65	25	60		
1164	24.5	26	64	25	59		
1166	25	26	63	24	55	10.5	5.25
1172	25	26	64	25	59		
1176	25	26	65	25	60		
1180	24.5	26	64	24	57	14.6	7.3
1190	25	26	69	24	61	37.7	18.85
1200	25	26	75	25	71	218.5	109.25
1210	25	26	79	25	77	329.2	164.6
1220	25	26	79	25	77	269.8	134.9
1230	25	26	81	24	73	121.3	60.65
1240	25	26	82	24	73	135.2	67.6
1260	25	26	82	25	78	59.5	29.75
1280	25	26	83	24	74	35.4	17.7
1300						35.1	17.55

Figure 4-3, PhD Dissertation, 2/96		Baudu predictions		R/Ro for		Carbon Rod	
R/Ro for ACC20 and 572		Baudu predictions		packed ACC20		R and R/Ro (McIntos	
50	91.7	1.00	0.83	29	1.00		
60	88.6	0.97	0.81	28	0.97		
70	85.6	0.93	0.796	27	0.93		
80	82.7	0.90	0.784	26	0.90		
90	79.9	0.87	0.774	25	0.86		
100	77.5	0.85	0.766	24	0.83		
110	74.7	0.81	0.759	23	0.79		
120	72.1	0.79	0.754	22	0.76		
130	69.1	0.75	0.751				
140	66.2	0.72	0.745				
150	25.6		0.42				
140	27.2		0.45				
130	29.2		0.48				
120	31.6		0.52				
110	34.6		0.57				
100	37.9		0.62				
89	42.5		0.70				
79	47.8		0.78				
67	54.3		0.89				
61	58.4		0.96				
57	61		1.00				
140						0.5818	0.8641
123						0.5953	0.8842
98						0.6127	0.9100
72						0.6316	0.9381
20.2						0.6733	1

Figure 4-4, PhD Dissertation 2/96
Cloth Adsorbent Isotherms

DRY: (0.0094g cloth)

TIME	GC Area	Conc.pp	Ohm	
0	0		54.2	
8	0		55.13	
15			55.52	
25			55.65	
34			55.76	
41	0			
47			55.76	
61	0			
160			55.79	
181	3.17	2.4		
201	6.65	4.9		
210			56.23	
221	10.35	7.7	55.89	
241	13.84	10.3	56.27	
257			56.2	
271	18.62	13.8	56.76	13 mg TC
281	19.96	14.8	56.67	
361	24.56	18.2	57.07	
421	23.35	17.3	56.88	
541	23.18	17.2	57.05	
661			56.89	
781	20.55	15.3	56.71	
901	20.32	15.1	56.9	
1021	19.61	14.6	56.83	
1141	20.21	15.0	56.93	
1261	18.96	14.1	57.23	
1301	19.57	14.5	56.46	
1321	20.78	15.4	55.78	
1341	22.25	16.5	57.09	
1366	21.24	15.8	55.9	
1381	14.72			
1401	31.29	29.4	55.45	
1421	42.6	40.0	54.82	
1441	94.85	89.1	54.12	
1461	262.72	246.9	54.54	
1481	388.17	364.8	54.1	

1501	457.82	430.3	54.1	
1521	491.51	461.9	54.18	
1541	458.41	430.8	53.96	
1561	504.05	473.7	54.11	33 mg/g
1581	489.89	460.4	53.82	
1601	484.71	455.6	53.81	
1621	493.2	463.5	54.02	
1641	499.6	469.5	53.74	
1661	525.4	493.8	53.95	
1681	496.6	466.7	53.67	
1711	508.8	478.2	53.61	
1741	500.5	470.4	53.79	
1771	510.3	479.6	53.76	
1801	513.3	482.4	53.74	
1861	535	502.8	53.75	
1981	535	502.8	53.43	
2101	536	503.8	53.23	
2221	547.7	514.8	52.99	
2341	523	491.5	53	
2461	547.9	514.9	53.06	
2581	532.3	500.3	52.78	
2701	565.8	531.8	53.4	
2801	551.8	536.1	53.28	
2813	530.2	515.1	54	
2825	548.9	533.3	55.71	
2837	753.4	731.9	57.35	
2849	959.8	932.4	58.75	
2861	1059.5	1029.3	60.11	
2873	1182.4	1148.7	60.4	
2885	1222.3	1187.5	61.01	
2897	1287.1	1250.4	61.2	
2909	1319.3	1281.7	61.3	
2921			61.5	
2933	1224	1189.1	61.4	
2945	1268.9	1232.7	61.9	71 mg/g
2957	1387.2	1347.7	62.2	
2977	1340.3	1302.1		
2997	1404.6	1364.6	63.3	
3017	1466.3	1424.5	63.4	
3037	1402.4	1362.4	64.1	
3057	1448.9	1407.6		
3077	1382	1342.6		

3097	1446.7	1405.5	64.5
3117	1478.9	1436.8	64.5
3147	1388.9	1349.3	64.8
3177	1409.9	1369.7	65
3207	1508.5	1465.5	65
3237	1488.7	1446.3	65.1
3297	1482.6	1440.3	65.26
3417	1444.1	1402.9	64.72
3537	1456.9	1415.4	65.46
3657	1544.4	1500.4	65.48
3777	1539.9	1496.0	65.53
3897	1369.1	1330.1	66.02
4017	1634.4	1587.8	65.79
4137	1497.4	1454.7	66.46

Fig 4-5, PhD Dissertation, 2/96

1500 ppmv humid feed to 48 sections of K-cloth (0.0792 g)

Flow 19.8 ml/min, not insulated or heat taped

Time	GC Area	Eff. Conc.	Ohms
0			190
10			210.8
30	3.3	2.29	249.6
50	0	0.00	252
70	0	0.00	248.6
90	0	0.00	246.4
110	0	0.00	245.5
130	0	0.00	242.8
150	0	0.00	242.2
170	0	0.00	255.4
190	0	0.00	258.9
210	0	0.00	259.8
230	0	0.00	259.9
250	0	0.00	262.1
270	0	0.00	261.9
290	4.7	3.26	263.9
310	356.4	247.50	263.3
330	1002.6	696.25	266.5
350	1614.4	1121.11	265.3
370	2041.8	1417.92	266.7
390	2077.4	1442.64	269
410	2062.1	1432.01	267
430	2212.1	1536.18	271
450	1913.3	1328.68	268.3
470	2249.6	1562.22	271.4
490	2029.4	1409.31	268.8
510	2156.4	1497.50	271.4
530	2090.5	1451.74	272.4
550	2050	1423.61	271.1
570	2251	1563.19	272.6
590	2045.2	1420.28	270.2
610	2212	1536.11	274.6
630	2024	1405.56	271.6
650	2245.2	1559.17	275.8
670	1996.7	1386.60	273.2
690	2222.8	1543.61	275.5
710	2066	1434.72	273

730	2265.7	1573.40	274.6
750	2091.7	1452.57	274.4
770	2218.4	1540.56	275.8
790	2136.7	1483.82	276.5
810	2221.98	1543.04	274.5
830	2145.4	1489.86	277.1
850	2112.8	1467.22	276.1
870	2151.9	1494.38	277.4
890	2065.6	1434.44	275.3
910	2032.6	1411.53	278.5
930	2168	1505.56	275.6
950	1915.8	1330.42	279
970	2127.8	1477.64	275.2
990	1864.8	1295.00	279.4
1010	2112.2	1466.81	276.3
1030	1932	1341.67	279.8
1050	2152.8	1495.00	276.7
1070	1876.9	1303.40	279.8
1090	2030.7	1410.21	277
1110	1721.2	1195.28	278.9
1130	2030.8	1410.28	278.5
1150	2220.3	1541.88	277.2
1170	2247.4	1560.69	279.3
1190	2128.7	1478.26	280.7
1210	1960.9	1361.74	280.3
1230	2145.4	1489.86	278.3

Fig 4-6, PhD Dissertation, 2/96

Resistance Changes with addition of compounds to K Cloth, Sep 95

Compounds-Dichloromethane (DCM), Methanol (MeOH), and Toluene (Tol)

Time	Resistance, Ohms		R/Ro
		MeOH	MeOH
	1	72.81	1.00
	5	76.4	1.05
	7	87.3	1.20
	8	91.3	1.25
	10	98.8	1.36
	11	100.7	1.38
	12	102.33	1.41
	13	103.4	1.42
	15	106	1.46
	16	106.9	1.47
	17	107.6	1.48
	18	108.2	1.49
	20	109.5	1.50
	22	110.6	1.52
	24	111.34	1.53
	26	111.7	1.53
	28	112	1.54
	30	112.3	1.54
	32	112.6	1.55
	34	112.7	1.55
	36	112.8	1.55
	60	113.7	1.56
			Toluene
	1	76.1	0.99
	2	75.6	0.98
	4	74.2	0.96
	5	74	0.96
	6	74.8	0.97
	7	75.6	0.98
	8	76	0.98
	10	75.4	0.98
	11	74.8	0.97
	13	74	0.96
	14	77.5	1.00
	15	78.9	1.02
	16	81.2	1.05

17	80.4	1.04
19	79.7	1.03
23	86	1.11
24	84.8	1.10
26	88.1	1.14
27	90.3	1.17
28	92.1	1.19
29	95	1.23
30	96.5	1.25
31	103	1.33
32	109.7	1.42
33	118.7	1.54
34	122.4	1.59
35	125.7	1.63
36	126.4	1.64
37	123.3	1.60
38	123.5	1.60
48	125.4	1.62
58	123.3	1.60

			R/Ro	
			DCM	TCE
1	85.5	57.8	1.00	1.00
2	88.6	57.8	1.04	1.00
3	88	57.2	1.03	0.99
4	87.4	56.1	1.02	0.97
5	88	55.2	1.03	0.96
6	89.2	54.1	1.04	0.94
7	94.6	53	1.11	0.92
8	100.6	52.4	1.18	0.91
9	104.2	54.1	1.22	0.94
10	106.7	53.4	1.25	0.92
11	107.9	56.2	1.26	0.97
12	108.7	59.8	1.27	1.03
13	109.5	63.5	1.28	1.10
14	109.9	66.4	1.29	1.15
15	110.2	68.6	1.29	1.19
16	110.5	68.1	1.29	1.18
18	110.5	68.2	1.29	1.18
20	110.6	69	1.29	1.19
30	110.6	69.4	1.29	1.20
40	113.7	77.9	1.29	1.21
50	113.8	77.4	1.30	1.20

60	113.9	75.4	1.30	1.17
70	113.9	75.9	1.30	1.17
	113.9	75.9	1.30	1.17
			R/Ro	
			CCL4	PCE
1	63.5	80.1	1.02	1.00
2	62.2	79.9	1.00	0.99
3	61.5	80	0.99	0.99
4	61.4	79.9	0.99	0.99
5	61.8	79.6	1.00	0.99
6	64.3	79.3	1.04	0.99
7	63.2	78.5	1.02	0.98
8	60.8	78.1	0.98	0.97
9	59.1	77.8	0.95	0.97
10	62.6	78.1	1.01	0.97
11	58.3	78.1	0.94	0.97
12	64.7	78.3	1.04	0.97
13	70.4	78.3	1.13	0.97
14	68.1	79	1.10	0.98
15	67.9	79.8	1.09	0.99
16	68.5	80.6	1.10	1.00
17	69.7	80.6	1.12	1.00
18	71.5	80.8	1.15	1.00
19	71.4	81.1	1.15	1.01
20	72.4	83.4	1.17	1.04
21	74.2	86.2	1.19	1.07
22	73.9	90.2	1.19	1.12
23	73.6	90.6	1.19	1.13
24	74.1	91.9	1.19	1.14
26	74.1	96.6	1.19	1.20
27	75.1	101.1	1.21	1.26
28	74.7	106.1	1.20	1.32
30	75.1	113.3	1.21	1.41
31	76.1	115.1	1.23	1.43
32	76.3	118	1.23	1.47
34	76.8	119.2	1.24	1.48
35	77.2	121.5	1.24	1.51
36	77.4	123.7	1.25	1.54
38	77.4	124.8	1.25	1.55
39	77.5	126.6	1.25	1.57
40	77.6	124.8	1.25	1.55
41	77.7	126.2	1.25	1.57

42	77.7	126.9	1.25	1.58
43	77.7	128	1.25	1.59
45	78.3	129.6	1.26	1.61
47	78.7	134	1.27	1.66
50	78.8	136.4	1.27	1.69
52	79.1	138.1	1.27	1.72
54	79.4	139.3	1.28	1.73
56	78.4	140.1	1.26	1.74
58	78.7	144.5	1.27	1.80
60	78.8	145.2	1.27	1.80
70	79.4	149.4	1.28	1.86
80	80.8	151.2	1.30	1.88

Fig 4-7, PhD Dissertation, 2/96
Resistance/Adsorbance test results, Sep 1995
K-Cloth with DCM and TCE

Time	DCM R	TCE R	DCM R/R	TCE R/Ro		
0	85.5	57.8	1.00	1.00		
1	88.6	57.8	1.04	1.00		
2	88	57.2	1.03	0.99		
3	87.4	56.1	1.02	0.97		
4	88	55.2	1.03	0.96		
5	89.2	54.1	1.04	0.94		
6	94.6	53	1.11	0.92		
7	100.6	52.4	1.18	0.91		
8	104.2	54.1	1.22	0.94		
9	106.7	53.4	1.25	0.92		
10	107.9	56.2	1.26	0.97		
11	108.7	59.8	1.27	1.03		
12	109.5	63.5	1.28	1.10		
13	109.9	66.4	1.29	1.15		
14	110.2	68.6	1.29	1.19		
15	110.5	68.1	1.29	1.18		
16	110.5	68.2	1.29	1.18		
18	110.6	69	1.29	1.19		
20	110.6	69.4	1.29	1.20		
30	113.7	77.9	1.29	1.21		
40	113.8	77.4	1.30	1.20		
50	113.9	75.4	1.30	1.17		
60	113.9	75.9	1.30	1.17		
1					54.3	0.99
2					54	0.99
3					54	0.99
4					53.65	0.98
5					53.5	0.98
6					53.3	0.98
7					53.1	0.97
8					53	0.97
9					52.8	0.97
10					52.6	0.96
11					52.45	0.96
12					52	0.95
13					52	0.95
14					51.8	0.95

15	51.5	0.94
16	51.3	0.94
17	51	0.93
19	50.65	0.93
20.5	50.3	0.92
22	50.1	0.92
23	49.85	0.91
24	49.65	0.91
26	49.3	0.90
28	48.95	0.90
30	48.75	0.89
32	48.5	0.89
34	48.2	0.88
36	48.05	0.88
38	48	0.88
40	48.3	0.88
42	48.6	0.89
44.5	49.2	0.90
47	49.45	0.91
50	49.6	0.91
53.5	50	0.92
56	50.4	0.92
57	50.7	0.93
59	51.1	0.94
60	51.3	0.94
63	51.6	0.95
66	51.9	0.95
70	52.15	0.96
82	52.4	0.96
90	52.5	0.96
100	52.5	0.96
110	52.55	0.96
120	52.6	0.96

Water plus TCE in equal volumes in static test

Time	Ohms
1.00	58.6
1.67	58.5
2.33	57.56
3.00	56.41
3.67	55.24

4.33	54.39
5.00	53.95
5.67	53.91
6.33	54.09
7.00	54.34
7.67	54.2
8.33	53.97
9.00	53.87
9.67	53.71
10.33	53.75
11.00	53.67
11.67	53.67
12.33	53.7
13.00	53.86
13.67	54.2
14.33	55.04
15.00	55.05
15.67	55.06
16.33	54.27
17.00	54.41
17.67	54.47
18.33	54.8
19.00	55.09
19.67	55.01
20.33	55.5
21.00	56.54
21.67	57.24
22.33	57.66
23.00	57.64
23.67	59.48
24.33	59.47
25.00	60.22
25.67	62.37
26.33	62.18
27.00	63.21
27.67	64.46
28.33	66.44
29.00	66.9
29.67	68.32
30.33	69.95
31.00	71.02
31.67	73.04

32.33	73.95
33.00	73.13
33.67	74.64
34.33	75.48
35.00	74.7
35.67	74.5
36.33	75.14
37.00	76.69
37.67	77.62
38.33	77.63
39.00	78.12
39.67	80.85
40.33	80.71
41.00	81.31
41.67	81.44
42.33	81.09
43.00	80.13
43.67	80.46
44.33	80.34
45.00	79.77
45.67	79.9
46.33	79.93
47.00	79.02
47.67	79.08
48.33	79.24
49.00	79.54
49.67	79.42
50.33	79.25
51.00	79.69
51.67	80.23
52.33	80.13
53.00	80.68
53.67	81.05
54.33	80.05
55.00	80.35
55.67	80.86
56.33	80.13
57.00	80.59
57.67	79.99
58.33	79.54
59.00	80.03
59.67	79.54

60.33	79.16
61.00	80
61.67	79.88
62.33	79.17
63.00	80.12
63.67	80.46

APPENDIX C

Additional Information on Thermal Catalysis of Trichloroethylene over Transition Metal Impregnated Ambersorb 572

This appendix contains information too detailed for the professional paper in Chapter 2. The information below is summarized in Chapter 2, and the references, tables, and figures are all the same.

AM-572-Mn

The experiments with AM-572-Mn (Table 2-6) were conducted with a dry feed at 175 °C. The catalyst appears to have an induction time as shown in Figure 2-5 where the effluent rises to about 80 percent of the influent. After the catalyst is activated, the effluent drops below detection limits (>99.9 percent conversion). During this induction time PCE was noted in the effluent, dropping off to below detection limits. Adding water to the feed reduces the TCE conversion efficiency to about 88 percent and PCE is once again to a detectable level. After 166 hours the system was turned off and the catalyst was noted to have increased in mass by about 8 percent. No chloride samples were taken to determine mineralization efficiencies.

In a separate run with AM-572-Mn with a humid feed at 210 °C and an EBCT of 3.8 s, no conversion occurred. Reducing the flow by 50 percent did not improve the performance. To determine if the temperature was too great for the oxidizing radical/carbenium ions, the temperature was reduced to 180 °C. Unfortunately this did not impact the conversion efficiency, as verified by chloride analysis. It appears that water in the system initially can impact the performance of the catalyst. The water probably blocks the access to the catalytic sites reducing or eliminating the oxidative power of this catalyst, even at elevated temperatures.

AM-572-Ti

The following experiments with the titanium impregnated Ambersorb 572 are summarized in Table 2-7. Using a pre-loaded AM-572-Ti at 105 °C and an EBCT of 12.7 s, no initial TCE was in the effluent. A chloride analysis showed 90 percent mineralization of TCE to HCl/Cl₂. After approximately 1300 minutes the

mineralization efficiency dropped to 77 percent and reached 28 percent (conversion was down to 99.6 percent) after 1600 minutes. At this point the temperature was raised to 150 °C and flow reduced to an EBCT of 23 s. The mineralization efficiency raised up to 47 percent initially but fell to about 20 percent a short time later. Increasing the temperature again to 175 °C increased the mineralization efficiency to about 50 percent. Increasing the flow from an EBCT of 35 s to 10 s, decreased the mineralization efficiency to about 30 percent. Increasing the flow again to an EBCT of 3.7 s increased the mineralization efficiency back to approximately 50 percent indicating a possible concentration effect. The back pressure by the catalyst bed would cause a slight increase in the concentration in the bed, especially at the leading edge. This increase could, in turn, cause an increase in the catalyst performance by increasing the concentration of the reactants on the surface.

After 120 hours the catalyst was removed and had a 6 percent mass loss after the experiments. This is in direct contrast to the findings of the other low temperature runs where by-products accumulated on the surface increasing the catalyst mass. A separate aliquot of the AM-572-Ti was rinsed (up to five times) in water and the pH of the rinsate was <2 as indicated by pH paper. The catalyst/adsorbent readily wet and a tremendous amount of heat was released. After eight flushings of Milli-Q® water the rinsate finally came out at pH 7. This means that the TiCl_4 had not fully reacted with the water in the room air. The reaction flow may have removed the excess chlorine causing the weight loss. However, this would also put the mineralization quantities in question as to their validity.

Another portion of the original batch of AM-572-Ti was rinsed once in Milli-Q® water as described. This material, designated as AM-572-Ti(W), was dried and pre-loaded form for the following experiments. As the catalyst heated up to 200 °C under a TCE feed flow (EBCT of 3.3 s), approximately 240 mg TCE came off in the effluent. Subtracting the amount of TCE fed during this time and the amount destroyed (as verified by chloride analysis) this results in approximately 1/3 of the initial 100 mg TCE/g catalyst loading being desorbed. Also noted in the effluent were other by-

products. The flow was reduced (EBCT of 31 s) and the TCE effluent tailed off to non-detectable levels leaving only a small amount of PCE still in the effluent.

After a short interruption (12 hr) where the reactor cooled to room temperature without flow (and was exposed to Joule heating as part of the experiments for Chapter 3), the reactor was restarted again at 200 °C (EBCT of 11 s). The effluent continued to remain below detection limits for TCE, but now instead of PCE, small amounts of carbon tetrachloride and chloroform appeared in the effluent. After approximately 10 hours a third peak was noted, later identified as hexachloroethane (C_2Cl_6). A chloride analysis at this point showed the mineralization efficiency to be 58 percent. Approximately 16 hours later this had dropped to 35 percent and significant amounts of C_2Cl_6 were in the effluent. After 30 additional hours the mineralization efficiency had dropped to 20 percent, however TCE was still non-detect in the effluent.

After 220 hours (excludes interruption) the flow was increased to obtain an EBCT of 3 s. At this flow the catalyst only lasted about 14 hours before TCE broke through and was detectable in the effluent along with a new compound (tentatively identified as pentachloroethane). However, even with TCE in the effluent and all the by-products being formed, the mineralization efficiency of the catalyst was 36 percent. The reactor was allowed to continue operating with the TCE concentration slowly increasing. As the TCE increased the C_2Cl_6 decreased and the others remained essentially constant. A re-check of the catalytic activity a day later indicated that the mineralization efficiency had stabilized at approximately 37 percent. Total on-stream catalyst time was over 285 hours, ending with the TCE effluent concentration approximately one half of the dry 1500 ppmv feed.

AM-572-Co

Cobalt was the final transition metal to be used to impregnate the Amborsorb® adsorbent. The conditions reported here are summarized in Table 2-6. Initial flows

(EBCT of 7 s to 49 s) up to 145 °C showed no catalytic activity. Raising the temperature to 190 °C (EBCT of 24 s) dramatically drops the TCE effluent but also starts to show chloroform in significant quantities. A chloride analysis at the point where the TCE was approximately 20 percent of the influent as determined by the GC, indicated a mineralization efficiency of about 17 percent. The TCE concentration in the effluent continued to drop and eventually went non-detect, with only chloroform remaining at a relatively constant level.

The flow was increased to an EBCT of 9.6 s to determine if the TCE would return to the effluent. While TCE was not seen, the chloroform levels increased slightly and slight amounts of carbon tetrachloride appeared. The mineralization efficiency went up to 47 percent. A GC/MS sample of the effluent indicated a new, barely detectable peak, phosgene. The flow was again increased to an EBCT of 2.8 s, which rapidly (within 4 hrs) yielded TCE in the effluent (4 ppmv) and also PCE in the effluent.

Reducing the reactor flow and temperature (EBCT of 32 s; 130 °C) caused the adsorption isotherms to shift, causing initial decreases in effluent concentrations. After this had re-equilibrated only chloroform, carbon tetrachloride and PCE remained in the effluent. A chloride analysis indicated a mineralization efficiency of 27 percent, even though the TCE was non-detect in the effluent. Increasing the flow to an EBCT of 9.6 s did not initially change the product spectrum, however, the mineralization efficiency decreased to 20 percent. After 2 days under these conditions TCE was noted in the effluent (2 ppmv). Another increase in flow (EBCT of 3 s) yielded significant quantities of TCE in the effluent (900 ppmv) which stayed relatively constant for the remainder of this 280 hour experiment. The catalyst mass increased by approximately 30 percent.

In a subsequent run the cobalt oxide catalyst was started at 190 °C. In this run the cobalt showed an induction period similar to the manganese as shown in Figure 2-5. The addition of water to the feed stream showed deactivation of the catalyst so the run

was stopped. No chloride samples were taken to confirm mineralization.

To determine the nature of the induction period, an aliquot of the initial 100 g batch of AM572-Co was placed in a tube furnace and heated to 250 °C in air over night. Some of this material, AM572-Co(H), was put into the steel reactor (25 s EBCT; 280 °C). Only a 67% conversion was obtained, with chloroform and PCE as the major by-products. The catalyst suffered a 12 percent weight loss during the run.

Since the $\text{-SO}_3\text{H}$ group can be ion exchanged, a new batch of catalyst was made by passing cobalt nitrate (1 M) through a bed of plain Ambersorb 572. As expected the adsorbent did not have much exchange capacity. This catalyst, AM 572-Co(e), at 180 °C (1 s EBCT) also had an induction period, after which complete conversion (>99.9 percent) is achieved, but the mineralization efficiency is only 7 percent. Shortly afterwards the catalyst completely deactivates. Heat treating the AM-572-Co(e) as above to make AM 572-Co(e)/H showed a standard adsorption curve (short loading with breakthrough) and no catalytic activity.